Synthesis and chemosensing ability of novel pyrene-isoxazole-calix[4]arene constructs

A thesis submitted to the National University of Ireland, Maynooth for the MSc.

By Haowen Diao (BSc. Hors).

NUI MAYNOOTH

Ollscoil na hÉireann Má Nuad

Department of Chemistry,

National University of Ireland, Maynooth,
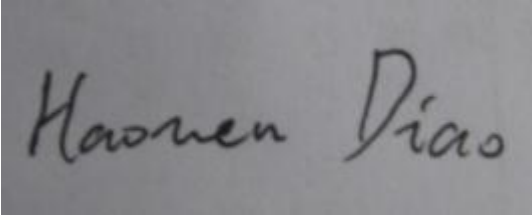
Maynooth,

Co. Kildare,

Ireland.

Oct 2012

Research supervisor: Dr. Frances Heaney

Head of Department: Dr. John Stephens

Declaration

This is to certify that the materials presented in this thesis has not been submitted before for a Degree to this or any other university, except where acknowledged and cited. The thesis is the author's original work.

Haowen Diao

October 2012

Acknowledgements

This is the third year I stay in Ireland. How to say, that is a good time also a challenge for me to study and live here. There are really a few people I need to thank for. Firstly, I would like to thank my supervisor, Dr. Frances Heaney, for her guidance, patience and strict attitude on research over the course of my study in Maynooth.

Thanks to Dr. John MacGinley for his cooperation on fluorescence study and assisting me with the further study.

Thanks to Dr. Bernie Creaven who helped us with the NMR study in Tallaght.

Thanks to postgrads that helped me a lot and invited me join the lab family when I started. We played soccer, hockey and lots of sports together. Particular thanks for Naill Maher, my partner on fluorescence study who assisted me with all fluorescence experiments and data analyze. We together got through a lot of problems.

Thanks to the postdocs who presented me knowledge and advice, in particular John Murphy, Collin Freeman and Trish Owens.

To the stuff of chemistry department, I would like to thank Noel (for fixing anything I needed on laptop), Ken, Ria, Babara and Ollie (for all the mass specs analysis).

Last, I would like to thank Ruiyao for your love, encouragement and support.

Dedication

To my parents,Yanjun and Huiqin, with respect and love.

Thanks for everything.

Abstract

This master thesis describes the preparation and analysis of a new chemosensor built up of the following elements: a pyrene reporter unit, an isoxazole unit functioning as linker and ion-binding moiety and a calixarene scaffold as ion-binding moiety – **PIC.**

The first chapter gives an introduction to the known properties, synthetic routes and relevant applications of both isoxazoles and calixarenes. Special attention is given to coordination properties of isoxazoles and to the application of calixarenes as valuable scaffolds for the creation of robust molecules with diverse functionality and chemosensing applications.

In the second chapter, all results achieved are discussed. The synthesis of all model compounds and of the functional calixarene **PIC** is discussed. The structural interpretation of the new compounds is presented including analysis of NMR data. The targeted compound **PIC** was synthesized and it's structure-confirmed by X-ray crystallography. The ability of **PIC** to function as an ion selective detector was studied by fluorescence spectroscopy. It was found to selectively detect Cu^{2+} ions even in the presence of a range of other heavy metal ions. Sensitivity was found to be higher towards copper perchlorate than all other copper salts studied. The stoichiometry of **PIC-Cu^{2+}** binding was established as 1:1, but it was not possible to say if the quenching of the fluorescence of the host by the guest was by static or dynamic processes.

In the final part of the results chapter the possibility to introduce regioselectivity to the strain-promoted nitrile oxide cycloalkyne cycloaddition by employment of reacting partners bearing groups capable of *H*-binding was studied. Unfortunately regioselectivity did not result.

Chapter 3 reports all the experiments carried out. All compounds were characterized

by ^{1}H, ^{13}C NMR, IR spectra and Mass spectrometry data. This is followed by a complete list of all the reference materials used in this thesis.

The final part is the Appendix, in which the complete characterization data of **a**nthracene-**i**soxazole-**c**alixarene, (**AIC**) is presented**.** Details are given of some analytic techniques used, eg. NMR, COSY and HSQC. A poster is also presented.

List of abbreviations

Ar	Aromatic ring
CH$_3$CN	Acetonitrile
CDCl$_3$	deuterochloroform
cm^{-1}	Wavenumbers
DBU	1,8-Diazabicyclo[5.4.0]undec-7-ene-2,3,4,6,7,8,9,10-Octahydropyrimido[1,2-a]azepine
DCM	Dichloromethane
DMF	Dimethylformamide
d	Doublet
dd	Doublet of doublets
Δ	Reflux temperature
δ	Chemical shift
e.g.	Example
eq.	Equivalent
g	Gram
HPLC	High-performance liquid chromatography
IR	Infrared
J	Coupling constant
DMF	N,N-dimethylformamide
m.p.	Melting points
M	Molar
m	Multiplet
min	Minute
mL	Milliliter
NMR	Nuclear magnetic resonance
Ph	Phenyl group
ppm	Parts per million
r.t.	room temperature
s	Singlet

SiO$_2$	Silica gel
s.m.	starting material
t	Triplet
TBAF	Tetrabutylammonium fluoride trihydrate
TEA	Triethylamine
μL	Microliter
μM	Micromolar
UV/vis	Ultraviolet/visible

Contents

Chapter 1
Introduction

Introduction:

1.1 Isoxazole chemistry

1.1.1   Overview

The parent isoxazole is a five membered heterocyclic with an oxygen atom in position 1 and a nitrogen atom in position 2. As shown in Figure 1.1, it is an aromatic structure. A 3D model of the isoxazole ring is shown in Figure 1.2.
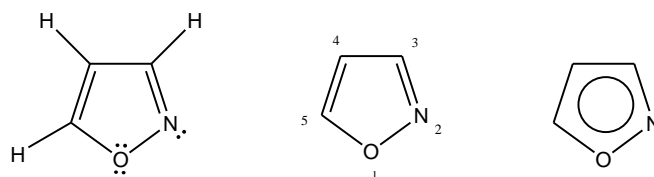
Figure 1.1.Stucture of the parent isoxazole ring
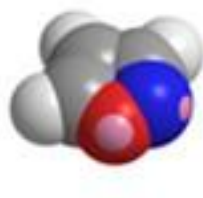
Figure 1.2. 3D Model of isoxazole ring.

Isoxazoles are a class of heteroaromatic molecules.[1] As well as being useful synthetic intermediates, they are important biologically active motifs which feature in lots of agrochemical and pharmaceutical products.[2] Isoxazoles are also widely found in natural products from various sources, *e.g.* ibotenic acid, isolated from mushrooms named *Amanita muscaria* and *Amanita pantherina*.[3] Certain isoxazoles are shown to be potent, selective agonists of human cloned dopamine D4 receptors[4] and others exhibit activity as $GABA_A$ antagonists,[5] and COX-2 inhibitors.[6] Others have ulcerogenic and antinociceptive anticancer properties.[7] In addition to applications as biologically active units isoxazoles can also be valuable scaffolds for construction of chiral ligands.[8]

1.1.2 Isoxazole preparation.

The presence of an isoxazole ring as a substructure in a large range of natural and

synthetic products makes their preparation an important synthetic goal. The challenge to develop new routes for the synthesis of isoxazoles has been taken on by many organic chemists. Generally speaking, isoxazoles can be obtained by two main synthetic routes: cyclisation of acetylenic oximes, themselves generated from the reaction of hydroxylamine with acetylenic aldehydes/ketones and [3+2]cycloaddition between alkynes and nitrile oxides.[9]

In an example of the first gold(III)-catalyzed cycloisomerization the α,β-acetylenic oximes **2** have been shown to afford substituted isoxazoles **3** under moderate reaction conditions, (Scheme 1.1).[10] Products can be obtained in excellent yield, *e.g.* when R^1 = Ph, R^2 = 4-MeC$_6$H$_4$, **3** was obtained: in 95% yield. The required α,β-acetylenic oximes (**2**) were easily obtained in good yield by stirring a mixture of α-acetylenic ketones/aldehydes (**1**) with hydroxylammonium chloride and 10% NaHCO$_3$ in methanol. When R^1= Me or H, E/Z oximes were formed in a 1:1 mixture while for R^2=Ph, the Z-isomer was obtained as the major product.

R^1 = Me, Ph, H;

R^2 = Ph, 4-MeOC$_6$H$_4$, 2-NCC$_6$H$_4$, 2-hydroxybutyl, SiMe$_3$, 4-MeC$_6$H$_4$.
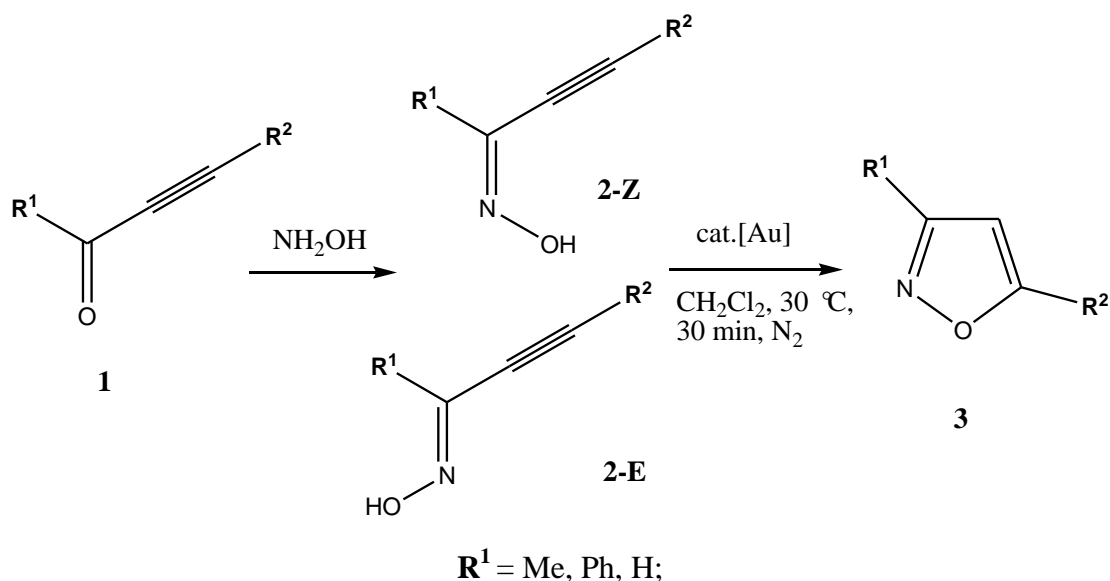
Scheme 1.1. Synthesis of isoxazoles **3** by gold-catalyzed cyclisation.

The proposed mechanism of cyclisation is shown in Scheme 1.2.[10] π-Activation of carbophilic AuCl$_3$ with the triple bond leads to a π-complex which undergoes a *5-endo-dig* cyclization to afford the cyclized intermediate which following

deprotonation and subsequent deprotection, results in the formation of **3** in good yield. Interestingly, a range of cationic gold complexes, like AuBr$_3$ or AuCl, promoted the reaction as well. However they are not as effective as AuCl$_3$, neither did the reaction proceed without a catalyst.[10]
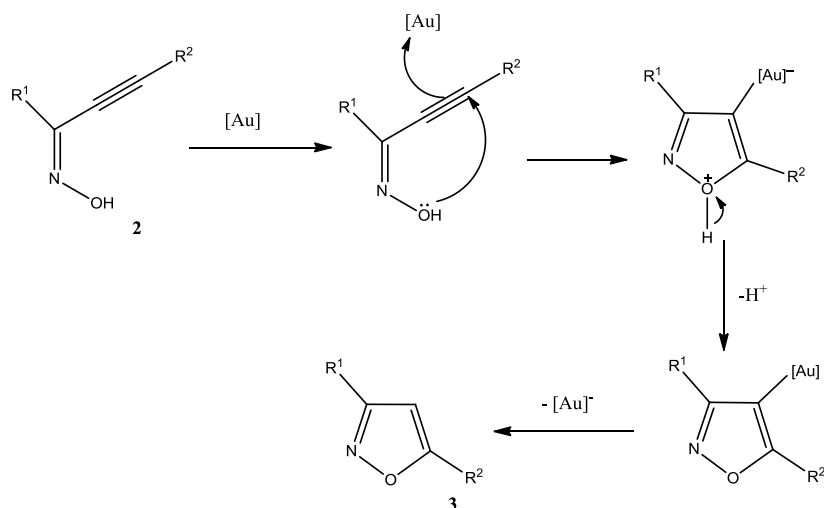
Scheme 1.2. Proposed mechanism for the gold (III)-catalyzed cycloisomerization of acetylenic oximes

In one example of the cycloaddition approach a thermally promoted reaction between alkynyl iodides and nitrile oxides was shown to give isoxazoles with good regioselectivity.[11] The reaction gave the 4-iodo-5-phenyl isomer **6A**, the alternative 4-phenyl-5-iodo isomer **6B** apparently was not found. The study involved reaction between the *N*-oxide and 2 equivalents of alkynyl iodide in DMF at 100 ℃ under microwave activation. After 20 min, the desired product was obtained in 83% yield (equation 1.1).[11]
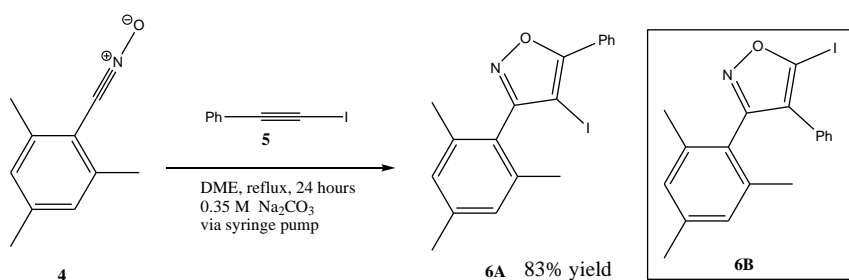
Equation 1.1. Synthetic route to isoxazoles by [3+2] cycloaddition.

Frequently nitrile oxides are unstable so *in situ* generation is necessary. Often this involves dehydrohalogenation of chlorooximes. In one example, the ketoalkynes **9**, themselves generated from reaction of the monosubstituted alkynes **8** and acid chlorides **7** in the presence of a palladium catalyst**,** were trapped regioselectively by the dipoles formed from *in situ* reaction of the chlorooximes **10** and triethylamine. After 30 minutes of microwave heating, the isoxazoles **11** were obtained in good yields (Scheme 1.3, Table 1.2). The mechanism[12], a typical cycloaddition, is shown in Scheme 1.4.
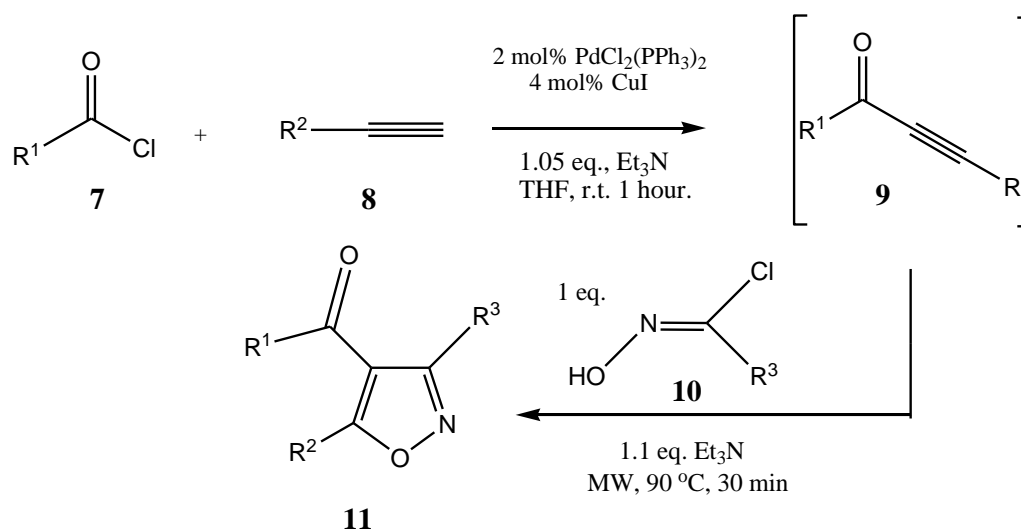
R^1	R^2	R^3	yield
2-thienyl	Me_3Si	$4\text{-}MeOC_6H_4$	77%
$4\text{-}O_2NC_6H_4$	*n*-butyl	$4\text{-}MeOC_6H_4$	56%
$4\text{-}MeOC_6H_4$	*n*-butyl	$4\text{-}MeOC_6H_4$	64%
$4\text{-}ClC_6H_4$	*n*-butyl	$4\text{-}MeOC_6H_4$	59%
$4\text{-}F_3CC_6H_4$	*n*-butyl	$4\text{-}MeOC_6H_4$	56%

Scheme 1.3. Dipolar cycloaddition route to isoxazoles **11**.
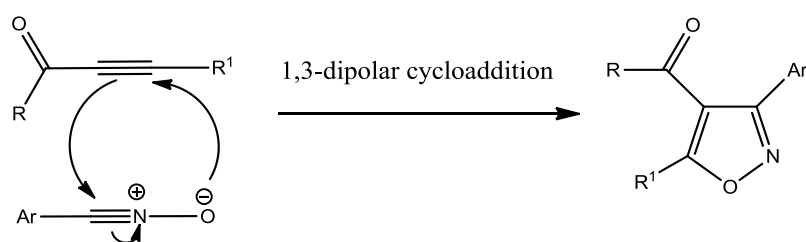
Scheme 1.4. The mechanism of 1,3-dipolar cycloaddition.

1.1.2.   Coordination chemistry of isoxazoles.[13]

Since their first preparation by Claisen in 1888,[14] isoxazoles have been well studied due to their potential application as multifunctional materials in luminescence, gas adsorption, fluorescence, catalysis and so on. A great deal of interest has been shown in isoxazole-metal complex formation. However rational control in the synthesis of coordination compounds is still a big challenge. Researchers have attempted to learn the relationship between heterocyclic structure and complex formation. Important features of isoxazole and its derivatives which help them serve as ligands include:

(1). Isoxazoles are heterocyclic π-conjugated systems with *N-* and *O-* as potential donor atoms for coordination to metals.

(2). Isoxazoles offer a large number of bridging modes depending on the functional groups substituted on the isoxazole ring.

(3). Isoxazoles have nitrogen atoms and oxygen atoms as hydrogen bonds acceptors, so many kinds of secondary non-covalent interactions can potentially contribute to isoxazole complexation.

The structures of selected isoxazole ligands are shown in Chart 1. In the formation of isoxazole-metal complexes it has been reported that the ring can act as either a monodentate or bridging bidentate ligand.

Chart 1. The structures of selected isoxazole ligands.[15]

5-methylisoxazole

12

3,5-dimethyl-isoxazole

13

3-methyl-5-phenylisoxazole

14

3,5-diphenylisoxazole

15

3-amino-5-methylisoxazole

16

4-amino-3,5-dimethylisoxazole

17

5-amino-3,4-dimethylisoxazole

18

3-phenylisoxazole

19

4,5-naphthisoxazole

20

n=1,2

4,5-cycloalkylisoxazole

21
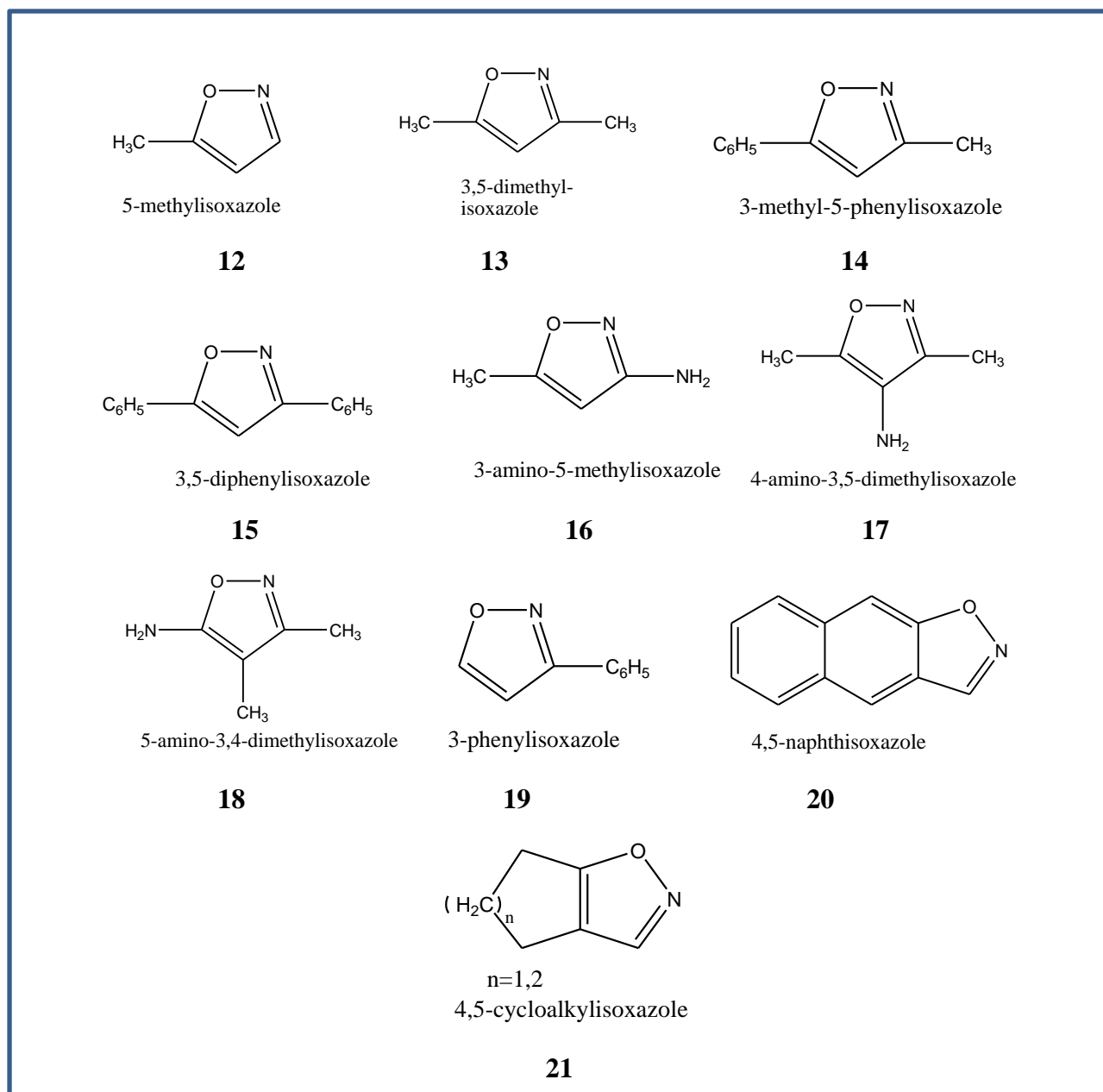
For most metal ions, the major mode of monodentate binding is through the ring nitrogen atom when the isoxazole is aryl-substituted or alkyl- substituted (Figure 1.4, Mode A).[15] However, all the Zn(3-methyl-5-phenylisoxazole)$_2$ (**14**)[16] and the ZnBr$_2$ complexes of 3,5-dimethylisoxazole (**15**) coordinate through the ring oxygen atom (Figure 1.4, Mode B). Binding through the N$_{ring}$ dominates among complexes formed from 3-amino-5-methylisoxazole (**16**); on the other hand, complexes to Pd, Pt, Cd and Zn favor the oxygen binding which is consistent with the known oxophilicity of Pd

and Pt. However, this behavior is not observed in alkyl/aryl-substituted isoxazole adducts. Except N_{amine} complexation has been observed for Ni(3-amino-5-methyl-isoxazole)$_3$ which is also the sole example of a tetrahedral Ni complex.

A. N_{ring} B. O_{ring} C. N_{amine}
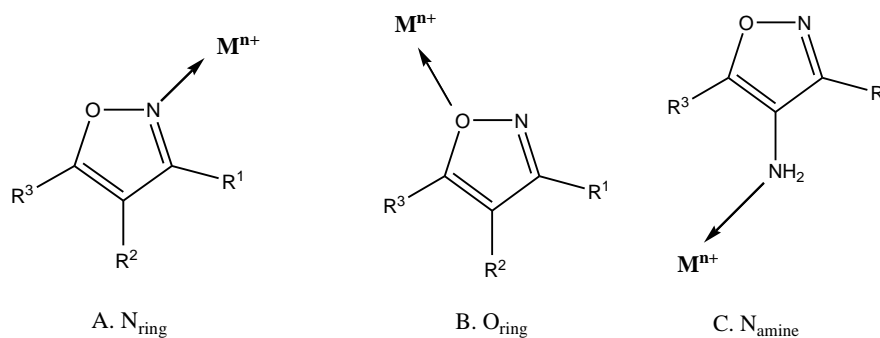
Mode A, M^{n+} = Hg(II), Zn(II), Fe(0), Fe(III) Cr(0), Co(III), Ag(I), Pd(I), Pt(I), Pr (III), Eu(III), Yb(III), Gd(III), Pt(IV).

Mode B, M^{n+} = Cu(II), Pd(I), Pt(I), Mo(0), Fe(0).

Mode C, M^{n+} = Cr(III), Ni(II), Cu(II), Ca(II), Ba(II), Fe(III), Pd(I), Pt(I), Co(II).

Figure. 1.4. Monodentate chelation modes of isoxazoles to metals.

The most common bridging binding modes of isoxazoles are shown in Figure 1.5. The parent isoxazole (**11**) and 3,5-dimethylisoxazole (**13**) can exhibit only Mode A binding involving both ring heteroatoms (Figure 1.5). Mode D and E involve contributions for the heterocyclic ring as well as a non-coplanar aromatic ring. Only 5-amino-3,4-dimethyl- isoxazole (**18**) exhibits Mode C binding (Figure 1.5).

A. Mode A; O_{ring}-N_{ring}

B. mode B; N_{ring}-N_{amimo}

C. Mode C; O_{ring}-N_{amino}

D. N-aryl bridging

E. O-aryl bridging
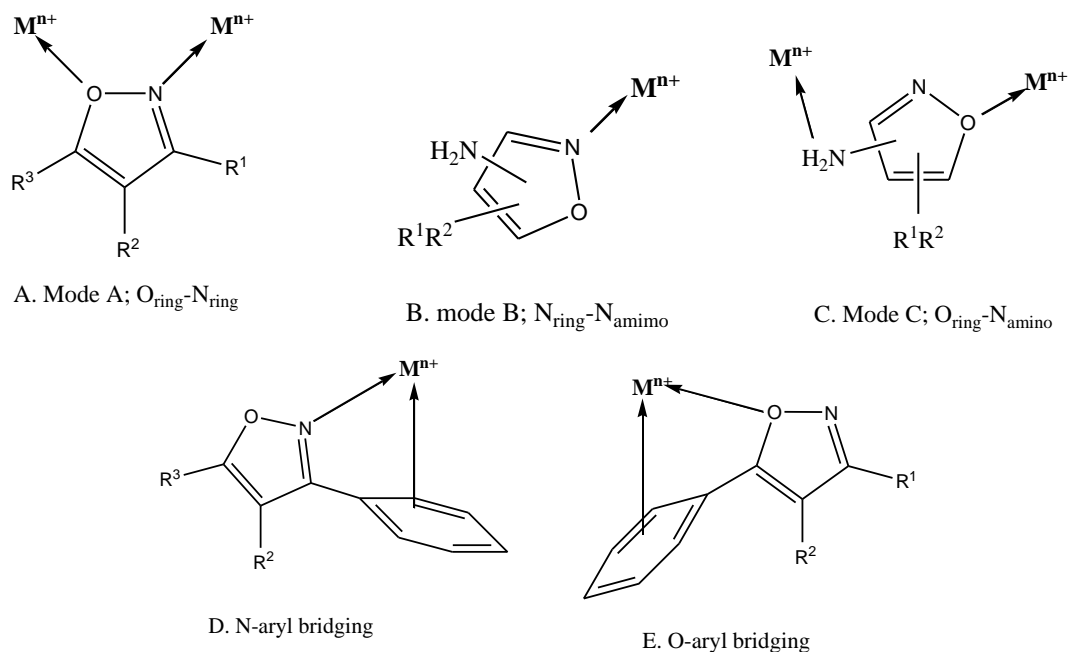
Mode A: **M** = Cr(III), Ni(II), Cu(II), Ca(II), Ba(II), Fe(III), Pd(I), Pt(I), Co(III).

Mode B: **M** = Co(III), Pd(I), Pt(I), Ni(II), Cu(II).

Mode C: **M** = Cr(III), Ca(II), Ba(II), Pd(I), Pt(I).

Figure 1.5. Bridging bidentate chelation modes of isoxazoles.

The possible resonance structures for 3-amino-5-methylisoxazole (**16**) and 4-amino-3,5-dimethylisoxazole (**17**) are shown in Figure 1.6. Electron donation from the oxygen atom can increase the electron density on the ring nitrogen atom of **16**. However, electron donation by the oxygen of **17** increases the electron density on the exocyclic amino group and so the ring nitrogen atom may not be such a strong donor atom for complexation. Although 16_{iii} appears quite similar to $\mathbf{17}_{iii}$, the observed behavior of the ligands[16] that structure $\mathbf{17}_{ii}$ plays a large role in the monodentate binding of **17**. For **16** it appears that the primary binding involves the N_{ring} atom while **17** got the N_{chain} atom binding to the ring.

16	
17	
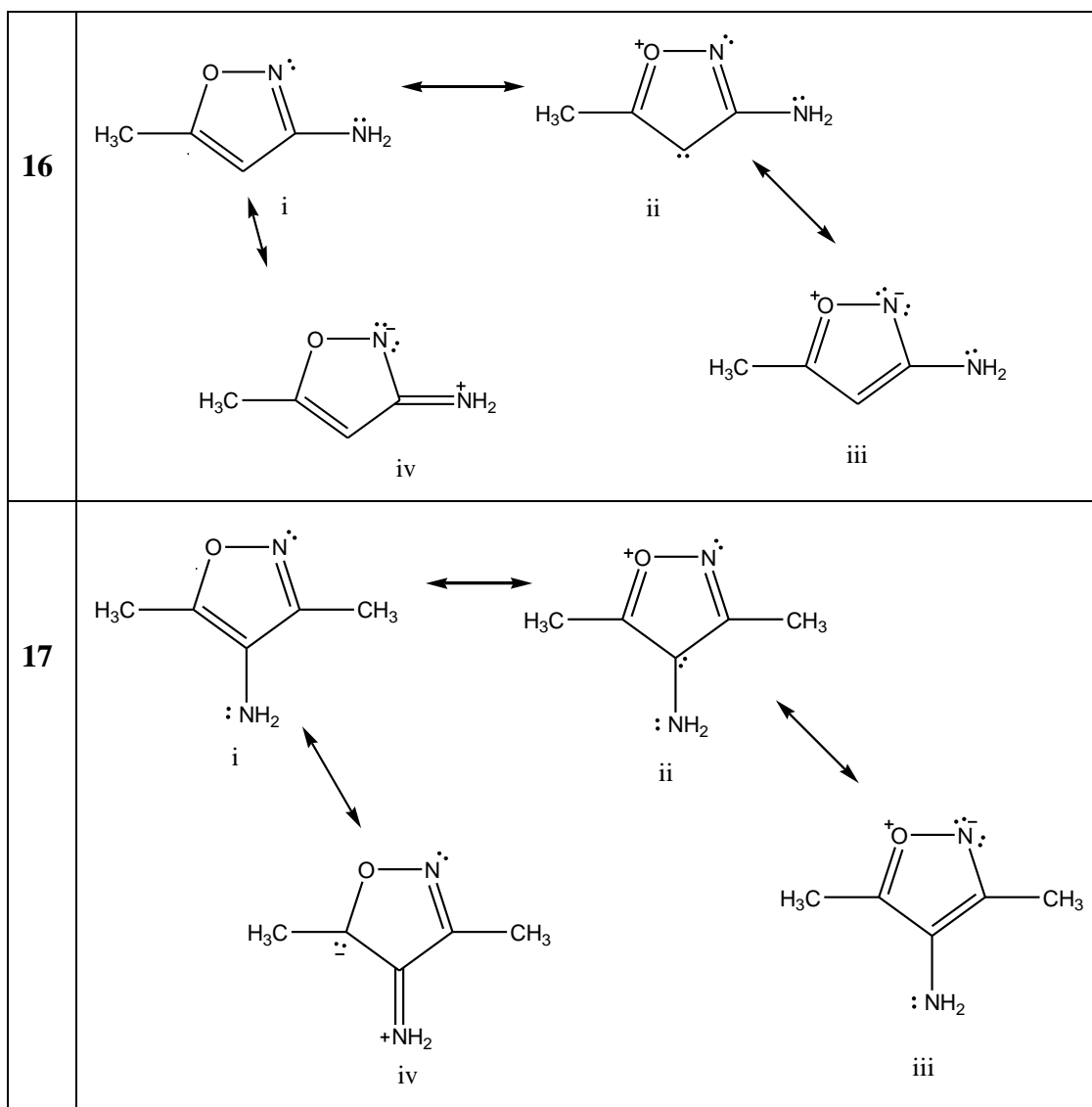
Figure 1.6. Resonance structures of 3-amino-5-methylisoxazole (**16**) and

4-amino-3,5-dimethylisoxazole (**17**).

In summary, the preparation and binding characteristics of metal-isoxazole complexes have been of interest for many years; however, there are still some issues which require attention. In particular, the preparation of multifunctional coordination compounds with potentially valuable fluorescent and adsorption properties is still a challenge.

1.2 Calixarenes.

1.2.1 History:

In 1872, Adolf von Baeyer pioneered the chemistry of calixarenes.[17] He studied the reaction of phenol and formaldehyde in the presence of a strong acid and noted formation of a red-brown resin with a marked viscosity increase. However, the structure of the substances he synthesized couldn't be determined due to the limited analytical techniques at that time. Calixarenes are a class of cyclooligomers formed by phenol-formaldehyde condensation. They have defined upper and lower rims and a central annulus. They exist as a cup-like shape (Figure 1.7). The name reflects similarity between the cyclic tetramers and a type of Greek vase named calix (Figure 1.8).

Figure 1.7. Cone conformation of calix[4]arene	Figure 1.8. Space-filling molecular model of a cyclic tetramer (left) & calixcrater (right).
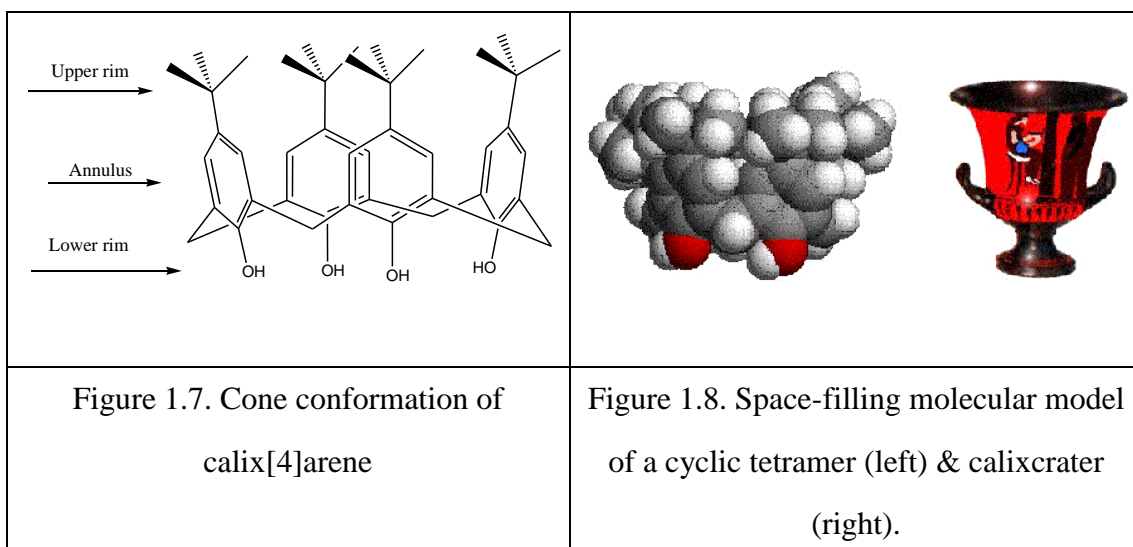
In 1894, the Lederer-Manasse hydroxyalkylation reaction[18] (Equation 1.1) was invented as a synthetic tool for the preparation of hydroxymethylphenols which brought calixarene synthesis one step further.

p-hydroxybenzyl alcohol   *o*-hydroxybenzyl alcohol
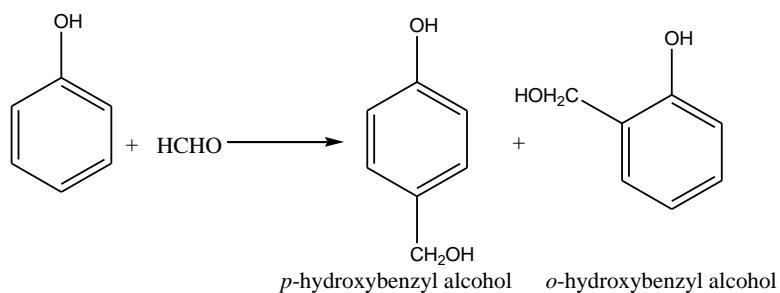
Equation 1.1. The Lederer-Manasse reaction.

In 1942 Alois Zinke made the first crystalline calixarene by the condensation of *p*-substituted phenols with formaldehyde. Two years later, following reaction between *p-tert*-butyl phenol and formaldehyde in the presence of sodium hydroxide in linseed oil he obtained a crystalline solid which didn't melt below 300 $^{\circ}$C. In 1955, another milestone was John Cornforth's realization of the potential of calixarene as a basket, analogous to enzymes. He repeated the experiments reported by Zinke which started with *p-tert*-butyl phenol but he formed two crystalline compounds. He proposed the compounds were diastereoisomers arising from hindered rotation about the methylene bridges.[19] Twenty years later, the word calixarene was proposed by C. David Gutsche. He was interested in the emerging area of enzyme mimics and, based on his awareness of phenol-formaldehyde chemistry.[17]

1.2.2   Structure of calixarene.

Calixarenes most commonly have four aryl rings, and such molecules are referred to as calix[4]arenes; those with 6 rings linked by methylene bridges are called calix[6]arenes and they can exist in up to eight different conformations, so are structurally more complex.[20] There are several different conformers of calix[4]arenes due to the potential for rotation of the Ar-CH$_2$-Ar bonds. The conformers are known as "cone", "partial cone", "1,2-alternate" and "1,3-alternate" (Table 1.1). The cone conformation (a) is the most stable for calix[4]arenes. In this conformation, all the OH groups are homoplanar.

Table 1.1: Four conformers of a calix[4]arene skeleton

(a). cone	(b). Partial cone	(c). 1,2-alternate	(d). 1,3-alternate
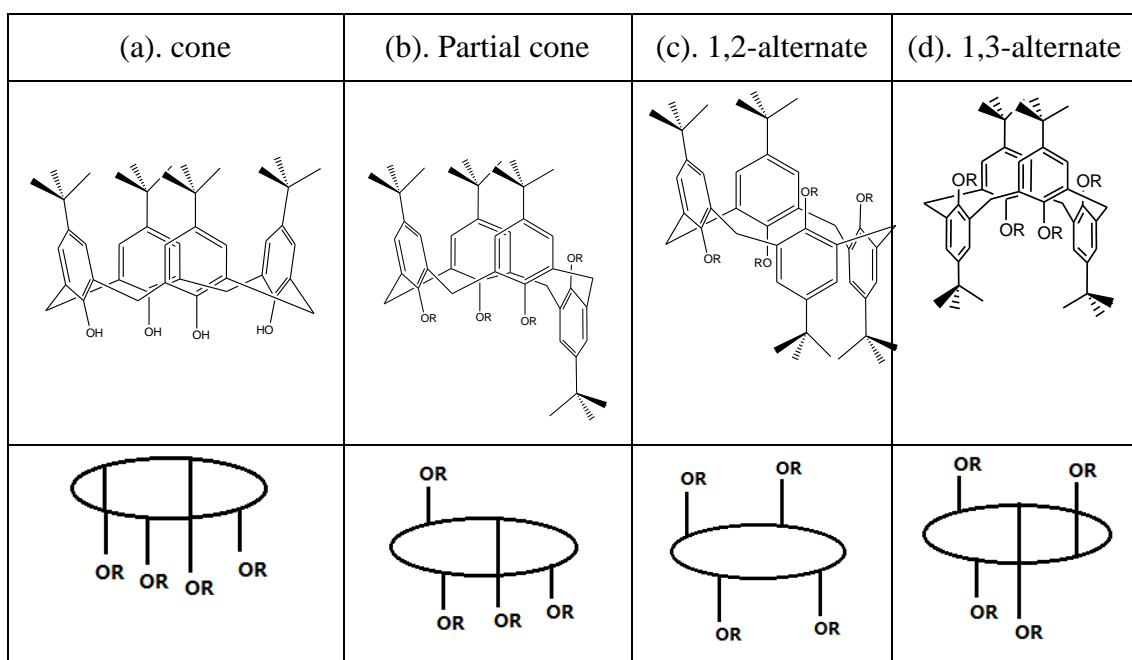
1.2.3 Synthesis of calix[4]arene

The preparation of *tert*-butylcalix[4]arene proved difficult for many years. Problems of poor yields were overcome after much experimentation varying parameters including the reaction temperatures. A one-step method[21] involving NaOH-induced condensation shown in Equation 1.2, of a *p*-substituted phenol and formaldehyde in diphenylether gave ca. 50% yield of glistening white rhombs, with a melting point of 342-344 ℃[22].
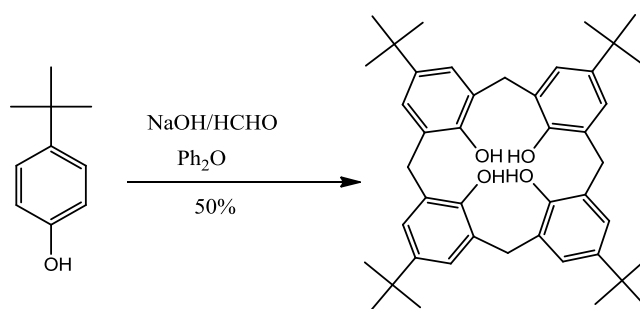
Equation 1.2. Zinke-Cornforth-Gutsche's procedure.

A general route to differentially substituted calix[4]arenes was developed by Hunter and Hayes.[23] Although the repetitive reaction sequence, requiring 10 steps, is more protracted than the one-step method (Equation 1.2), it allows substantial

variation in the structure of the final product through the use of different phenols at each arylation step. The starting material for the reaction was an *o*-protected *p*-cresol. Consecutive hydroxymethylation and acid-catalyzed arylation reactions lead to the formation of a linear oligomer. The product was finally cyclized with the removal of the protecting group (Scheme 1.5).
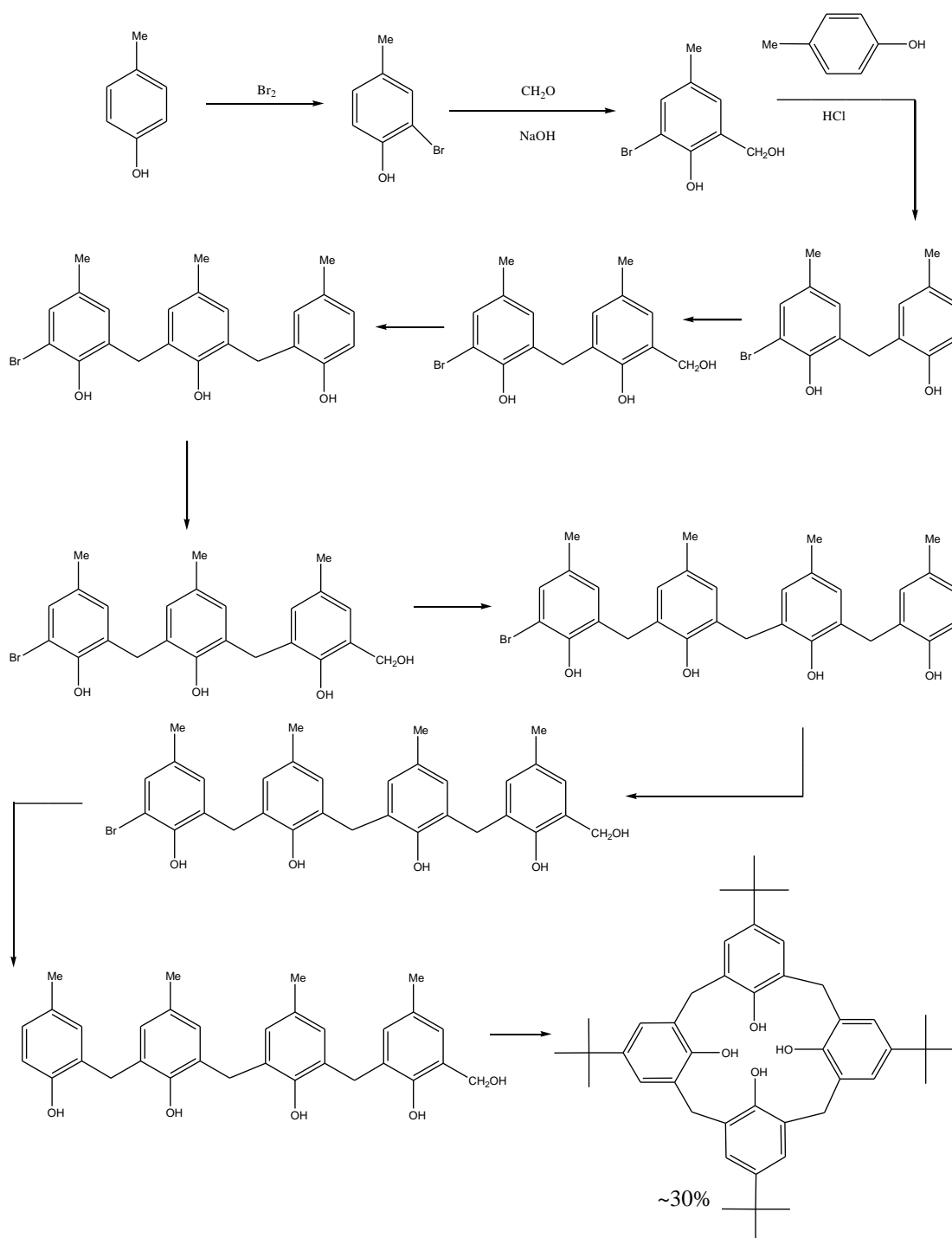
Scheme 1.5. Ten-step synthesis of tert-butyl calix[4]arene by Hunter and Hayes.[24]

The mechanism of the hydroxymethylation reaction between a bromo-protected phenol and formaldehyde (Scheme 1.5, second step) is believed to involve deprotonation to form a phenoxide ion prior to *C*-centered attack on the reactive carbon atom of formaldehyde (Scheme 1.6).[18]
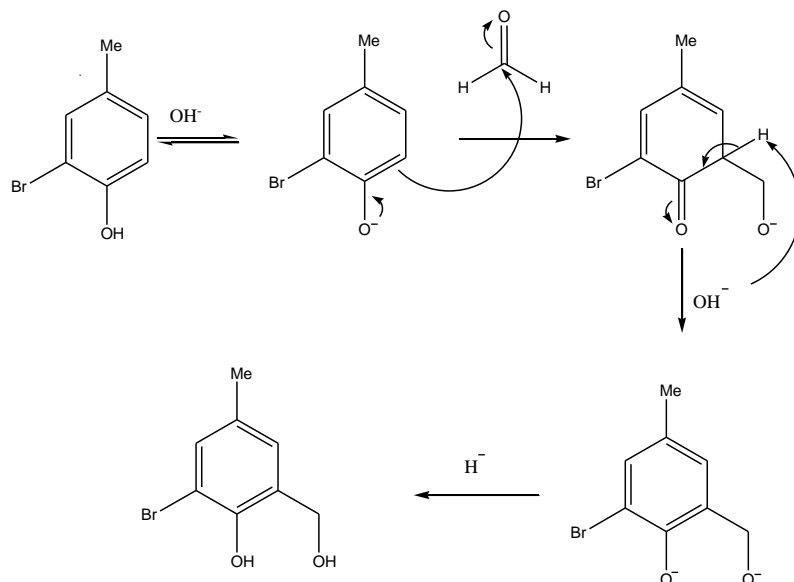
Scheme 1.6. The mechanism of the formation of hydroxylmethyl phenols.[18]

Under mild conditions the reaction terminates with formation of the hydroxymethyl compound, however, under more forcing conditions, it proceeds to form diarylmethyl compounds by way of quinonemethide intermediates as shown in Scheme 1.7. [18]
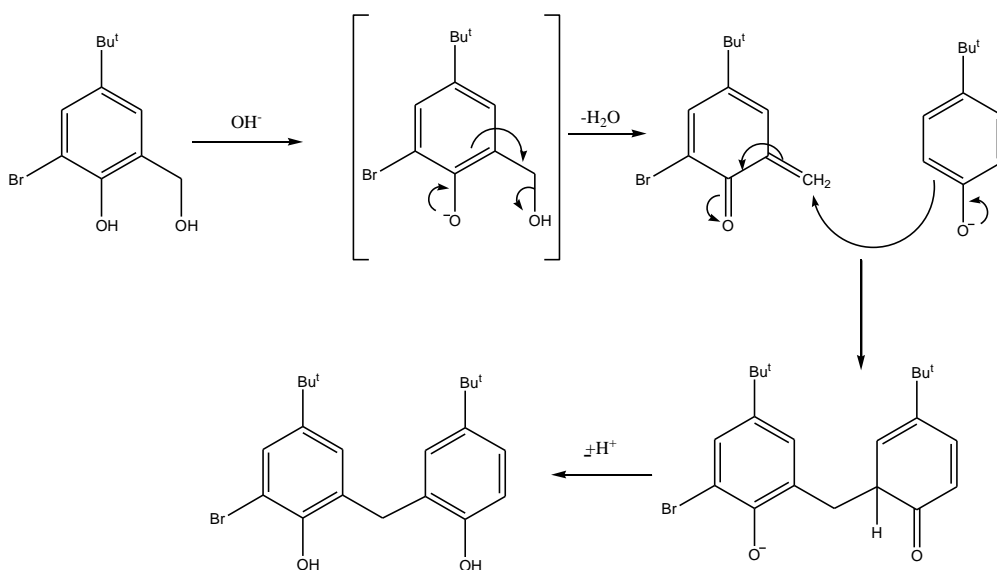
Scheme 1.7. Mechanism of dimer formation involving a quinomethide intermediate.

Sequential reactivity leads to linear oligomers suitable for cyclisation to calix[4]arenes (Scheme 1.8). The mechanism of cyclisation is still unknown. Gutsche and colleagues[25] proposed that 'effective circular hydrogen bonding should result in a hemicalixarene enhancing its stability and they believed that interconversion of this to calix[8]arene would require 'no conformational changes or any significant disruption to the hydrogen bonding array'. At high temperature in the presence of base, calix[8]arenes can interconvert to calix[4]arenes, in a process Gutsche likened to *'molecular mitosis'*.[18] This analogy arises as the calix[8]arenes are thought to pinch together in the middle and then split into a pair of cyclic tetramers (Scheme 1.8). However, no conclusive evidence has been published yet and the process remains under discussion.
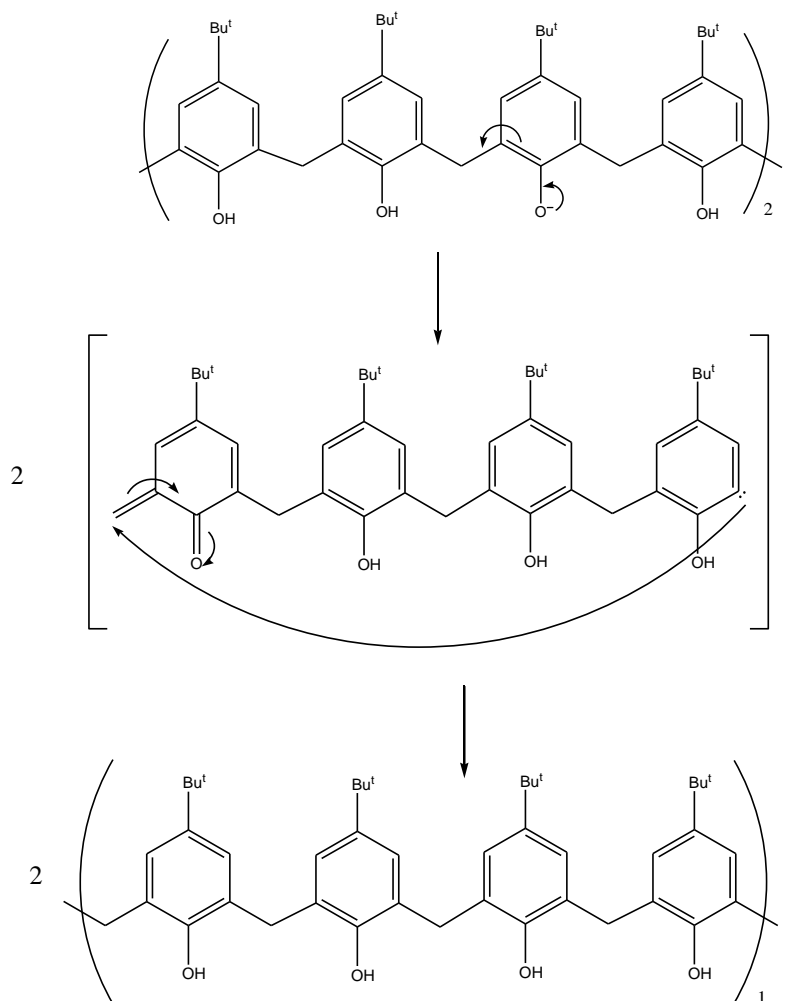
Scheme 1.8. *'Molecular mitosis'*: proposed conversion of calix[8]arenes to calix[4]arenes.

1.2.4. The properties of *t*-butyl calix[4]arenes.

1.2.4.1. Melting point[18]

The melting points of calixarenes are extremely high. Those with free hydroxyl groups usually have melting points above 250 ℃ *e.g.* the melting point of *t*-butylcalix[4]arene is 342-344 ℃. Melting point determination can be a very simple means to check the purity of *p-tert*-butylcalixarenes even when only a small amount of sample is available.

1.2.4.2. Solubility

Simple calixarenes are insoluble in water and in aqueous base. They are particularly soluble in organic solvents and sometimes it is difficult to obtain pure samples free from traces of solvent. Solubility is usually high in chloroform, dichloromethane, pyridine and carbon disulfide.[18]

1.2.4.3. Infrared Spectra

The most distinctive feature in the IR spectra of calixarenes is the OH stretch ranging from 3100-3500 cm^{-1}. The absorption is attributed to strong intramolecular hydrogen bonding.[26] In general, the IR spectra of variously substituted calixarenes exhibit similar OH absorptions, *e.g.* cyclic tetramer, 3180 cm^{-1}, cyclic pentamer, 3290 cm^{-1}; cyclic hexamer, 3170 cm^{-1}, cyclic heptamer, 3155 cm^{-1}. However, the cyclic octamers differ from other calixarenes and absorption is observed between 500 and 600 wavenumbers lower.[18]

1.2.4.4. NMR Spectra[18]

The ^{1}H NMR spectra of *p-tert*-butylcalix[4]arene, as a typical example of this class of compounds, is shown in Figure 1.9. The calix aromatic protons appear as a singlet at 7.05 ppm. The hydroxyl protons are also seen as a singlet at 10.34 ppm. The *tert*-butyl protons appear as a singlet at 1.21 ppm. The methylene bridge CH$_2$ protons are seen as doublets at 3.49 ppm and 4.23 ppm respectively. A temperature-dependent 'H NMR study, carried out by Kammerer and his co-workers,

showed characteristic changes in the chemical shift of the CH_2 groups as the conformation of the molecule varied with temperature. The signals for the CH_2 hydrogens appear as a sharp singlet above room temperature while they appear as a well-resolved pair of doublets at or below room temperature.[26]
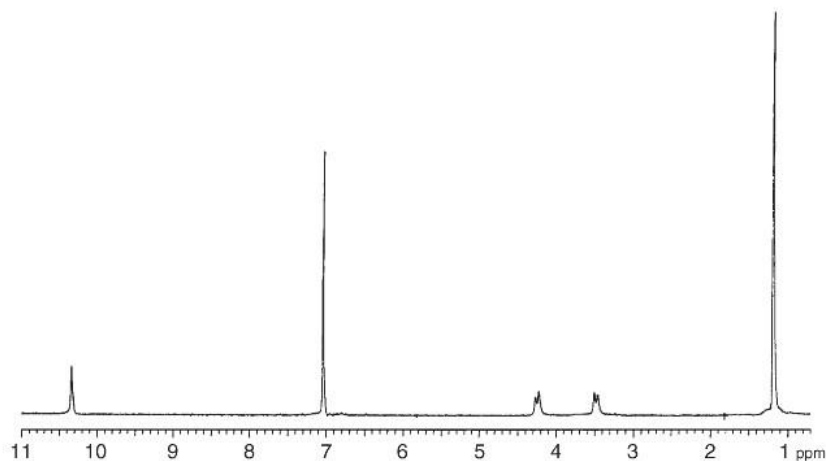
Figure 1.9. ^{1}H NMR spectrum of *p-tert*-butylcalix[4]arene (CDCl$_3$) at r.t.[18]

1.2.4.5. Applications of calixarenes as host molecules.[18]

Due to their attractive cavities, calixarenes can be considered like "baskets" with "functionality" and "shape" and calixarenes have become important players in host-guest chemistry. Indeed, in recent years much of the highlights of calixarene research have centered on designer molecules with unique abilities to act as sensors for metal ions, organic/neutral molecules and drug recognition applications including:

(i). calixarenes as chemical sensors.

   a). Cation receptors.

   b). Anion receptors.

   c). Receptors of neutral molecules.

(ii). Calixarenes in liquid-liquid extraction.

(iii). Calixarenes in transport through liquid membrane.

(iv). Calixarenes as Ion-Selective Electrodes.

1.2.5. Structural modification

Calix[4]arenes have two distinct regions available for modification: the lower and upper rim. The transformations which can alter significantly the physical and chemical properties of the parent compound are usually performed by:

(i) Functionalization at the *p*-positions of the aromatic rings *i.e.* the upper rim

(ii) Functionalization at the phenolic hydroxyls *i.e.* the lower rim

(iii) Substitution and replacement of methylene bridges by Si, S, SO_2, -CH_2-O-CH_2- and –CH_2-N(R)-CH_2- groups.

(iv) Modification of the aromatic "walls" of the calix cavity

(v) Extension of the calix[n]arene cavity by increasing n from 4 to 6 or 8.

1.2.5.1. Upper rim modification.[27]

After the removal of the *t*-butyl groups, modification at the upper rim has been explored. Upper rim derivatization requires careful selection of reagents and experimental conditions. *Ipso*-substitution[28] (where *Ipso*, describes as substation at the 1-position), has been carried out under a variety of reaction conditions. Under optimized conditions, calixarenes brominated at the *p*-positions as well as the methylene bridges can be obtained.[28]

A single step, (one-pot procedure) procedure is also reported for conversion of *p*-tert- butylcalix[n]arenes (Figure 1.11) to their *p*-acyl derivatives: thus **23** and **24** have been prepared[28]. The possibility to vary cavity size makes calixarenes interesting for a wide range of host-guest type interactions. Due to the potential for π-π interactions, (involving the aryl groups) and the potential for hydrogen bonding (involving the lower rim hydroxyl groups) the host molecules can encapsulate a wide variety of guests. The applications can be further expanded by structural modifications to the calixarene framework which modulate solubility, *e.g.* the groups of Makha and Rasston have synthesized water-soluble calixarenes with surface sulfonate groups. One approach to such compounds describing sulfonation of phenylsubstituted calix[n]arene **25** by treatment with sulfuric acid yields **26**[28]

(Scheme 1.9).

R^1	R^2	R^3	R^4
OH	H	CO-Ph	CO-Ph
OH	t-Bu	CO-C(CH$_3$)$_3$	CO-C(CH$_3$)$_3$
OMe	t-Bu	CO-CH$_3$	t-Bu
OMe	t-Bu	CO-CH$_2$CH$_3$	t-Bu

Figure 1.11. The one-pot procedure to *p*-acyl derivatives (n=4, 6, 8)
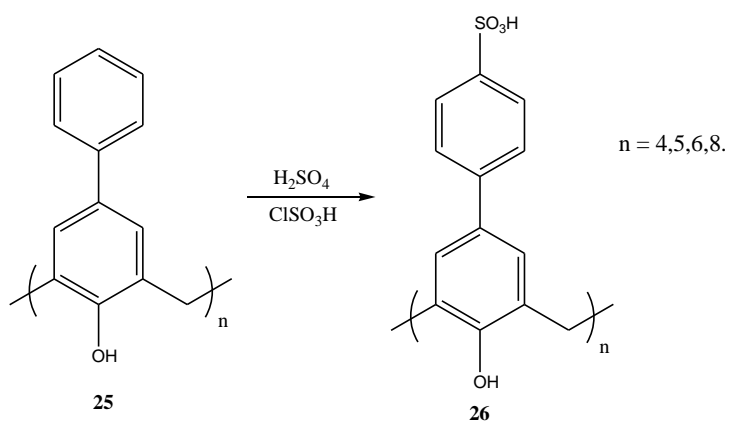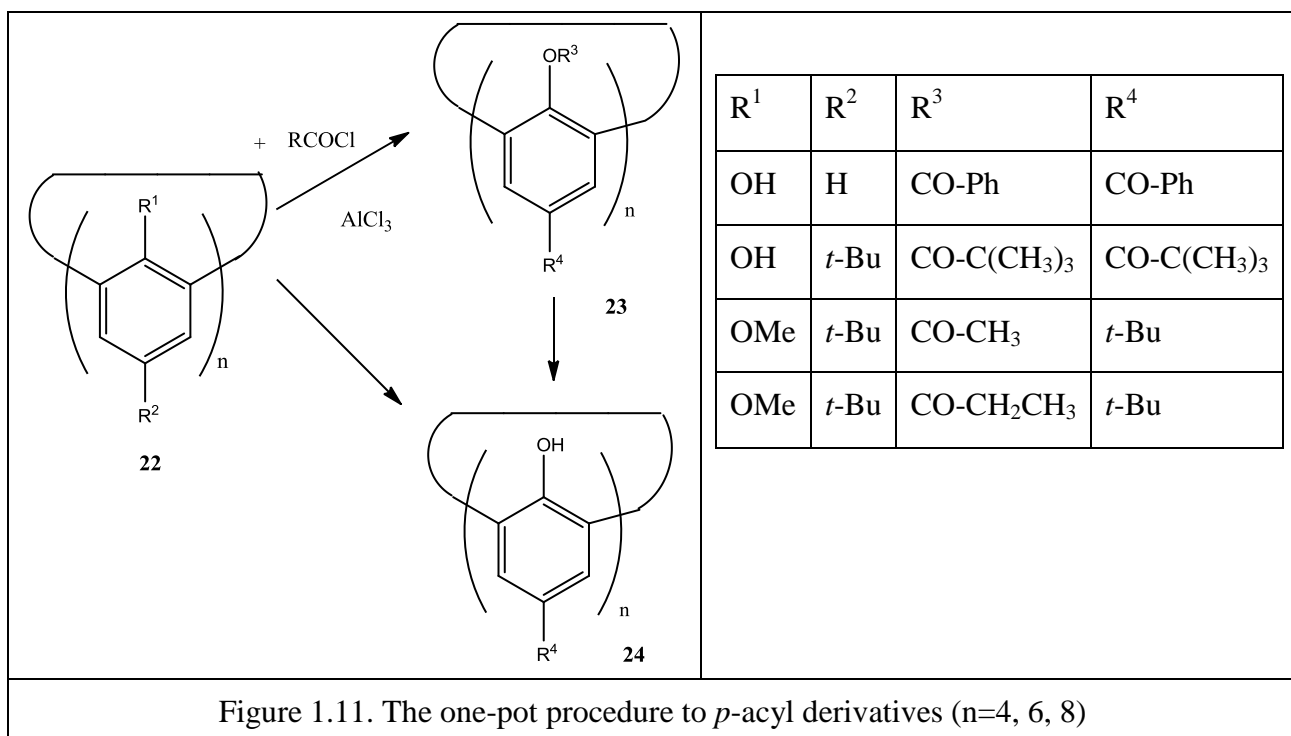

Scheme 1.9. Synthesis of sulfonated *p*-phenylcalix[n]arenes.

In conclusion, whilst functionalization of the upper rim, requiring the removal of the *t*-butyl groups is possible, it is more difficult than derivation of the lower rim. The latter has a readily functionalisable hydroxy group, thus lower rim derivation has been the main focus of attention.

1.2.5.2. Lower rim modification.

Due to the expansion of the cavity after lower rim substitution, complexation and inclusion of bigger guests, including heavy metals and organic molecules, can be facilitated. Thus, lower rim modification[24] has been the goal of many workers in this area. Lower rim modifications are relatively facile since the phenolic hydroxyl groups are good synthetic handles. A selection of lower rim modifications will now be discussed.

Bulky substituents including *m*- and *p*-methylbenzyl groups have been introduced by reaction of parent calix[4]arene **27** with the appropriate halo-compound in the presence of base (potassium carbonate, sodium carbonate). The reaction proceeds in acetonitrile at reflux temperature. The lower-rim substituted compounds **28** and **29** can be obtained in good yields (Scheme 1.10).[27]

$R^1 = p\text{-MeC}_6\text{H}_4, R^2 = m\text{-MeC}_6\text{H}_4.$
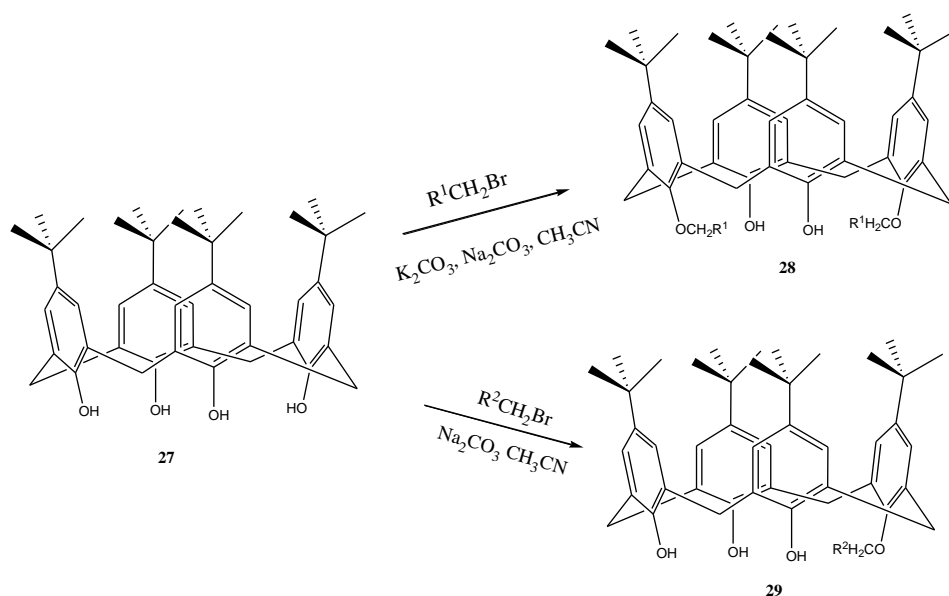
Scheme 1.10. Mono- and di-benzylation at the lower rim.

The unsymmetrical bis-alkyne **36** was prepared in two steps from the diprotected **30**.[29] The reaction of **30** with trimethylsilylacetylene **31** gave the expected **32** along with the unexpected iodinated derivatives **33-35**. The formation of **33-35** is thought to arise from metal-assisted iodide substitution. The iodinated **33** on treatment with phenylacetylene yielded the expected **36** (Scheme 1.11).
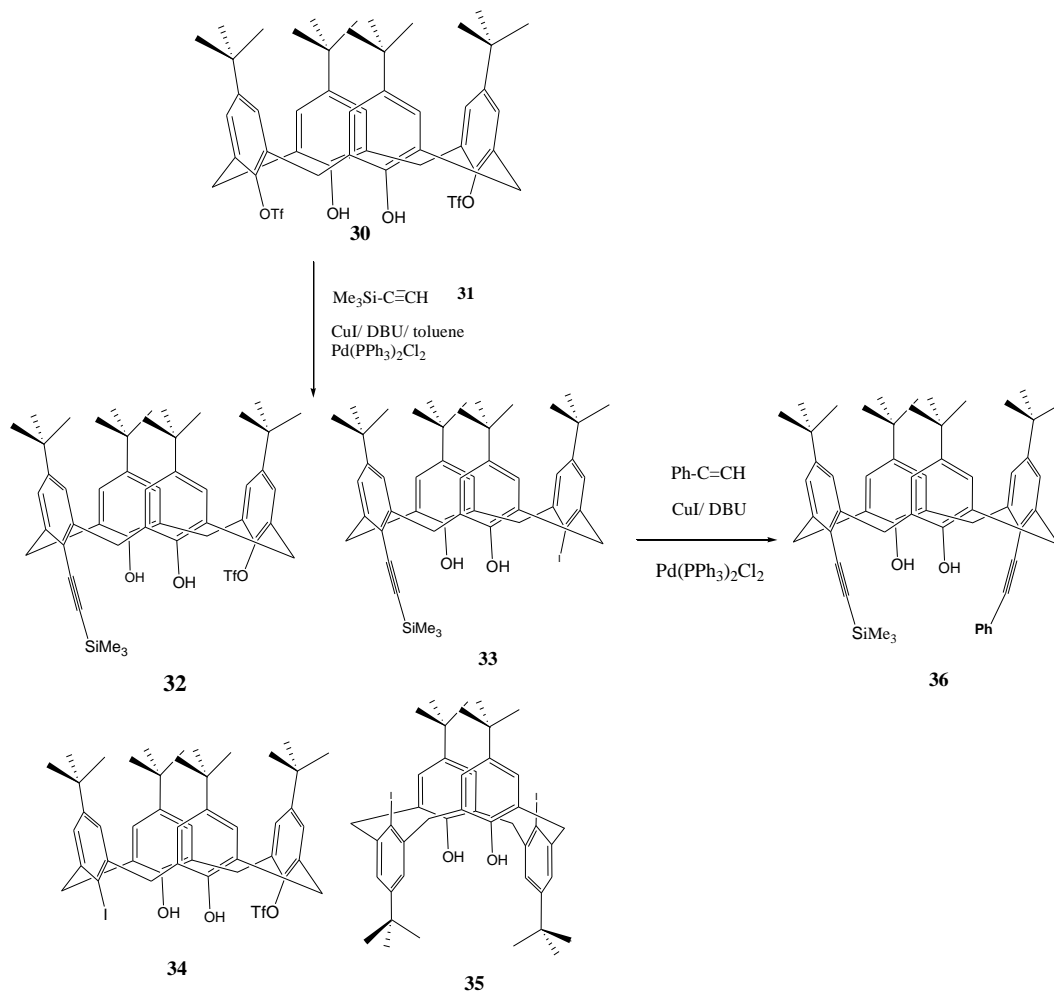
Scheme 1.11. Modification in lower-rim of calixarene.

Dimeric calixarenes have been formed by reaction at the lower rim, e.g. homocoupling of monoethynylcalixarene **38** led to bis-calixarene **39**. Following removal of the protecting group from **37**, by treatment with tetrabutylammonium fluoride (TBAF), dimerization occurred under the influence of CuI in toluene in the presence of DBU to yield the rigid bridged bis-calixarene **39** (Scheme 1.12). [29]
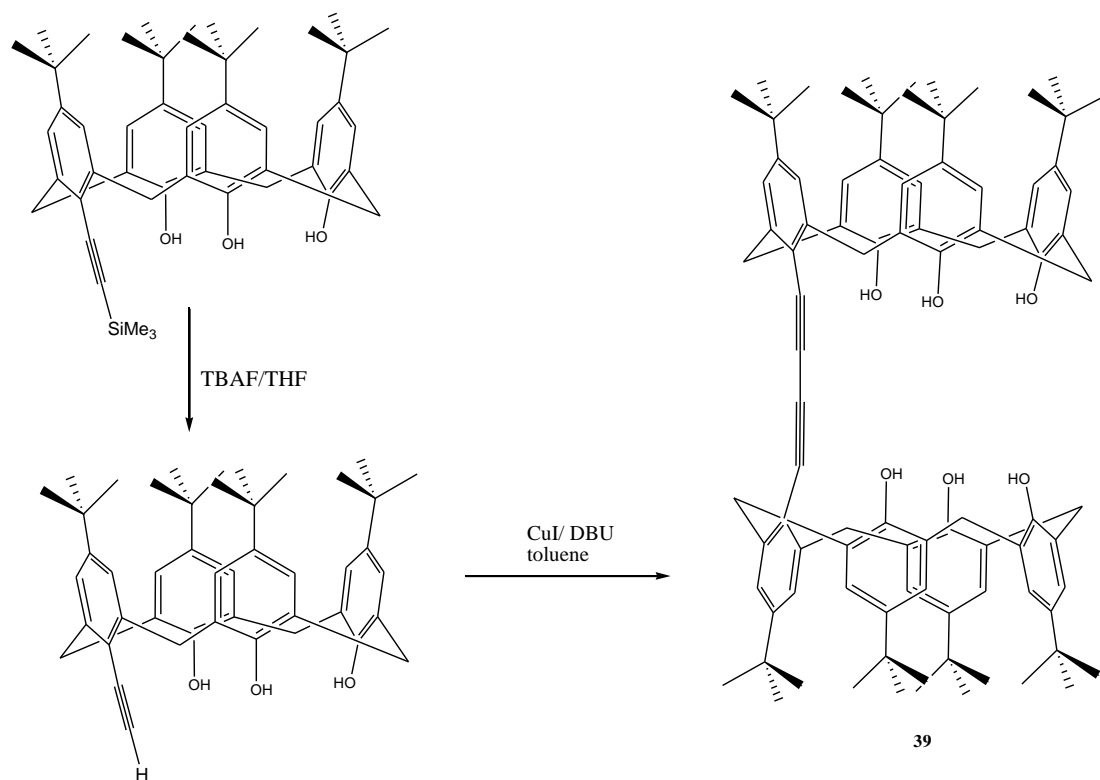
Scheme 1.12. Synthesis route to dimeric calixarenes.

1.2.5.3. Modification of both rims.[29]

Functionalization of both the lower and the upper rims of calixarene is known[30,31], and some examples are shown below. With the aim of constructing molecular logic gates[32], and also for the study of calixarene chromogenic chemosensors for both cations and anions, calixarene **44**, was synthesized. The synthetic route to the upper rim azo-functionalised calixarene **42** involved diazotization of the dipropargylcalixarene **40**, followed by treatment with p-nitroaniline **41**. Subsequent click cycloaddition with benzyl azide **43** in the presence of CuI yielded the calixarene **44** with both rims modified (Scheme1.13).
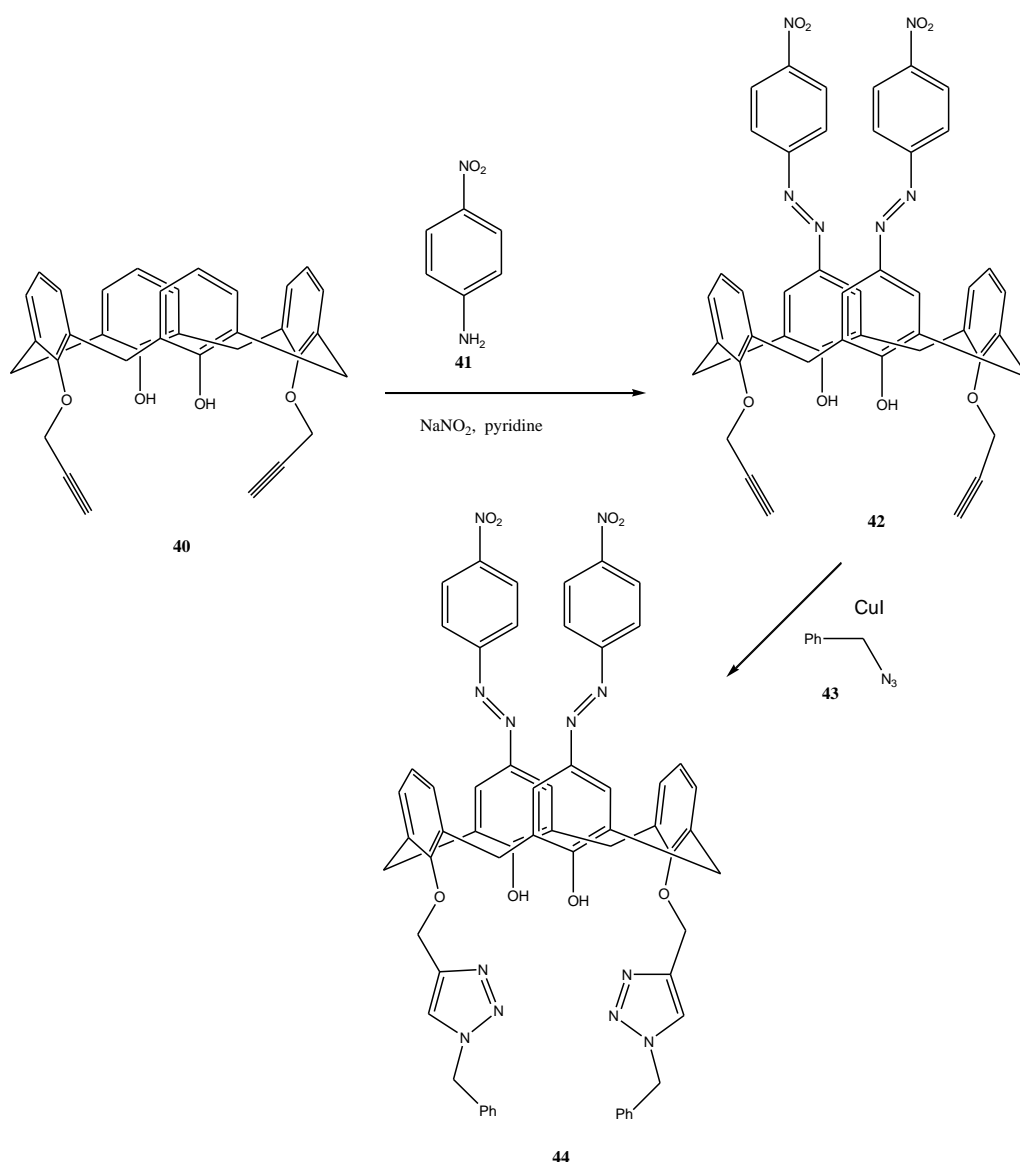
Scheme 1.13. Modification of both rims.

1.3 1,3-Dipolar cycloaddition.

Dipolar cycloaddition reactions are amongst the most important classes of reaction in organic chemistry which can be very attractive for high yielding regio- and stereoselective formation of 5-membered heterocycles.

In a 1,3-dipolar cycloaddition, also known as a Huisgen cycloaddition[33] (Scheme 1.14) a 1,3-dipole and a dipolarophile are united, providing fast access to a variety of five-membered heterocycles, as illustrated in formation of the triazole from reaction of an azide dipole with an alkyne dipolarophile. The dipole is defined by Huisgen as an a-b-c structure (Figure 1.12), with a positive and a negative charge distributed over

three atoms. There are also four π electrons in this structure.[34]
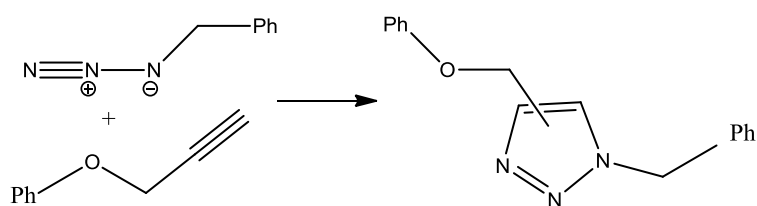
Scheme 1.14. Azide-alkyne Huisgen cycloaddition
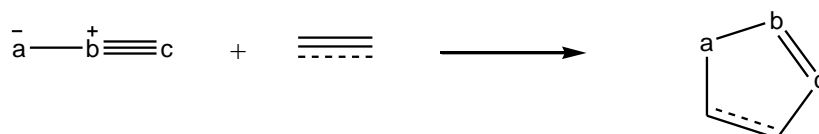
Figure 1.12. Generic 1,3-dipolar cycloaddition.

1,3-Dipolar compounds[35] contain one or more heteroatoms which are described as having at least one mesomeric structure that represents a charged dipole, examples of the most common dipoles are shown below (Figure 1.13).
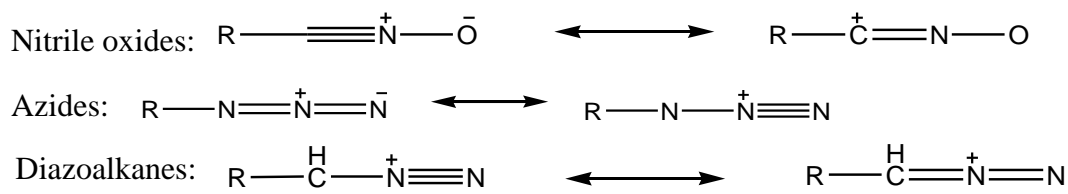
Figure 1.13. Examples of 1,3-dipolar compounds.

1.3.1 Nitrile oxides.

Isoxazoles, accessible from cycloaddition to nitrile oxide dipoles,[36] are amongst the most useful members of the 5-membered heterocycles. In general, nitrile oxides are unstable, therefore, they are often prepared *in situ* and used at once. There are several options for the generation of the dipole and access by way of oxime precursors is an attractive route.

In one example, the oxime **47**, prepared from the starting aldehyde **45,** following halogenation with NCS yielding the hydroximoyl halide **46,** and subsequent dehydrohalogenation, afforded the nitrile oxide **49.**

Alternative routes to these reactive dipoles involve triethylamine-mediated aryl isocyanate-induced dehydration of nitroalkanes **48** – this process is known as the Mukaiyama reaction[37]. Yet another approach involves furoxan thermolysis, *e.g.* furoxan **50,** itself stable under standard laboratory conditions, can be used as a convenient starting material for the generation of short-lived nitrile oxides upon heating at very high temperatures (Scheme 1.15).
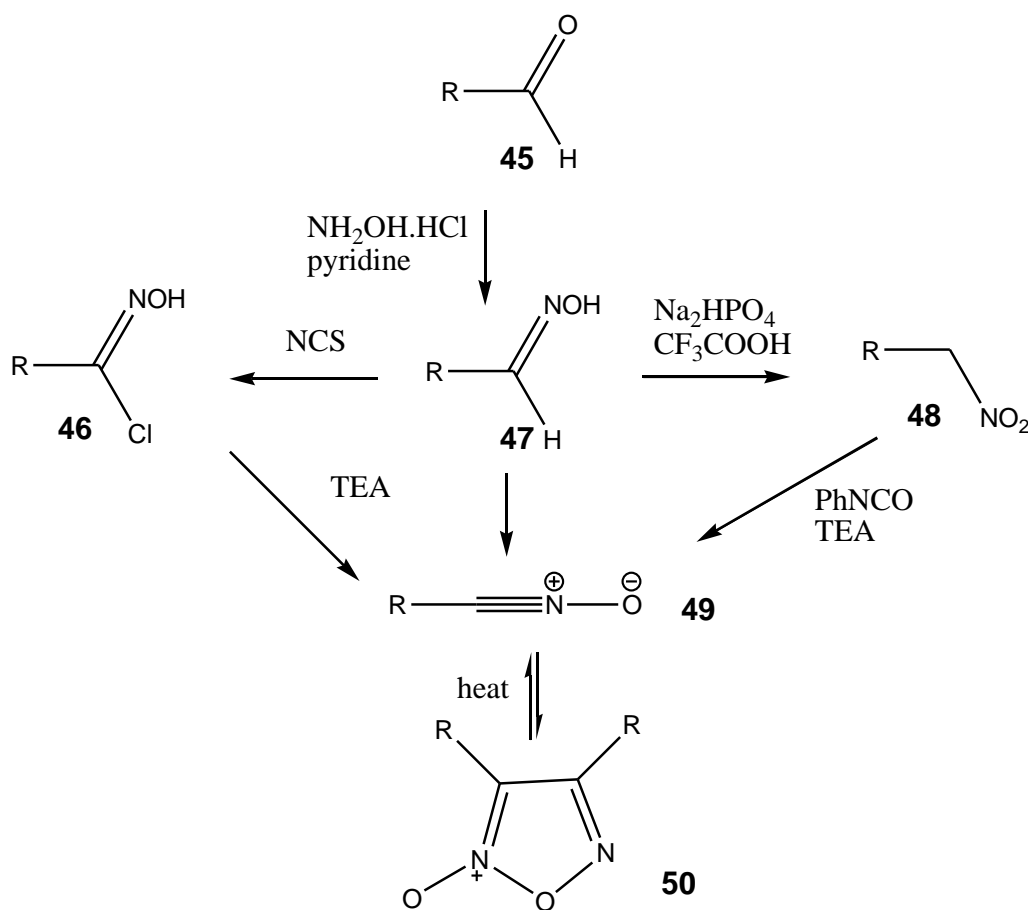
Scheme 1.15. Synthetic routes to nitrile oxides by a variety of possible routes.

Cycloaddition of nitrile oxides with substituted alkynes/alkenes can theoretically lead to 3,4- and 3,5-disubstituted isoxazoles/isoxazolines (Scheme 1.16). The 3,5-substituted isoxazoles are obtained with high regioselectivity in most cases[38].
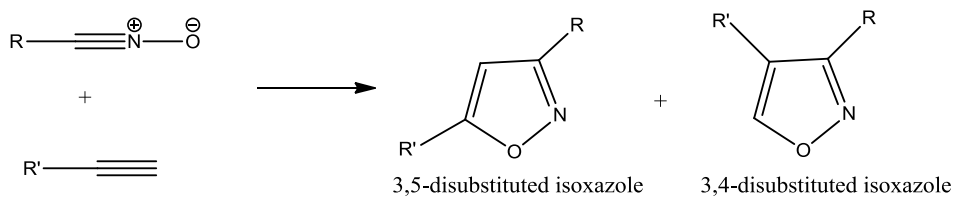
Scheme 1.16. Regioisomeric 3,4- and 3,5-disubstituted isoxazoles from nitrile oxide-alkyne cycloaddition.

1.3.2 Copper-catalyzed azide-alkyne cycloaddition.

The azide alkyne cycloaddition using copper as catalyst at room temperature is one of the most popular reactions in click chemistry. First reported by Meldal and co-workers, this reaction was extensively investigated by Valery V. Fokin and K. Barry Sharpless at the Scripps Research Institute.[33] The latter group recognized the reaction as a reliable catalytic process which offers an excellent level of selectivity and reliability as well as wide substrate scope. While the Cu(I)-catalyzed azide /alkyne reaction, widely referred to as a CuAAC reaction (copper(I)-catalyzed Azide-Alkyne Cycloaddition) leads to a triazole, mechanistically it is not a 1,3-dipolar cycloaddition (Scheme 1.17).
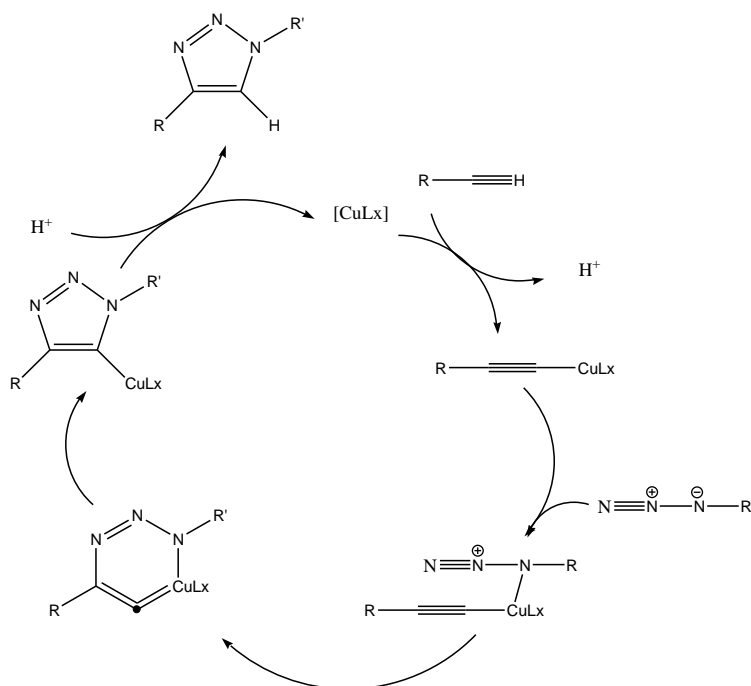
Scheme 1.17. . The proposed mechanism of the Copper-catalyzed azide-alkyne cycloaddition.

One proposed mechanism for the CuAAC reaction is shown in Scheme 1.17. Following π-coordination of the alkyne to Cu(I), the Cu-acetylide intermediate so formed activates the azide to make it more electrophilic. Following formation of the C-N bond, a copper-containing six-membered ring forms which subsequently rearranges to the five-membered triazole. Finally protonation yields the product - the source of the proton is believed to be the hydrogen which was removed from the terminal acetylene at the beginning of the cycle. Regeneration of the catalyst ligand complex allows further reaction cycles.[39]

1.4 Fluorescence spectroscopy[40].

Fluorescence spectroscopy is a type of electromagnetic spectroscopy which analyzes fluorescence from a sample, and can for example, be used to determine the concentration of various neutral or ionic species in solution. It involves using a beam of light, usually ultraviolet light, that excites the electrons in molecules of certain compounds and causes them to emit light. A complementary technique is absorption spectroscopy. The emission spectrum can be interpreted to give both qualitative and quantitative information[40].

Fluorescence is defined as the emission of a photon from an electronic excited state of a molecule at lower energy (longer wavelength) than the wavelength at which the photon was absorbed.[41] The Franck-Condon principle[42] is a rule in spectroscopy and quantum chemistry which describes the intensity of vibronic transitions. It states that when a molecule undergoes an electronic transition, as the nuclear configuration of the molecule exhibits no significant change; the electronic transition occurs faster than the nuclei can respond.[43] The simple diagram shown below describes the absorption by molecules to produce the first excited state, S_1, or the second excited state, S_2 (Figure 1.14).
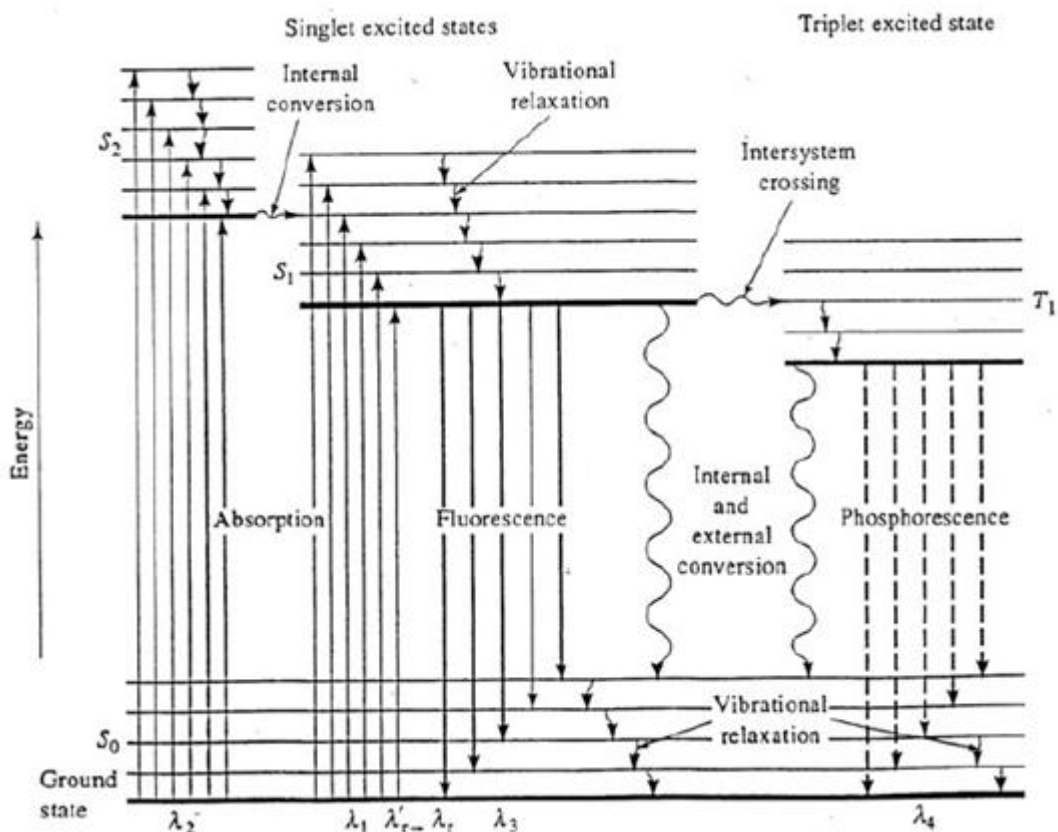
Figure 1.14. Electronic transition energy level diagram[40].

A vertical transition can occur from the lowest vibrational level of the electronic ground state, v''_o (Figure 1.15), to a given vibrational level of the first excited state, $S_1v'_n$. Upon relaxation energy is lost through non-radiative decay to the lowest vibrational energy level of the first excited state, $S_1v'_o$; the transition from energy level $S_1v'_o$ to energy level $S_0v''_n$ results in photon emission (fluorescence), non-radiative decay returns the electron to its lowest vibronic v''_o energy level in the ground state.

The energy of emission is less than that of absorption and therefore occurs at longer wavelength.[40] This difference in wavelength between absorbance and emission is called the Stokes shift (Figure 1.16).
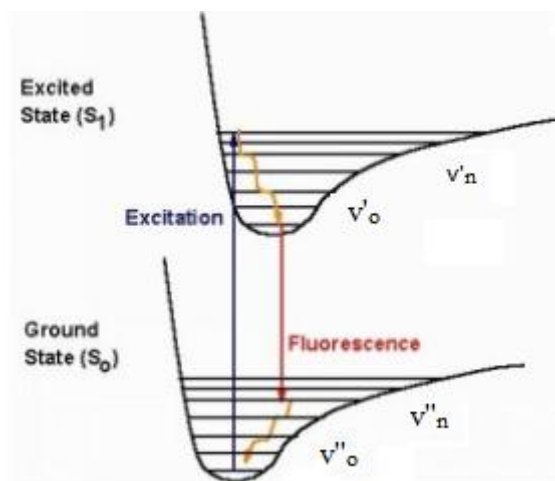
Figure 1.15. The difference in energy between absorption (excitation) and emission in solution[40].
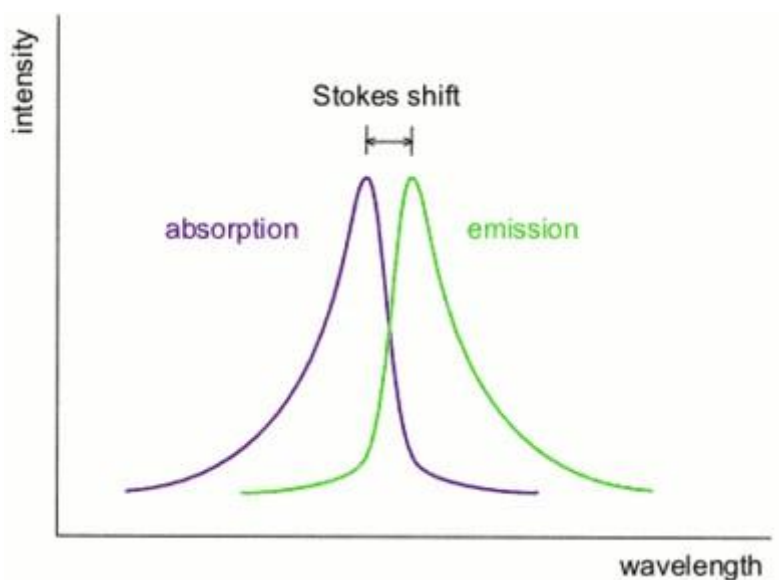
Figure 1.16. The Stokes shift[44].

1.5 Aim of this thesis

The aims of this thesis are as follows:

- To investigate 1,3-dipolar cycloaddition chemistry between nitrile oxides and alkyne-functionalised calixarenes as a route to isoxazole-derivatised calixarenes.

- To characterize the structure of these novel compounds, e.g. **PIC** (**65**).
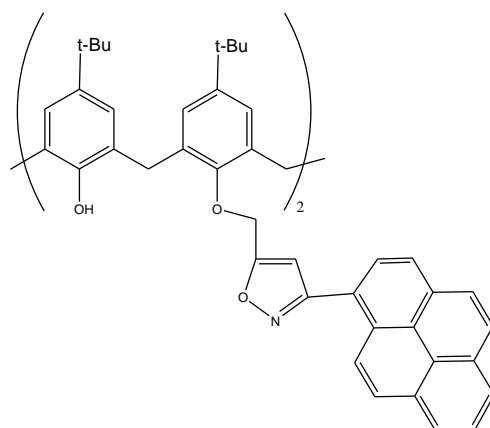
- To use fluorescence spectroscopy and NMR spectroscopy to investigate their potential as selective host molecules for metal cations.

Chapter 2

Result and Discussion

2.1. Overview.

"Click chemistry"[45] is popular nowadays due to its mild reaction conditions, high selectivity, high reaction yield and its potential usage in biological applications. In the literature to date, two novel, triazole-linked, pyrene-armed calix[4]arenes (**76** and **77**) were synthesized using "click" chemistry.[46]
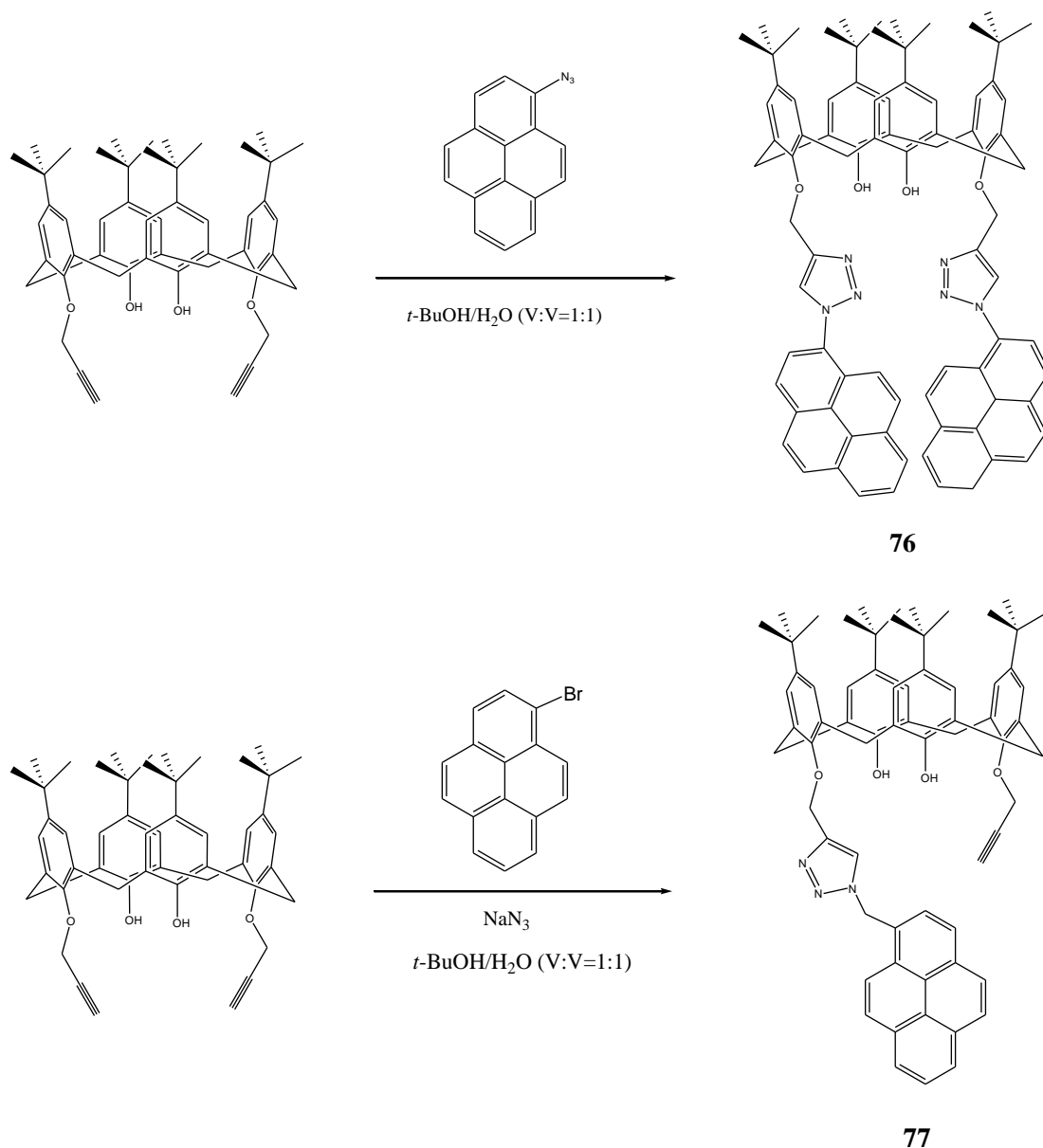
Scheme 2.1. Synthesis of two novel pyrene-armed *t*-butyl-calix[4]arenes (**76** and **77**).

Both **76** and **77** have been synthesized by Azide-Alkyne Cycloaddition[39] in the presence of Cu(I) salts. The azides and terminal alkynes united selectively to afford 1,4-disubstituted regioisomers of 1,2,3-triazoles as sole products (Scheme 2.2).
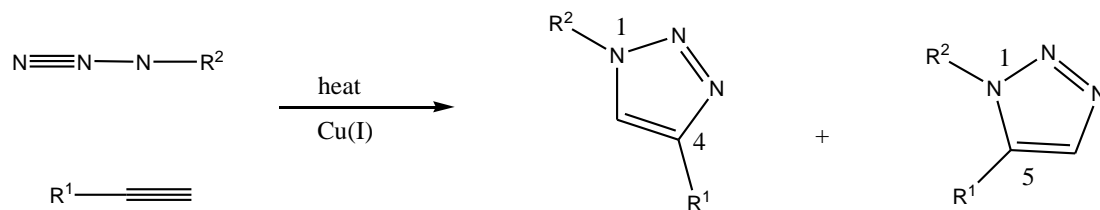
Scheme 2.2. Copper-promoted Azide-Alkyne Cycloaddition[47].

It is reported that compound **76** with two pyrene subunits on the lower rim of the *t*-butyl-calix[4]arene shows ratiometric fluorescence response to Zn^{2+}, and selective fluorescence quenching toward heavy metals like Hg^{2+}, Cu^{2+} and Pb^{2+}, while compound **77** with one pyrene subunit shows significant fluorescence quenching upon the addition of Cu^{2+} and slight quenching behavior toward Hg^{2+}. In its fluorescence spectrum, compound **76** displays weak monomer emission at 378 nm and strong excimer emission at 482 nm when excited at 343 nm in CH_3CN solution. In contrast **77** exhibits only monomer emission at 380 and 398 nm (Scheme 2.1)[46].

In this research I set out to study isoxazole analogs of compounds **65.** Since isoxazoles have unique coordinating properties and isoxazole preparation could be envisioned free from copper ions, which might be treated as guest species, we believed such molecules have potential to be effective chemosensors. The first part of this results chapter discusses synthesis of the new compounds, of general structure R-Isoxazole-Calix[4]arene (Figure 2.1). Introduction of R-isoxazole to the lower-rim of *t*-butyl-calix[4]arene was achieved by nitrile oxide alkyne cycloaddition chemistry.

	62	63	64	65	66
R =					
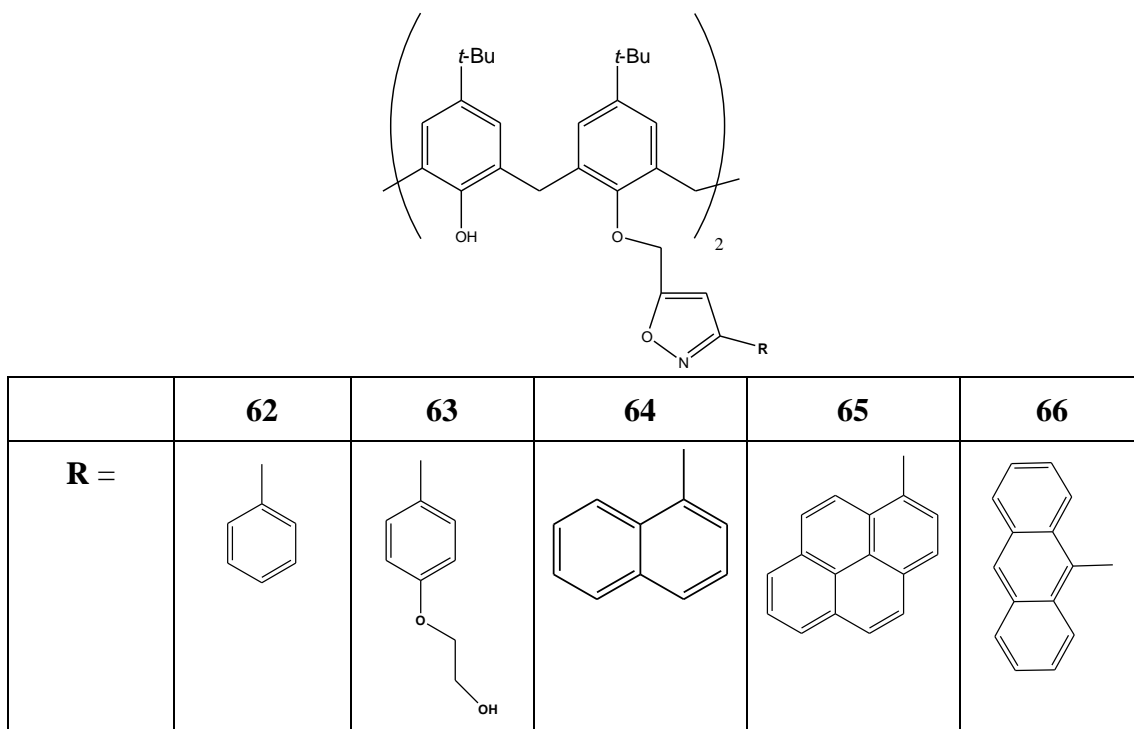
Figure 2.1. Structures of the R-Isoxazole-Calix[4]arenes **62-66** prepared in this research.

Isoxazole-modified calixarenes were accessed by 1,3-dipolar cycloaddition between a suitable nitrile oxide and alkyne. Chloramine-T (Figure 2.2), also known as the sodium salt of tosylchloramide or *N*-chlorotosylamide, sodium salt, was selected as the reagent for generation of nitrile oxides from oximes. This *N*-chlorinated and *N*-deprotonated sulfonamide is also used as a mild disinfectant and a biocide. It is a white powder which is unstable in water. Aqueous solutions are slightly basic, pH is 8.5. The molecule has an electrophilic chlorine atom and when it breaks down in water it yields the hypochlorite ion. It can be used as a source of electrophilic chlorine in organic synthesis.
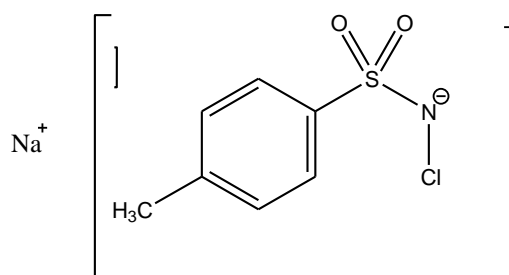
Figure 2.2. The structure of chloramine-T.

The initial oxime targeted was **56** which was prepared according to the method described by an earlier worker in the group, Dr. Colin Freeman.[48] In the former study *o-, m-* and *p*-hydroxethoxybenzaldehyde oximes (**54-56**) were found to undergo regioselective isoxazole formation following cycloaddition between the transient dipole and phenyl propargyl ether (Scheme 2.3). Thermal cycloaddition reactions of nitrile oxides with alkynes are often selective for the formation of the 3,5-disubstituted isomer[49] and in this chloramine-T-induced protocol the cycloadditions were found to be highly selective for the 3,5-disubstituted isomer. The regiochemical assignment of the major isomer, 5-substituted isomer, was determined from the resonance position of isoxazole ring proton in ^{1}H NMR spectrum which presented as a singlet in the range 6.59-6.76 ppm.[48] This signal represents the isoxazole H-4 proton while the C-5 position proton would be expected to appear further downfield, in the range of 7.50-8.50 ppm.

o- = **54**; *m-* = **55**; *p-* = **56**.

3,5-disubstituted isomer   3,4-disubstituted isomer

R^1 = -O-CH$_2$-CH$_2$-OH, R^2 = -CH$_2$-O-Ph.
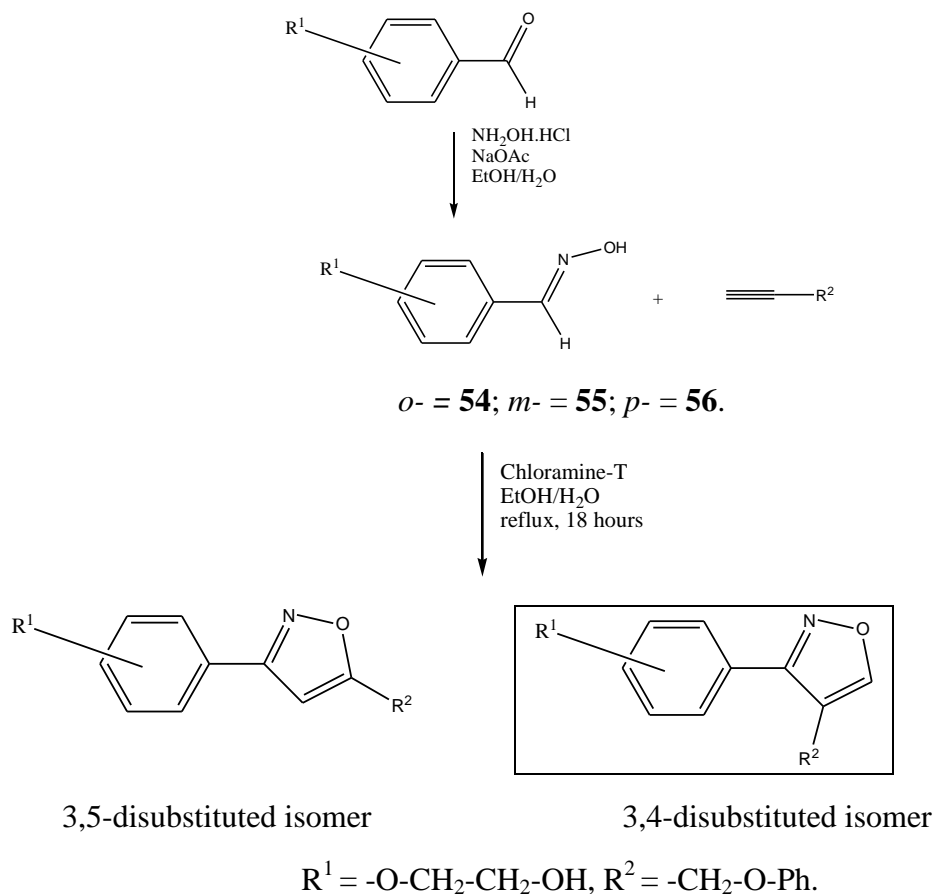
Scheme 2.3. Regioselective nitrile oxide alkyne cycloaddition.

The mechanism of nitrile oxide alkyne cycloaddition is shown below (Scheme 2.4).
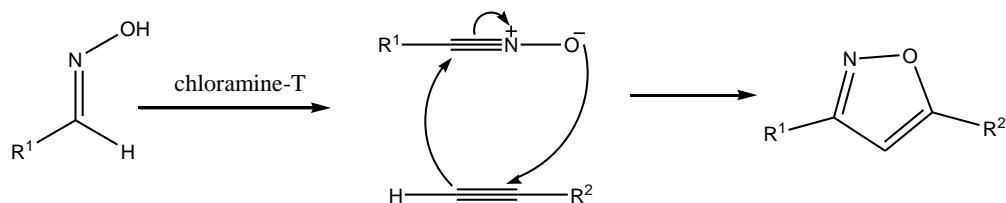
Scheme 2.4. The mechanism of cycloaddition reaction.

The consideration of the energy separations of HOMOs (Highest Occupied Molecular Orbitals) and LUMOs (Lowest Unoccupied Molecular Orbitals) leads to three reactivity types in these cycloadditions.[12] For the Diels-Alder addition and 1,3-dipolar cycloaddition the possible occurrence are classified in three types:

● Type 1. LUMO (olefin) controlled reactions.

The dipole contains a high HOMO which overlaps with the LUMO in the dipolarophile. This kind of dipole is referred to as a nucleophilic dipole or HOMO-controlled dipole. The dipoles add to electrophilic alkenes readily. Electron-withdrawing groups (EWG) on the dipolarophile would expedite the reaction by lowering the LUMO, while electron-donating groups (EDG) would decrease the reaction progress by raising the HOMO.[50]

● Type 2. LUMO (Diene or Dipole) controlled additions

HOMO of the dipole pairs with LUMO of the dipolarophile or HOMO of the dipolarophile pairs with LUMO of the dipole. This two-way interaction undergoes as the energy gap in either direction is very similar. A dipole of this class is referred to as an ambiphilic dipole or a HOMO-LUMO-controlled dipole, which includes nitrile imine, nitrone, nitrile oxide, carbonyl oxide, and azide. Any of these substituents on the dipolarophile would expedite the reaction by lowering the energy gap between the two interacting orbitals.[50]

● Type 3. LUMO-controlled dipole (an electrophilic dipole)

This kind of dipole has a low LOMO which overlaps with the HOMO of the dipolarophile. This kind of dipole is referred as an electrophilic dipole or a LUMO-controlled dipole, which includes ozone and nitrous oxide. EWGs on the

dipolarophile decelerate the reaction, while EDGs accelerate the reaction.[50]

2.2. Synthesis of oximes.

The synthesis of oximes from precursor carbonyl compounds is well reported.[48] Typical reaction conditions using hydroxylamine hydrochloride in the presence of sodium acetate were employed to make the oximes targeted for study during this research (Figure 2.3).
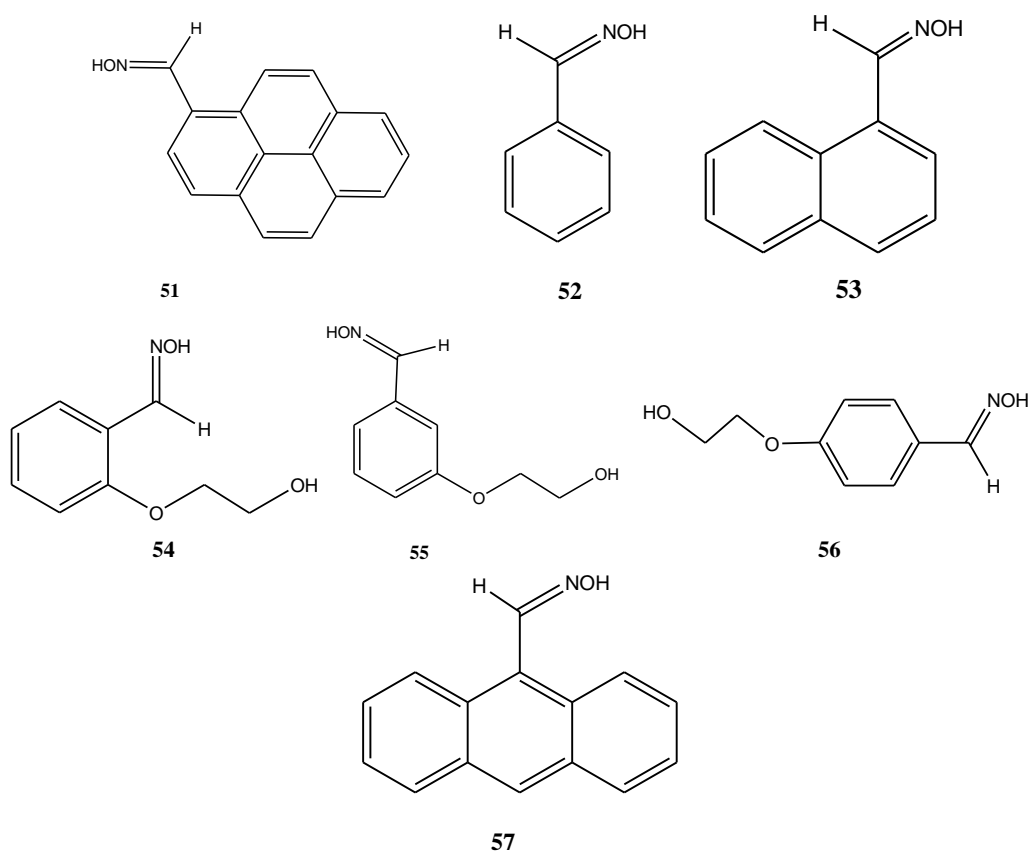
Figure 2.3. The structures of oximes (**51-57**) used in this thesis.

Typically the reaction mixtures were heated at reflux for 1 hour to afford the product in excellent yield (80-96%). The general reaction of oxime formation is shown in (Equation 2.1) and the accepted mechanism is illustrated (Scheme 2.5).[51]
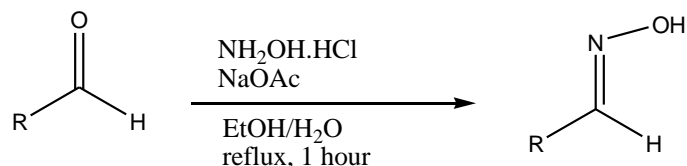
Equation 2.1. Formation of oximes from carbonyl precursors
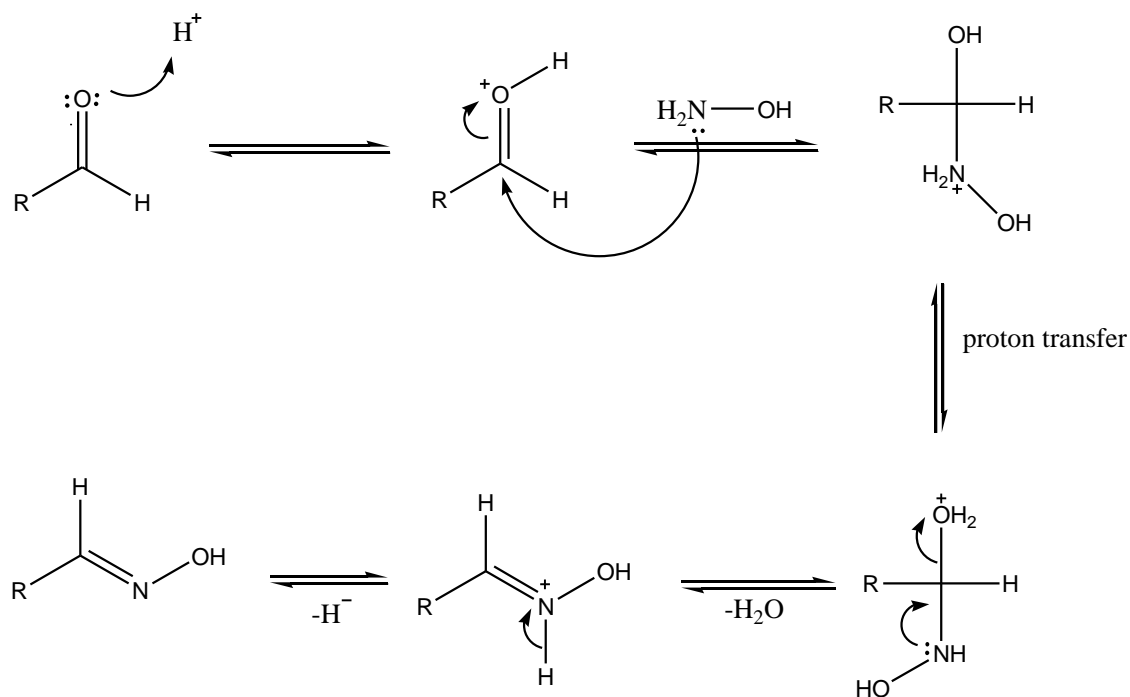
Scheme 2.5: Mechanism of oxime formation.

2.3. Synthesis of model compound **59**

Before experimenting with propargylated calix[4]arenes reactivity was explored with 1-*t*-butyl-4-(prop-2-ynyloxy)benzene **59** as a model compound. The desired alkyne **59** was prepared by the treatment of propargyl bromide and 4-*t*-butylphenol in the presence of K_2CO_3 at room temperature over two nights. The product was obtained as a pale yellow oil (86% yield). The synthesis route is shown below (Equation 2.1)[52].
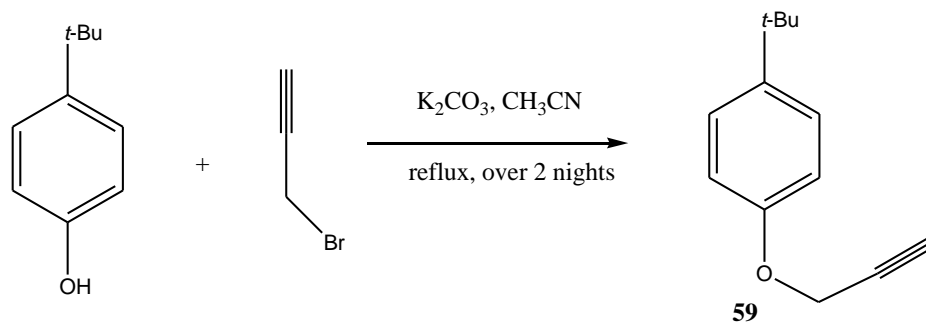
Equation 2.1. Synthesis of the model alkyne, 1-*t*-butyl-4-(prop-2-ynyloxy)benzene
(**62**).

2.4. The model reactions

2.4.1. Synthesis and characterization of **60.**

With the required oximes and the model alkyne, **59**, the initial reaction was explored with the 9-anthracene carbaldehyde oxime **57** (0.5 eq. to **59**) in the presence of chloramine-T (1.0 eq. to **57**) in aqueous ethanol. The reactants were heated at reflux for 6 hours. The equation is shown below (Equation 2.2).
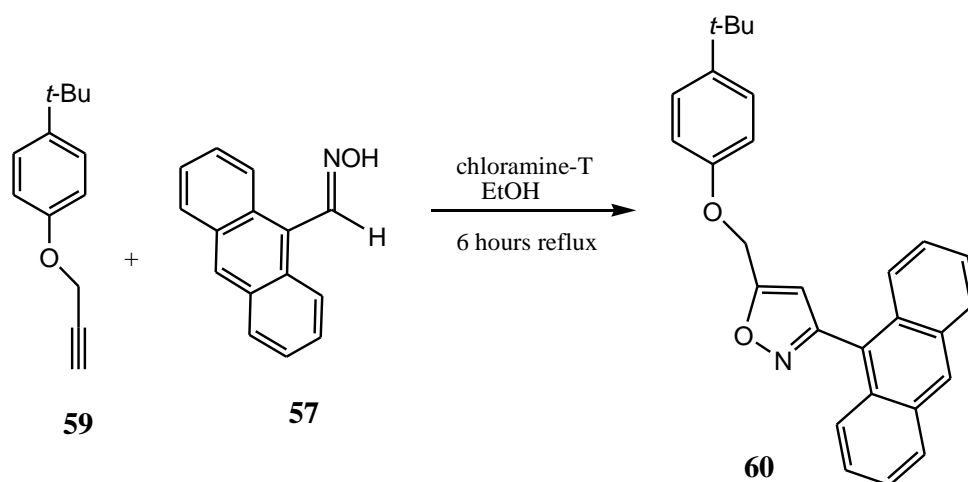
Equation 2.2. The model cycloaddition reaction of 9-anthracene carbaldehyde oxime
57 and **59.**

The ^{1}H NMR spectrum of the crude reaction products, shown in Figure 2.4, displays a singlet signal at ~6.58 ppm, typical of a 3,5-disubstituted isoxazole. There was no compelling evidence for the presence of the alternative 3,4-disubstituted regioisomer. This is in keeping with the expected regioselectivity of the nitrile oxide

cycloaddition[49]. The signal of OCH$_2$ protons of the product presented as a singlet at 5.38 ppm and that of the starting alkyne at 4.66 ppm. The crude product was purified by flash column chromatography (SiO$_2$, DCM:Petroleum ether, 1:2). The pure product was obtained as a yellow gum in excellent yield, 98%. ^{1}H NMR spectrum of the pure product (containing a slight trace of CH$_2$Cl$_2$) is shown in Figure 2.5.
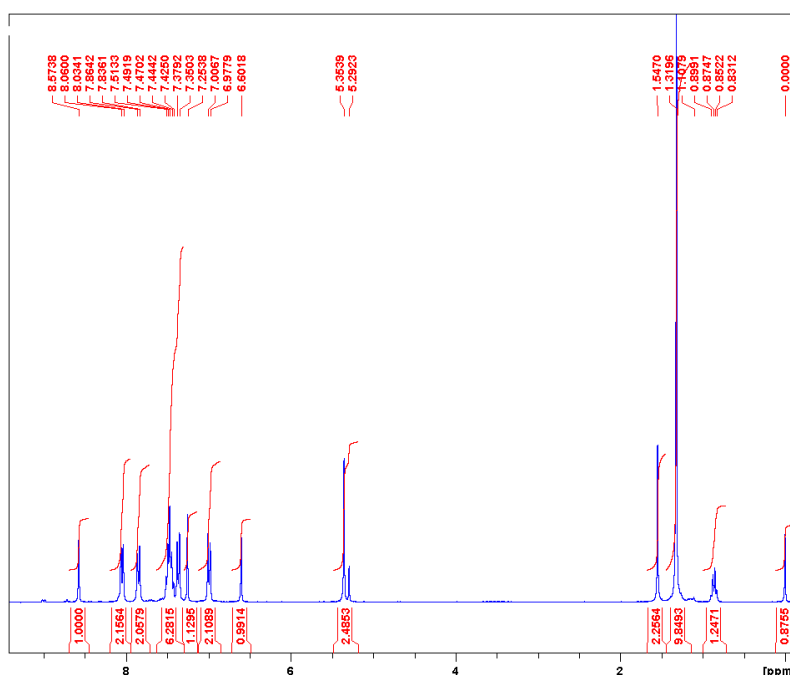
Figure 2.4. The ^{1}H NMR (300 MHz, CDCl$_3$) of **Crude** product **60.**
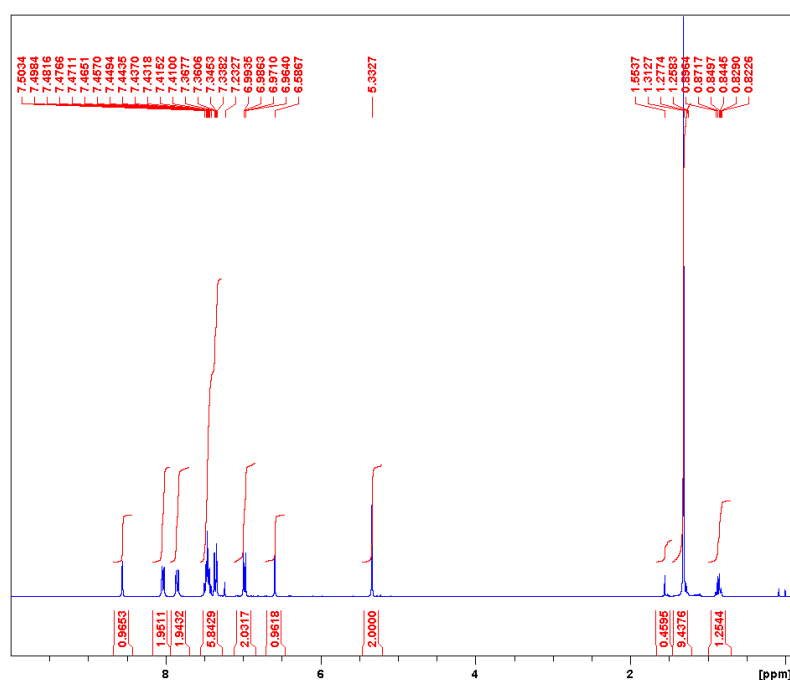
Figure 2.5. ^{1}H NMR (300 MHz, CDCl$_3$) of the **pure** product **60**.

2.4.2. Synthesis and characterization of **62**.

With the success of the cycloaddition to the model alkyne to hand the next significant goal was to experiment with nitrile-oxide based functionalization of a dipropargylated calixarene. Pyrene- and anthracene- appended calixarene molecules were the main compounds of interest for fluorsecence-based chemosensing applications; however, the large size of these rings suggested initial ground work should involve more *compact* nitrile oxides. Thus, the nitrile oxide generated from benzaldehyde oxime was the first dipole studied with the bis-propargyl calix[4]arene. The reactants were combined as follows: propargylated calix[4]arene (1 eq.) and benzaldehyde oxime (3 eq.) were mixed at reflux (solvent EtOH) in the presence of chloramine-T (4 eq.) for 6 hours (Equation 2.3). The product was purified by flash column chromatography (SiO$_2$, DCM:MeOH = 100:1) to afford the product in 44% yield. The ^{1}H NMR spectrum (Figure 2.6) shows the product contains a little impurity. Product formation was confirmed by the characteristic resonance of the OCH$_2$ protons. The OCH$_2$ protons present at 4.68 ppm in starting material bis-propargylcalix[4]arene whereas they present at 5.20 ppm in the product **62**. Despite the trace impurities, the formation of **62** has been a sufficiently successful model reaction to encourage the quest to form pyrene and anthracene analogues by the same synthetic route.
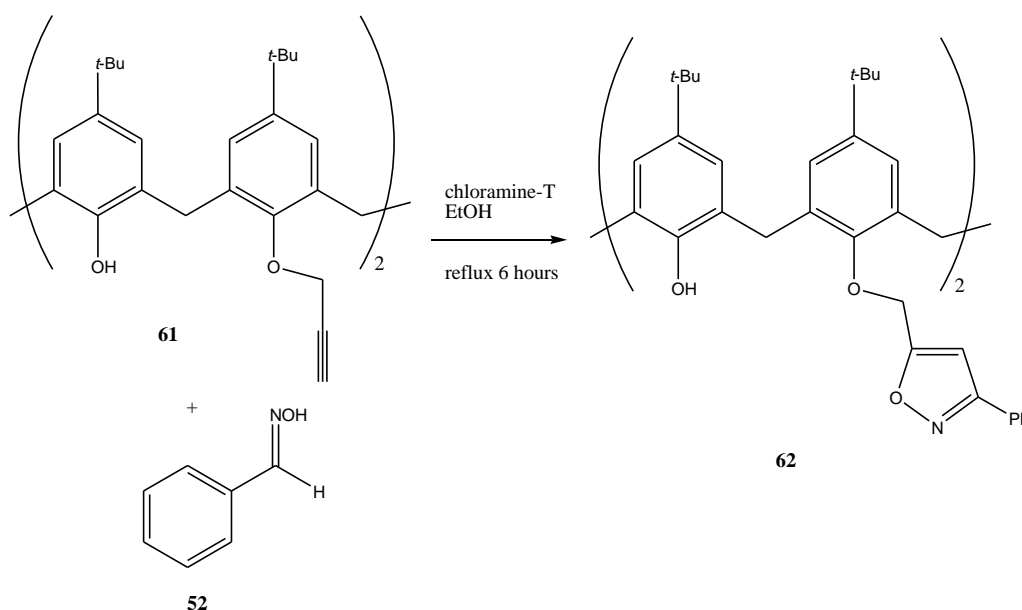
Equation 2.3. The model cycloaddition reaction leading to **62**.
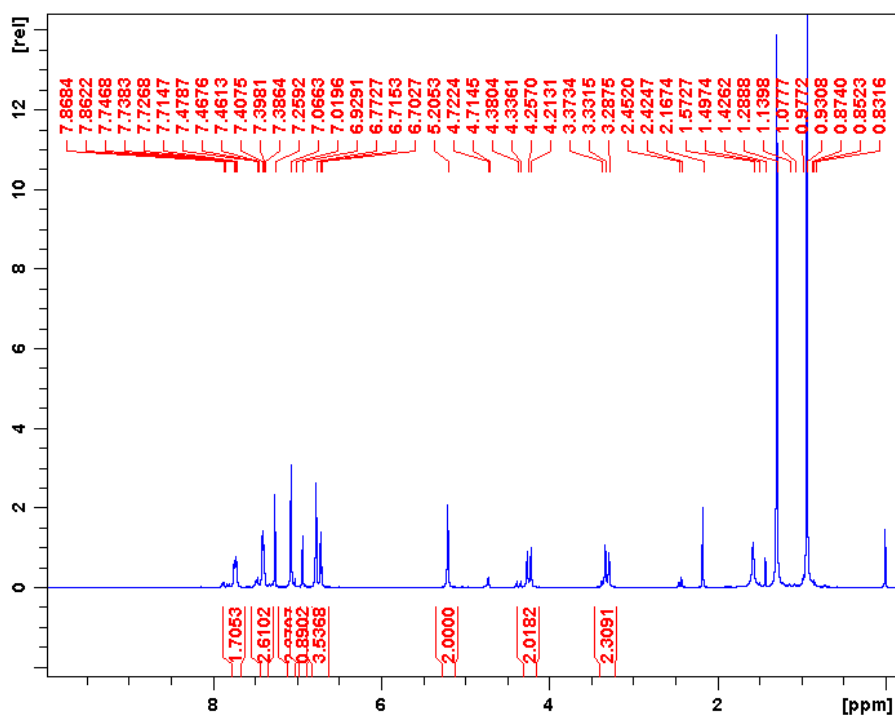
Figure 2.6. ^{1}H NMR (300 MHz, CDCl$_3$) of purified **62**.

2.4.3. Synthesis and characterization of **63**.

Prior to experimenting with the large aryl oximes, the potential to introduce additional functionality to modified calixarene frameworks was explored by reaction between 4-(2-hydroxyethoxy)benzaldehyde oxime **56**, which is a larger structure than **52**, and the propargylated calixarene A (**61**) reaction of 2-(5-*t*-butyl-3-ethyl-2-(prop-2-ynyloxy)benzyl)-4-*tert*-butyl-6-methylphenol(*t*-butylcalix[4]arene–alkyne) with **56** was set up under conditions parallel to that studied with benzaldehyde oxime (Equation 2.4). However, after 6 hours reaction time, product formation, as judged from the relative integrals of the signals representing the OCH$_2$ protons of the starting material and cycloadduct in the ^{1}H NMR spectrum, had progressed only to about 20% completion. The signal of OCH$_2$ in the propargylated calix[4]arene (starting material) appears at 4.70 ppm while it appears at 5.20 ppm in the desired product. Thus, the reaction was repeated and heating allowed continuing overnight. The extended duration increased the extent of reaction and following purification by column chromatography (SiO$_2$, EtOAc:hexane:methanol = 7:12:1) product was obtained in ~45% yield.
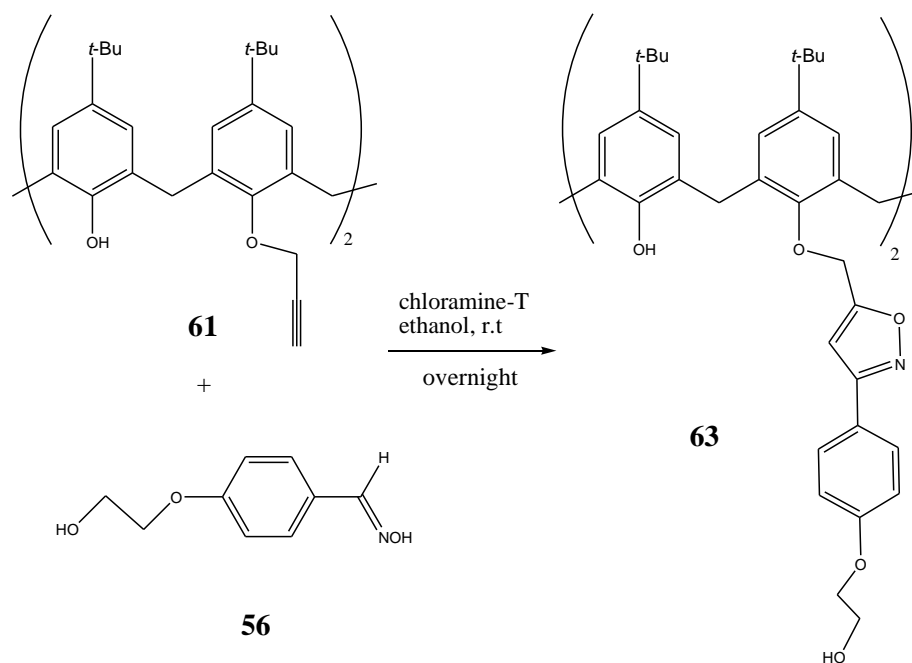
Equation 2.4. Synthesis of compound **63**.
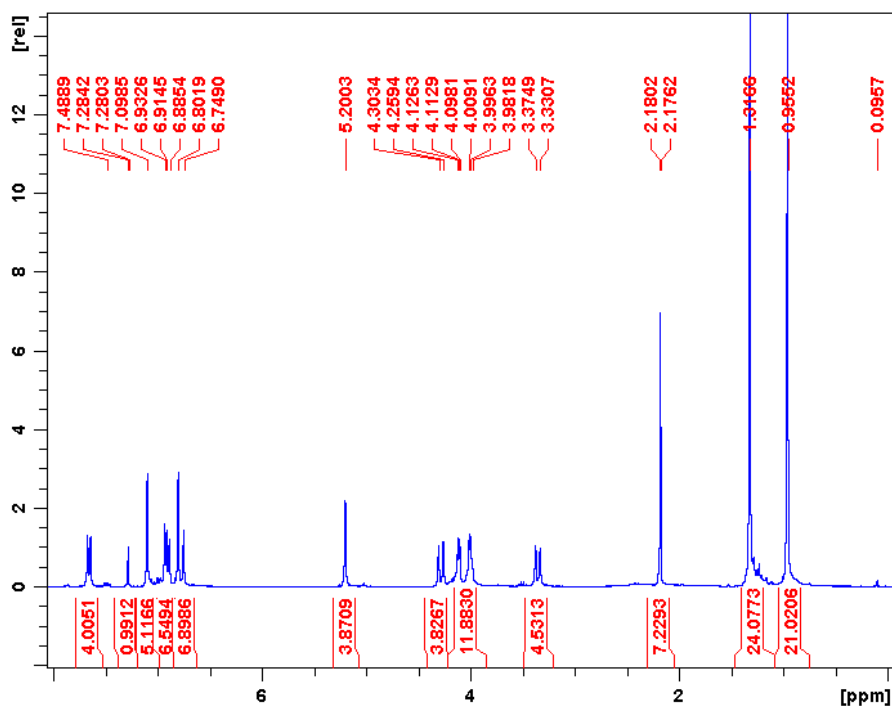
Figure 2.7. ^{1}H NMR (300 MHz, CDCl$_3$) of purified **63**.

2.4.4. Synthesis and characterization of **64.**

Reaction of the propargylated calix[4]arene with 1-naphthaldehyde oxime **53** was studied as a model reaction for a *larger* aromatic nitrile oxide (Equation 2.5). Following a protocol parallel to that described above[50], the product was furnished in a

poor yield (around 15%) after 6 hours reaction time as judged by the relative integration of the OCH$_2$ protons which present as a singlet at 4.68 ppm in the starting material and at 5.20 ppm in the desired product. However, after overnight (15 hours) heating of the reaction mixture, and following purification by column chromatography (SiO$_2$, DCM:hexane, 85:15), the product was obtained in 43% yield. The ^{1}H NMR spectrum of **64** is shown below (Figure 2.8).
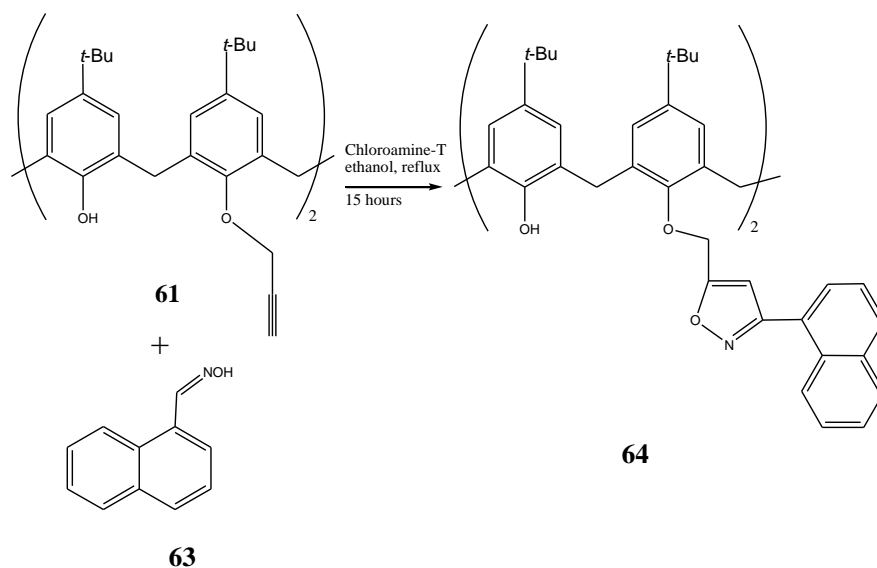
Equation 2.5. The synthesis of model compound **64.**
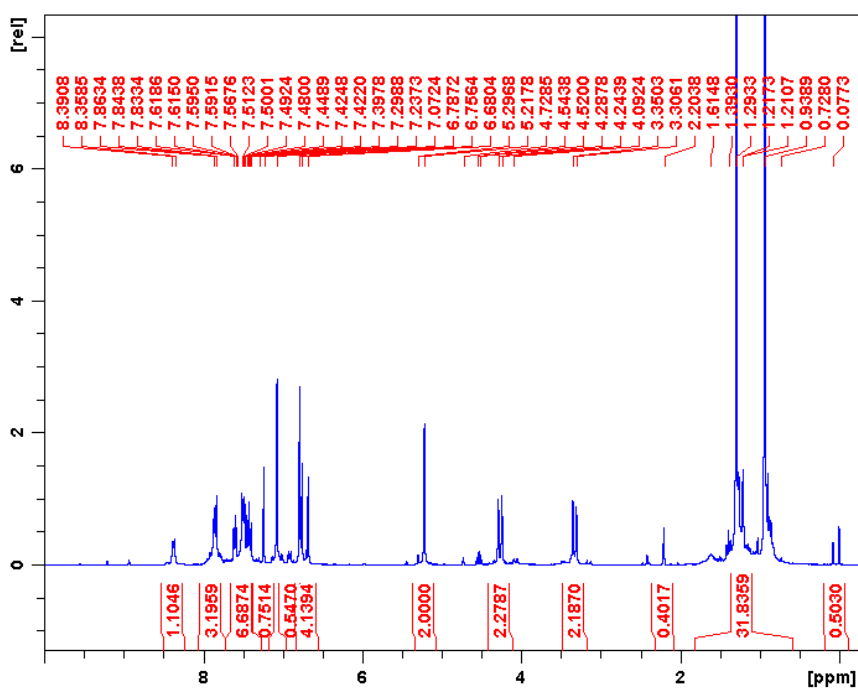
Figure 2.8. The ^{1}H NMR (300 MHz, CDCl$_3$) spectrum of purified **64**.

2.5. Synthesis and characterization of goal compound 65.

With a number of successful model reactions to hand, cycloadditions of propargylated *t*-butyl-calix[4]arenes with 1-pyrenecarbaldehyde oxime and 9-anthraldehyde oxime were attempted. Formation of the **p**yrene-**i**soxazole-**c**alix[4]arene **65** (herein after known as **PIC**) and the anthracene-isoxazole-**c**alix[4]arene **66** (herein after known as **AIC**) were key synthetic goals. The syntheses of **PIC** and **AIC** are shown below (Figure 2.9).
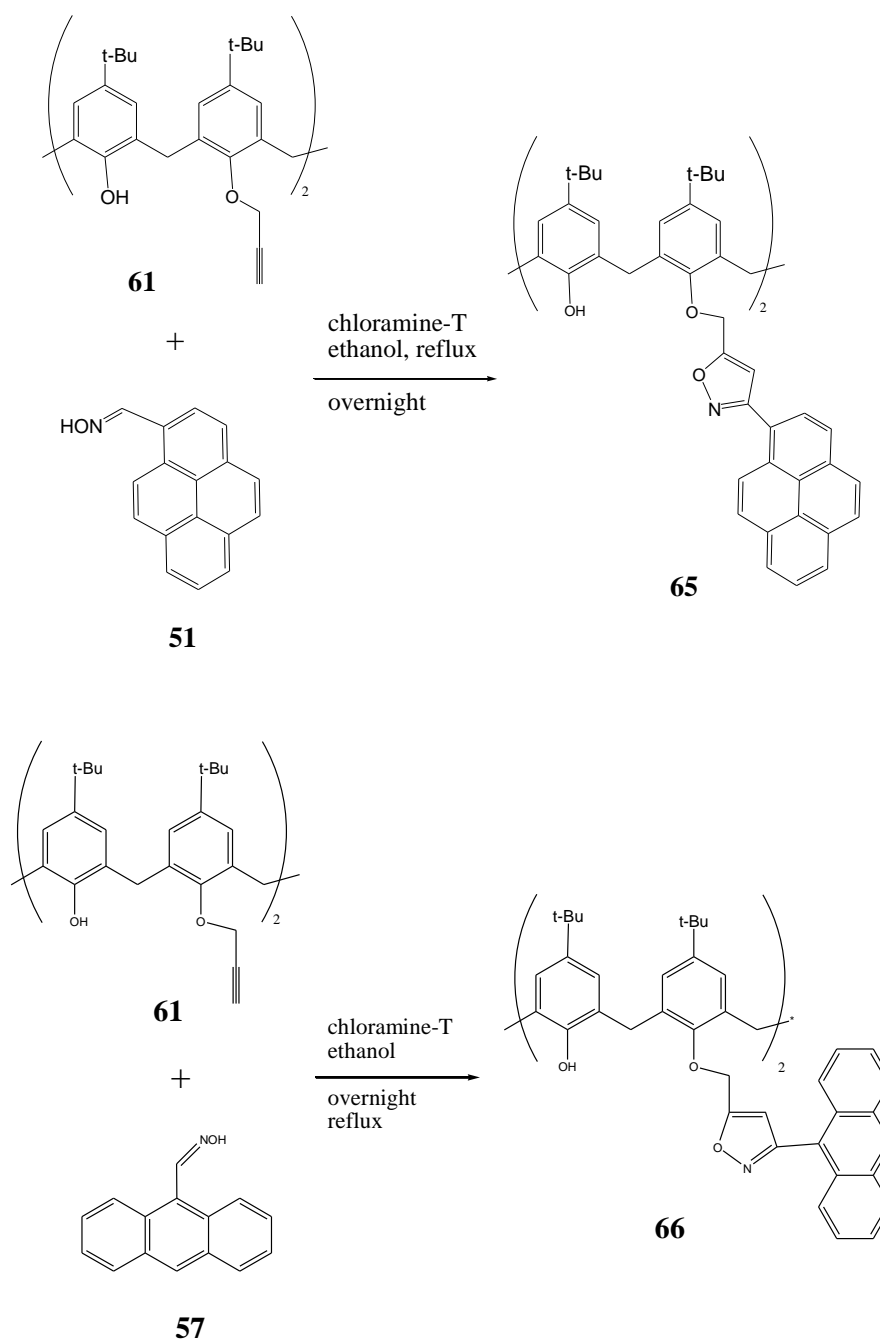
Figure 2.9. The synthesis routes to **65** and **66**.

The attempted cycloaddition route to **PIC** was studied as above, initially the reaction was allowed to proceed for six-hours and the ^{1}H NMR of the product is shown below (Figure 3.10), again progress of the reaction was determined following analysis of the O-CH$_2$ proton resonance signals. The starting material, *t*-buytlcalix[4]arene–alkyne, exhibits a singlet at 4.68 ppm with the analogous product signals present, also as a singlet, at 5.28 ppm in the product. For the six-hour-reaction crude, the starting material is approximately one-fourth of the desired product. Attempted purification by flash column chromatography (SiO$_2$, DCM: petroleum ether, 1:2) was only partially successful: the desired product was obtained in ~30% yield. The ^{1}H NMR spectra of the crude sample following six-hour reaction and purified product are shown below (Figure 2.10 and 2.11). The experiment was considered unsatisfactory because of the poor yield and the mediocre quality of the material after chromatography.
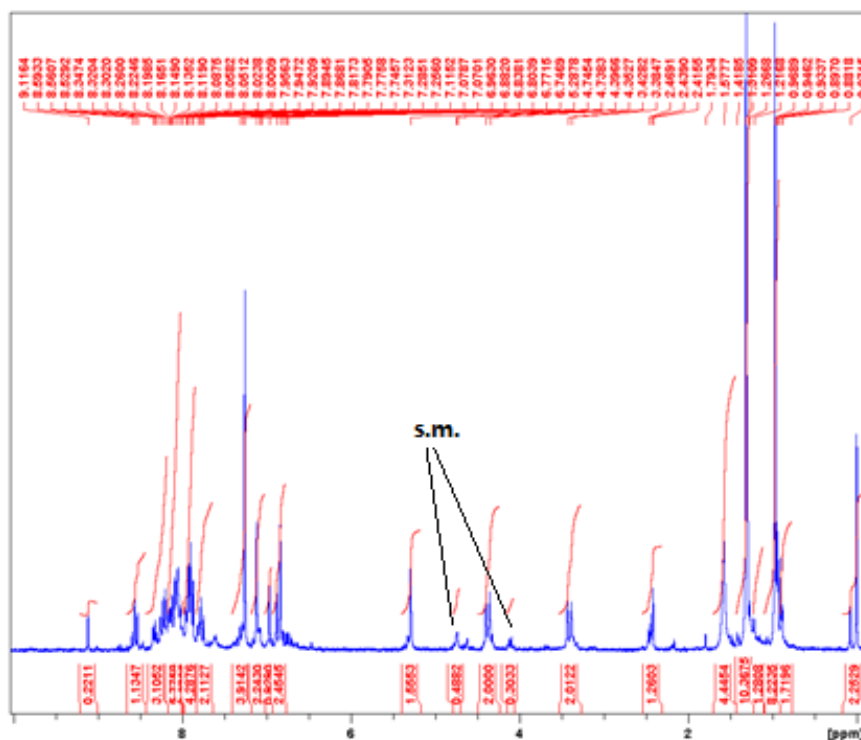
Figure 2.10.The ^{1}H NMR (300 MHz, CDCl$_3$) of crude **65** (6 hours reaction time).
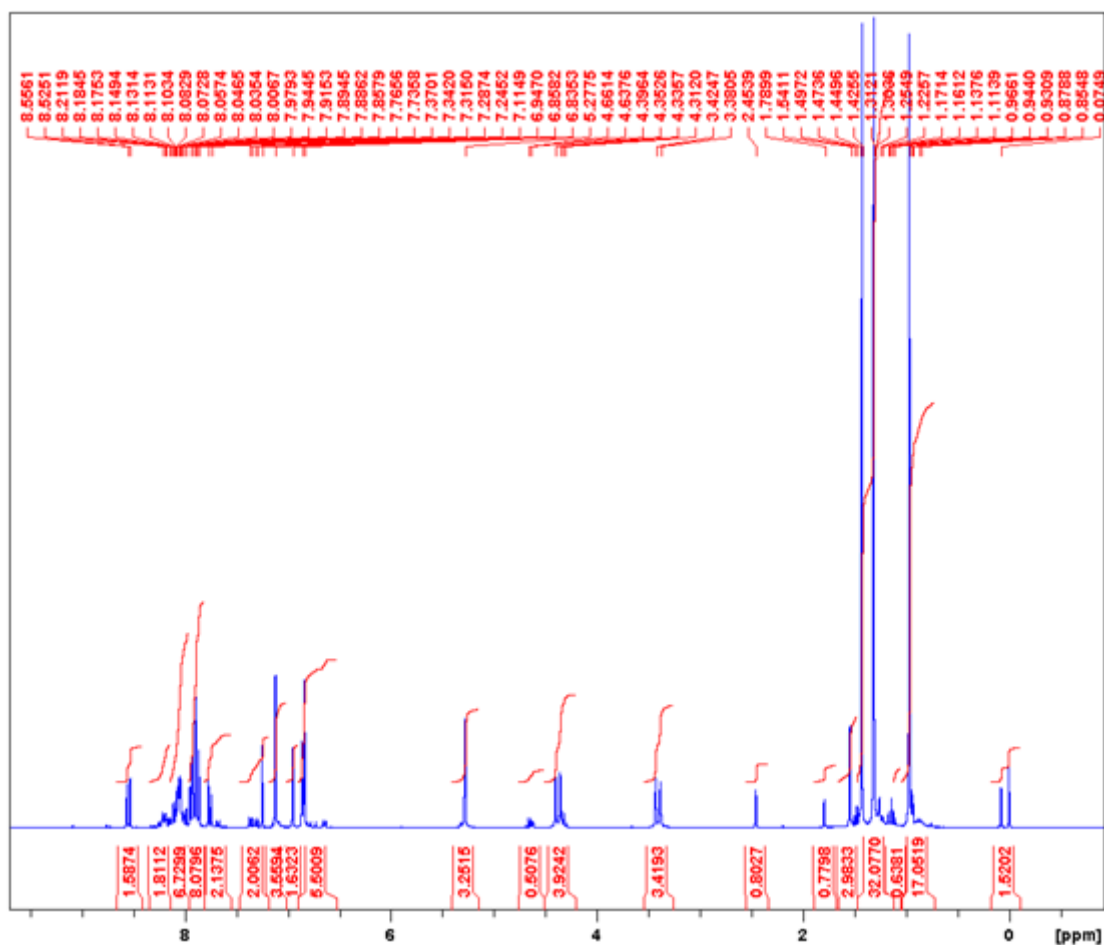
Figure 2.11. The ^{1}H NMR (300 MHz, CDCl$_3$) of purified **65**

To improve yield, and facilitate product purification, the reaction was repeated extending the reaction time from 6 to 18 hours. After this interval analysis of the crude products by ^{1}H NMR spectroscopy suggested the reaction was significantly more successful, data shown in Figure 2.12. After purification by column chromatography, the product was allowed to slowly crystalize from DCM and petroleum ether (1:5) over 2 days. The crystals were collected and analyzed. The ^{1}H NMR of crystals is shown in Figure 2.13.: it indicated the product was obtained highly pure.

The preparation of **AIC** was achieved in an analogous fashion. Details of the experimental approach are included in that section and the full structural analysis of this molecule is detailed in the appendix as a representation of the interpretative skills of the author.
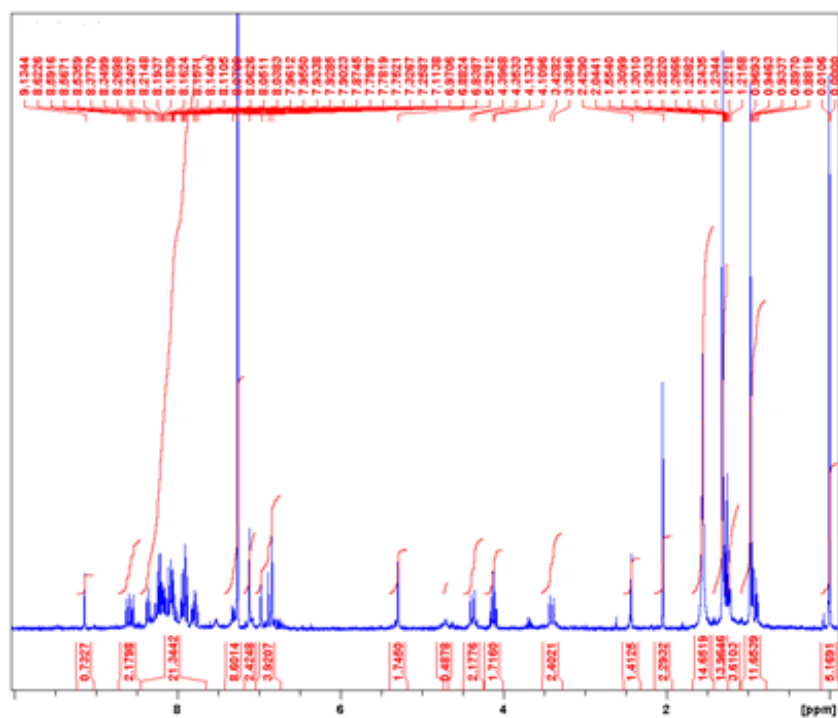
Figure 2.12. The ^{1}H NMR (300 MHz, CDCl$_3$) of crude **65 (**18 hours reaction time).
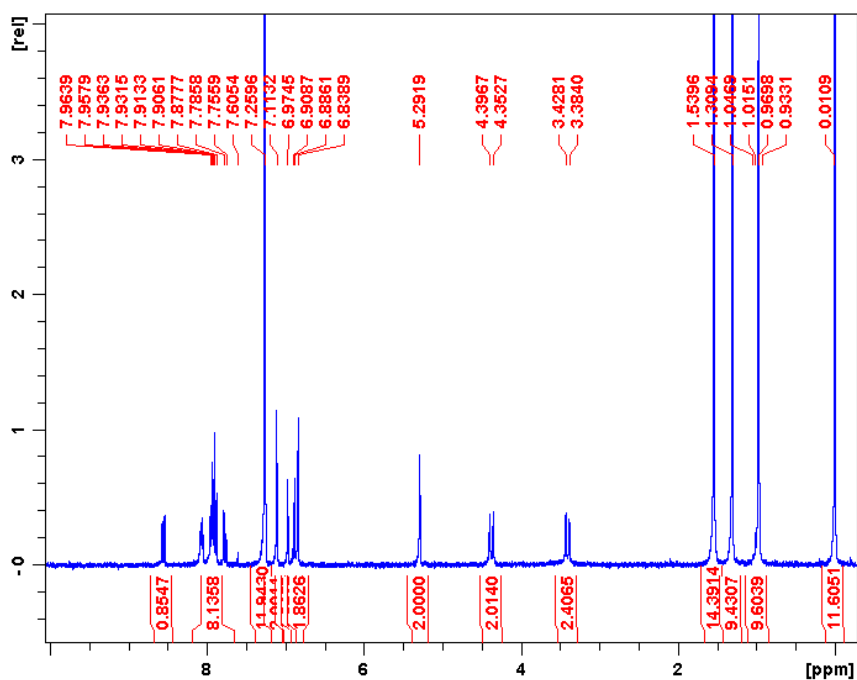
Figure 2.13. The ^{1}H NMR (300 MHz, CDCl$_3$) of crystallised **65 - PIC**.

In collaboration with Dr. John Gallagher of Dublin City University, the structure of **PIC** was unambiguously confirmed by a single crystal X-Ray structure

49

determination. Two views of the structure are shown in Figure 2.14. The pyrene rings are not parallel as expected. So it caused a big fluorescent change while some metal ions were added which will be talked in the next part.[53] However, the packing of **PIC** molecules can been seen to be dominated by a parallel alignment of the pyrene rings from neighboring **PIC** as shown in Figure 2.15.
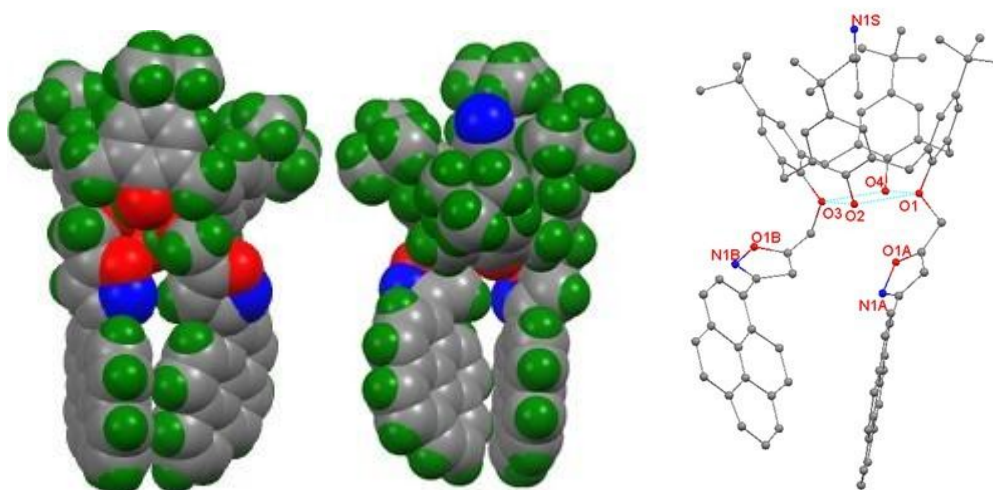
Figure 2.14. The crystal structure of **PIC.**
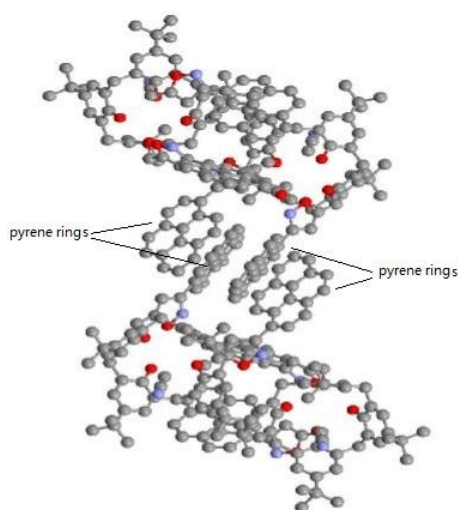
Figure 2.15. The X-ray structure determined for **65**

2.6. Fluorescence study.

    2.6.1. Overview.

In the past decade, the synthesis of new ligands for the simultaneous

complexation of cationic and anionic species has been reported. Because they are significant heavy-ion pollutants there is great interest in the development of fluorescent chemosensors for detection of Cu^{2+} and Hg^{2+} ions. Sensing Cu^{2+} is also important because whilst it is an essential trace element in biological systems, it is toxic at certain levels and its accumulation in the human body may cause the hepatic cirrhosis even at submicromolar concentrations.[54] Generally speaking, the sensing of metal ions with selective analytical reagents is a challenge for biological and environmental applications.

Most calix[4]arene-based fluorescent sensors for metal ions are designed based on photophysical changes that occur following ion binding, for example, photoinduced electron transfer (PET),[55] excimer/exciplex formation[56] and metal-to-ligand charge transfer processes (MLCT).[57] Excimer emission has been frequently reported with bis-fluorophore-substituted chemosensors which change conformation upon binding metal ion guests. Typical chemical sensors comprise two distinct components, a reporter unit (e.g. a fluorophore) and an ionophore. Pyrene moieties are widely used as fluorogenic units due to their relatively efficient excimer formation and emission.[58] A pyrene-appended triazole-ligated calix[4]arene has been reported for the detection of Cd^{2+} and Zn^{2+}. The detection of metal ions was monitored by changes in fluorescence spectra[59] (Figure 2.17).

Host-guest chemistry[60] can be considered a subset of supramolecular chemistry, it studies and attempts to explain complex formation between two, or more, molecules or ions that are held together by unique structural relationships, it attempts to explain molecular recognition.

Upon excitation, pyrene units can respond by monomer or excimer emission depending on compound structure or the conditions of the experiment. In one example which illustrates the relationship between compound structure and emission profile, the pyrene-appended calix[4]arenes shown in Figure 2.16 were studied.[59] The simple compound **M**, bearing one pyrene ring responds to excitation with a typical monomer emission (**M**). The more complex structure **B**, bearing two pyrene subunits reponds on the other hand with a typical excimer emission (**B**) (Figure 4.1).

Fluorescence spectra of **M** and **B** in recorded in CH$_3$CN at 6.0 μM are shown in Figure 2.17. Following excitation at 343 nm, the emission spectrum for **B** displays a weak monomer and a strong excimer band at 395 and 476 nm, respectively, whereas **M** exhibits only a monomer emission with maximum intensity at 395 nm.[59]
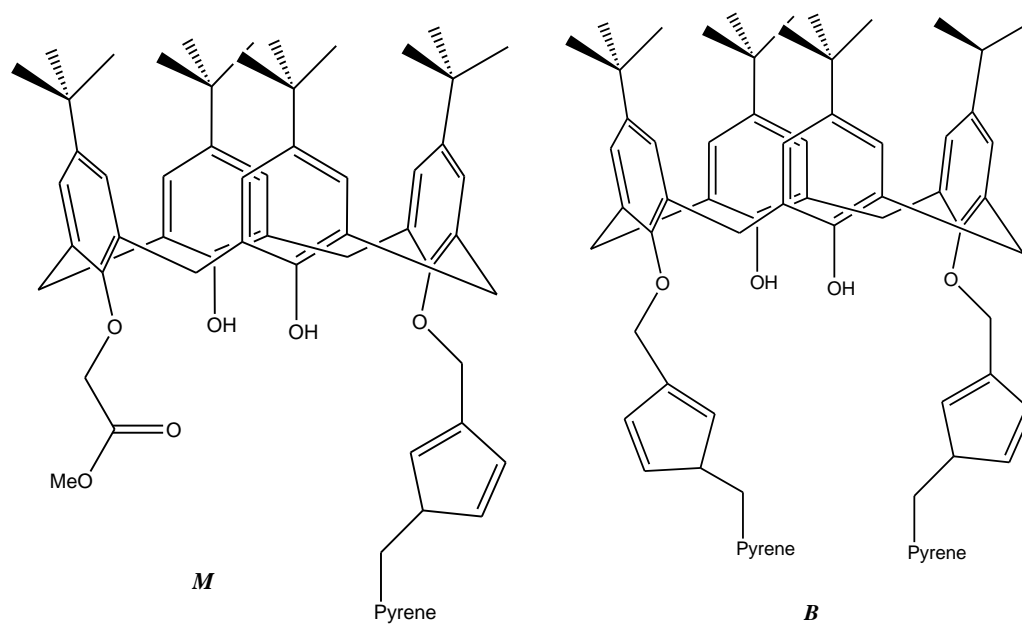
Figure 2.16. The structures of pyrene appended calixarenes **M** and **B**.
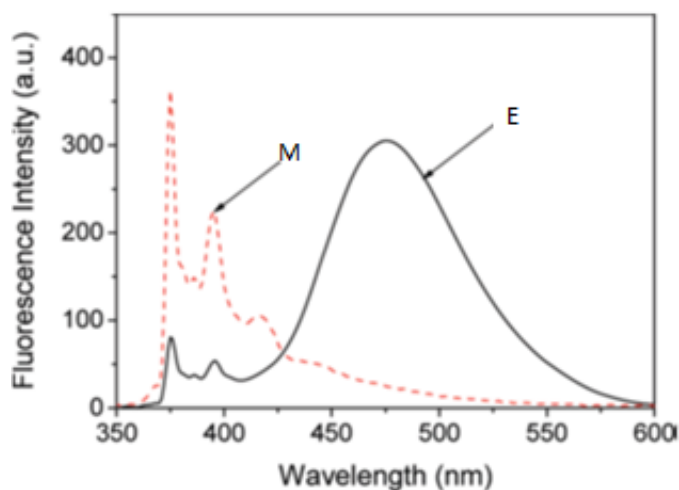
Figure 2.17. The fluorescent spectra of pyrene appended calixarenes **M** and **B**

2.6.2. Fluorescence study on **PIC** (**60**, pyrene-isoxazole-calixarene) and **monoPiM** (momopyrene-isoxazole-modle).

In this thesis, I constructed **PIC**, *p-tert*-butyl-calix[4]arene functionalized with an

isoxazole linked pyrene moiety. The construct was prepared by a 1,3-dipolar cycloaddition between an alkyne-modified calixarene and a pyrene-bearing nitrile oxide. To understand if the emission profile of **PIC**, arose from individual pyrene subunits (monomer emission) or if it would be a feature of intramolecular pyrene-pyrene interaction (excimer emission) 5-[(4-*tert*-butylphenoxy)methyl]-3-(pyren-6-yl)isoxazole, **monoPiM** was also constructed (Figure 2.18).
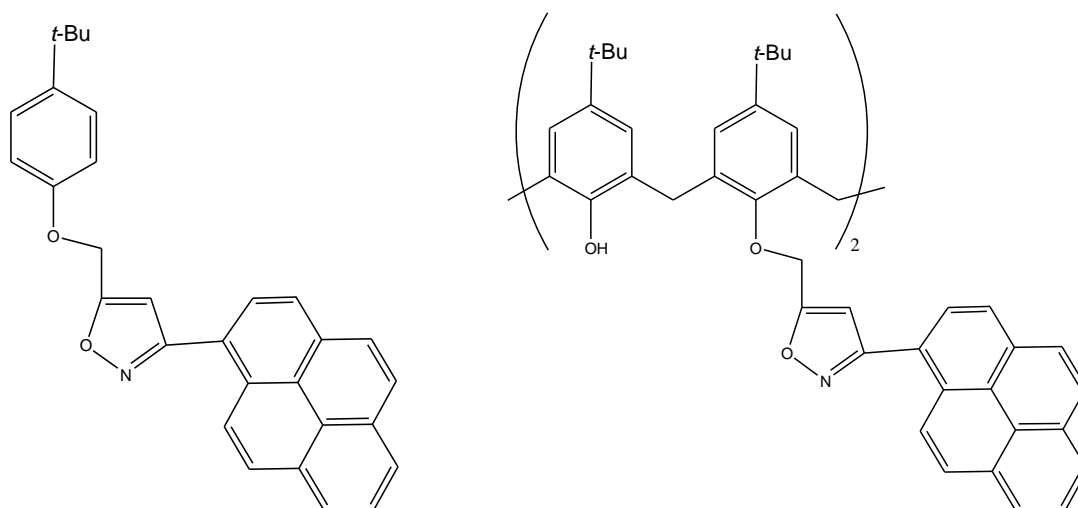
Figure 2.18. The structures of **monoPiM** (left) and **PIC** (right).

2.6.2.1. UV/Vis Spectral analysis of **monoPiM** and **PIC**

Samples of **PIC** and **monoPiM** were prepared, 6.0 μM in HPLC grade CH$_3$CN, for analysis by UV spectroscopy. Spectra were recorded on a *UV 500, DISC PD 2000-1* instrument. Initially a blank spectrum was recorded – *i.e.* CH$_3$CN was used as the UV-spectral background. After that the samples were studied; three absorptions were observed for **PIC**, at 242 nm, 275 nm and 343 nm while two absorptions were found for **monoPiM** at 274 nm and 346 nm; the data for both compounds are shown below in Figures 2.19a and 2.19b. This information was used to determine the optimal wavelength for excitation in subsequent fluorescence studies. HPLC grade acetonitrile was chosen as solvent.
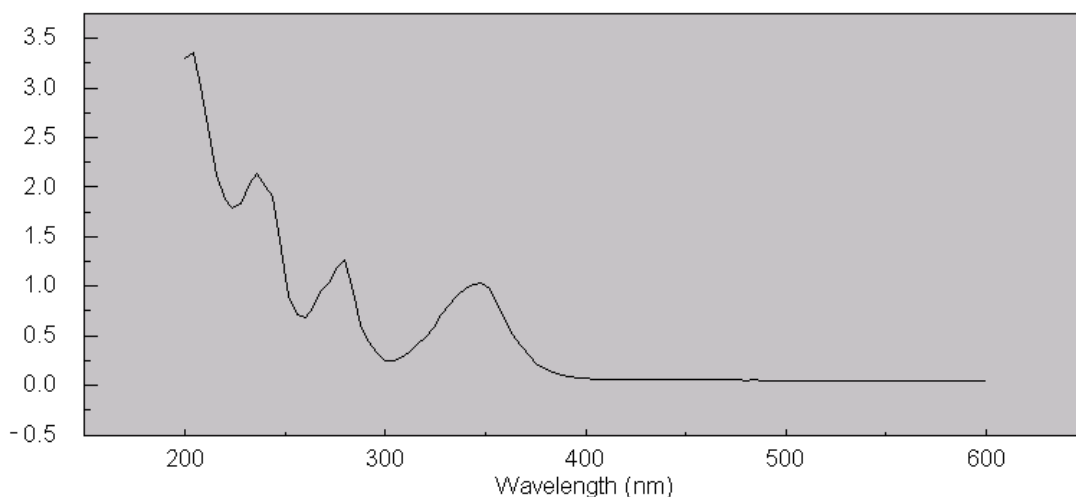
Figure 2.19a. The UV data of **PIC** (6.0 μM) in HPLC grade CH_3CN.
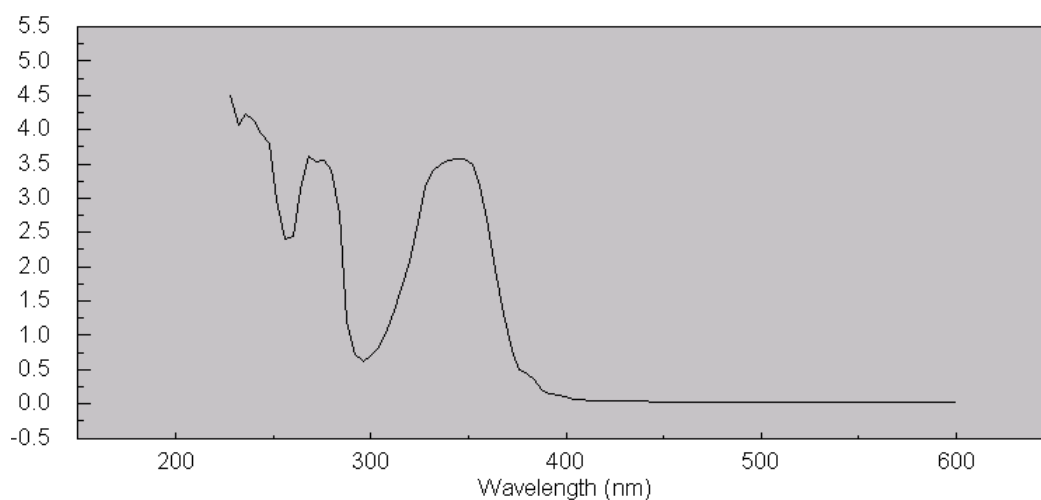
Figure 2.19b. The UV data of **monoPiM** (6 μM) in HPLC grade CH_3CN.

2.6.2.2. Fluorescence Spectroscopy.

Fluorescence spectra, in emission mode, were recorded using a *Jasco FP6300* fluorescence spectrophotometer. Samples were prepared, at 6.0 μM concentration and 3000 μL fluorescence cells were used. Initially excitation wavelength for both compounds was explored at λ_{max} of all absorption bands. The optimized parameters for acquisition of the fluorescence data are shown in Table 2.1.

Compound	Excitation (nm)	Start (nm)	Stop (nm)	Band width Ex. & Em. (nm)	Sensitivity
PIC	343	350	650	2.5, 2.5	high
MONOPIM	274	280	650	2.5, 2.5	high

Table 2.1 The parameters for acquisition of the fluorescence spectra (solvent HPLC

grade CH_3CN)
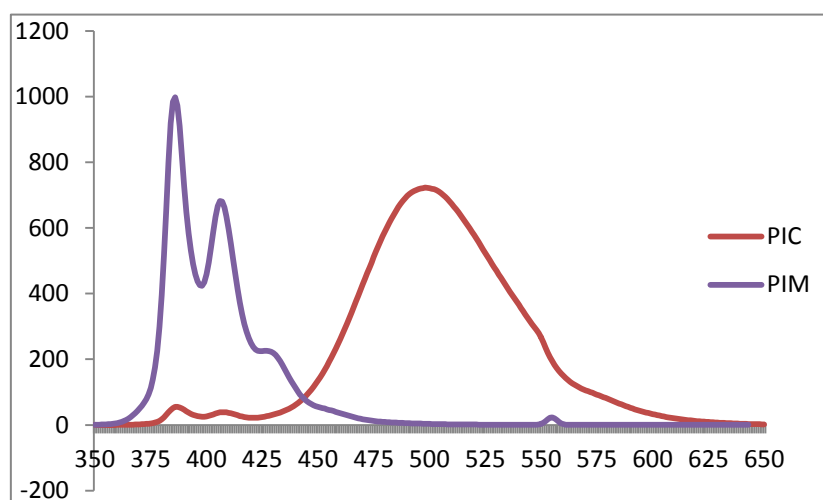
Figure 2.20. Fluorescence spectra of **PIC** and **monoPiM** (6.0 μM) in CH_3CN.

Excitation at 343 nm for **PIC** and at 274 nm for **monoPiM**.

The fluorescence spectra of **PIC** and **monoPiM** shown in Figure 2.20 are distinctly different.[53] **PIC** shows weak monomer emission bands at 386 nm and 406 nm, and a strong excimer emission band centered at 498 nm. **MonoPiM** exhibits strong monomer emission bands at 386 nm and 406 nm. One reason for the different behaviours is the possibility for π-π stacking of the pyrene rings of **PIC** in acetonitrile. Another reason why excimer emission may dominate in **PIC** is that the pyrene rings may be optimally positioned for an intramolecular interaction between one excited pyrene unit (pyrene[*]) with a ground-state pyrene unit where two pyrenes units are parallel.[61]

The potential for **PIC**, and possibly **monoPiM**, to sense heavy metal ions pivots on the coordination chemistry of isoxazoles. As mentioned in the Introduction of this

thesis a range of bis-isoxazoles have been observed to form complexes of Cu^{2+}, Co^{2+} and Fe^{2+} amongst others. The pyrene rings will not bind to the heavy metals. Thus **PIC** very attractively presents a calixarene scaffold, with two isoxazole units as potential metal-ion binding sites, and two pendant pyrene units capable of informing on the inclusion, or otherwise, of guest ions by a change in intensity, or emission mode of its fluorescence response. In contrast, **monoPiM**--featuring only one isoxazole binding site and no opportunity for intramolecular excimer emission--may neither form effective complexes, nor emit useful diagnostic signals.

2.6.2.3. A study of the potential of **monoPiM** and **PIC** as ion-selective host molecules.

    PIC and **monoPiM** were used as potential hosts to sense for a range of metal-ions. Stock solutions of host samples were prepared at 12 μM in CH_3CN, solutions of guests were prepared, in the same solvent, at 1200 μM. For all analyses, the total volume of *materials* in the cuvette was maintained at 3000 μL and the concentration of host was kept at 6.0 μM. The concentration of the guest salts in the cuvette was varied from 6.0 μM to 600 μM, *i.e.* 1 to 100 equivalents guest to host. In measuring host-guest samples, appropriate quantities of **PIC/monoPiM**, salt solution and solvent were added to the cell (quantities summarized Table 2.2). The sample was shaken by hand for 60 seconds to optimize mixing of host and guest. After this interval, the exterior walls of the sample cell were cleaned with fluorescence tissue before the cuvette was placed in the spectrofluorimeter. Due to the potential for deviation in the readings spectra for all mixtures were recorded three times.

    Prior to measurement of the experimental samples, background data was recorded for the solvent, a blank run with acetonitrile was measured under the same conditions as were to be employed for the sample (i.e. same excitation wavelength and emission window). This information was used to auto-zero the equipment.

Volume of Compounds / Host: guest (eq.)	PIC (μL)	M^{n+} (μL)	MeCN (μL)
1:1	1500	15	1485
1:10	1500	150	1350
1:100	1500	1500	0

Table 2.2. The volumes of host, guest and *added* acetonitrile used to prepare host:guest samples varying from 1:1 to 1:100 equivalents; e.g. host: guest= 1:1, 1500 *u*L of host, 15 *u*L of guest and 1485 *u*L of CH$_3$CN are needed to make up the desired 3000 *u*L sample.

2.6.2.4. Fluorescence spectral analysis of **PIC**.

To determine the ability, if any, of **PIC** to sense metal-ions, changes to the fluorescence profile of the host molecules upon addition of the perchlorate salts of a variety of heavy metal cations, like Cu^{2+}, Hg^{2+}, Ni^{2+}, Zn^{2+}, Co^{2+}, Fe^{2+}, Ag^{2+}, Pb^{2+}, Cd^{2+} and Cu^{1+} in CH$_3$CN were recorded. For each sample, fluorescence spectra were recorded in triplicate. The following samples were analyzed for each salt, host alone, host (6 μM) + 1 eq. guest (6 μM); host (6 μM) + 10 eq. guest (60 μM); host (6 μM) + 100 eq. guest (600 μM) and the fluorescence spectra are depicted below – Figures 2.21 a-h. All measurements were done three times, and for a given run, all intensities fell within a narrow range.
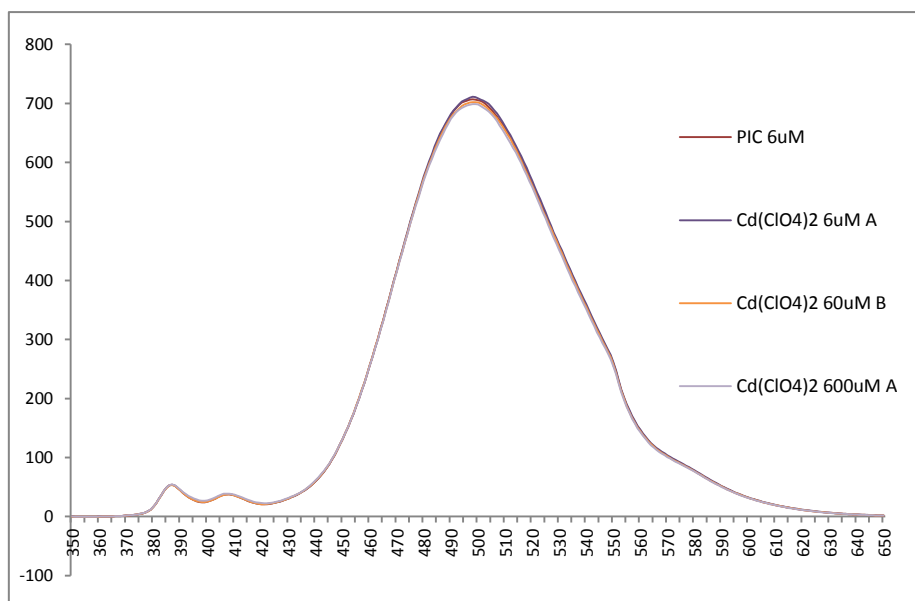
Figures 2.21a. Emission spectra of **PIC** (6 μM) in CH_3CN upon addition of 1 eq., 10 eq. and 100 eq. of $Cd(ClO_4)_2$.
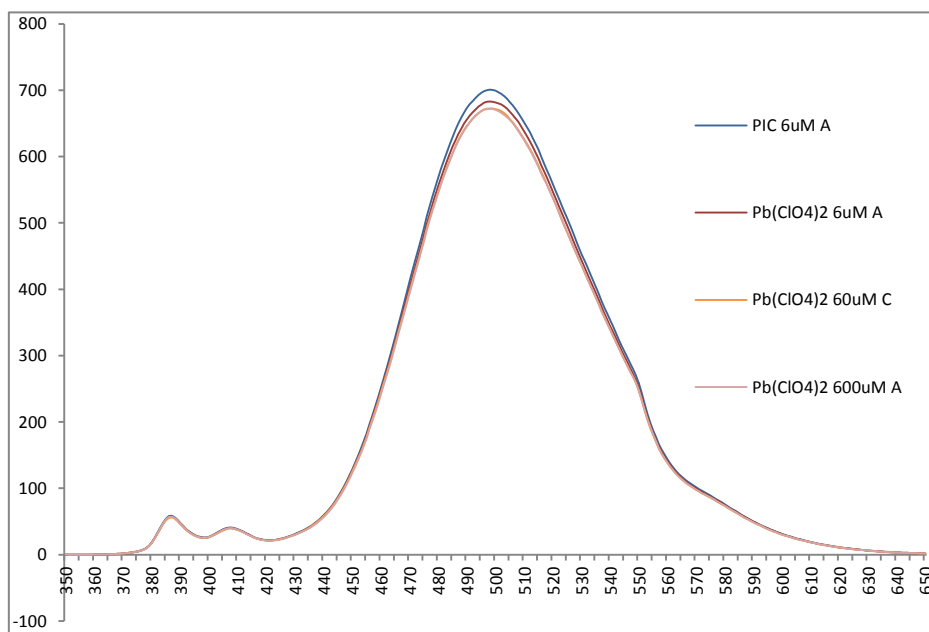
Figures 2.21b. Emission spectra of **PIC** (6 μM) in CH_3CN upon addition of 1 eq., 10 eq. and 100 eq. of $Pb(ClO_4)_2$
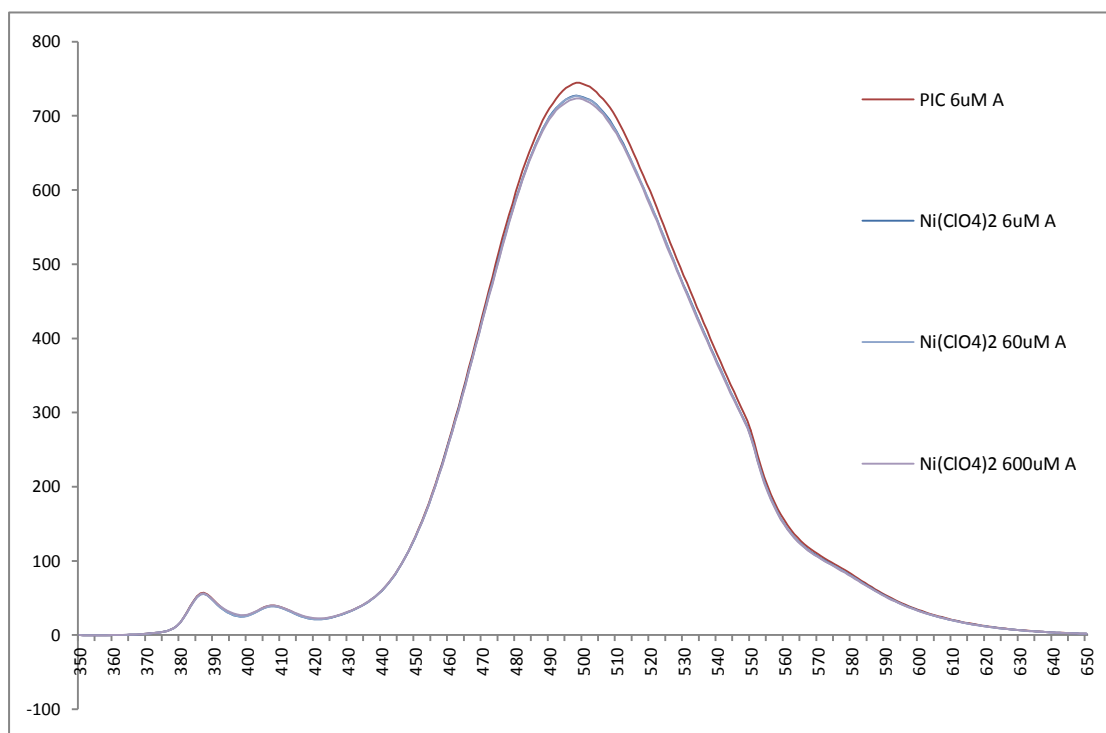
Figures 2.21c. Emission spectra of **PIC** (6 μM) in CH$_3$CN upon addition of 1 eq., 10 eq. and 100 eq. of Ni(ClO$_4$)$_2$.
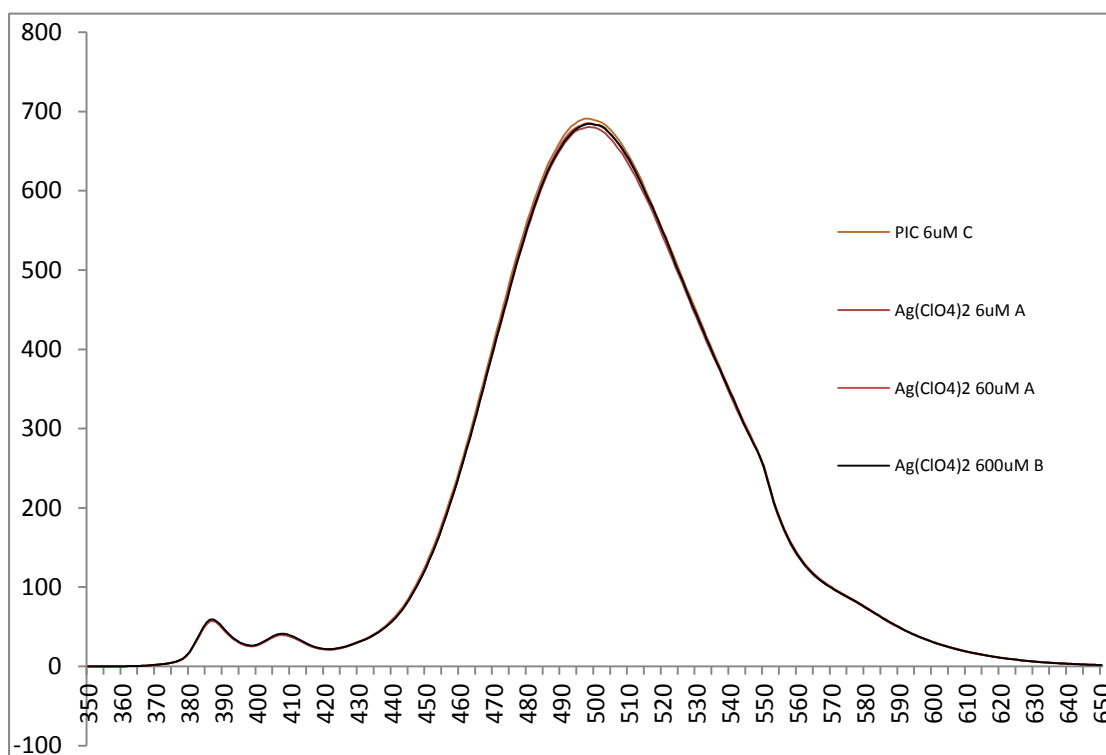
Figures 2.21d. Emission spectra of **PIC** (6 μM) in CH$_3$CN upon addition of 1 eq., 10 eq. and 100 eq. of Ag(ClO$_4$)$_2$.
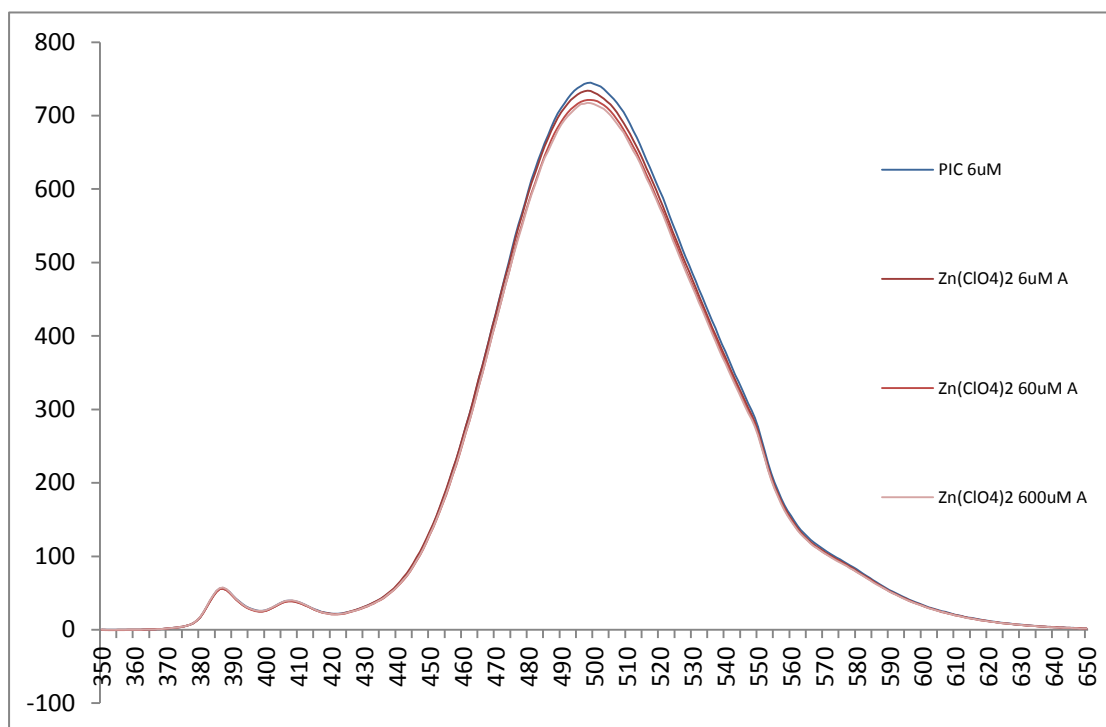
Figures 2.21e. Emission spectra of **PIC** (6 μM) in CH$_3$CN upon addition of 1 eq., 10 eq. and 100 eq. of Zn(ClO$_4$)$_2$.
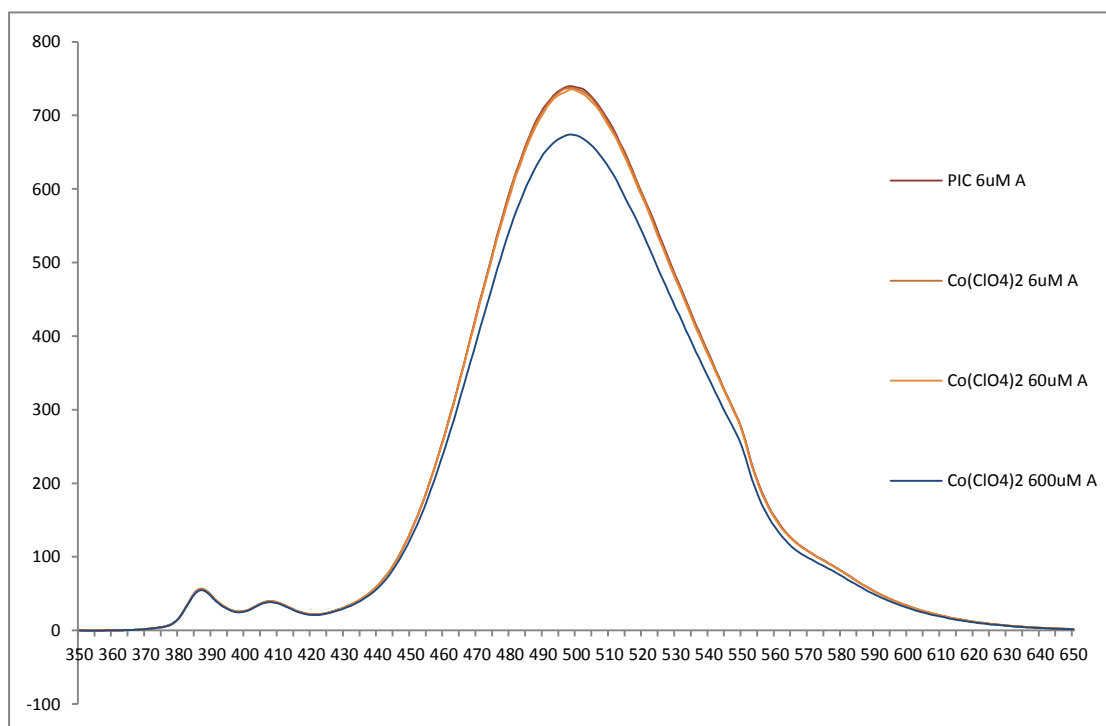
Figures 2.21f. Emission spectra of **PIC** (6 μM) in CH$_3$CN upon addition of 1 eq., 10 eq. and 100 eq. of Co(ClO$_4$)$_2$.
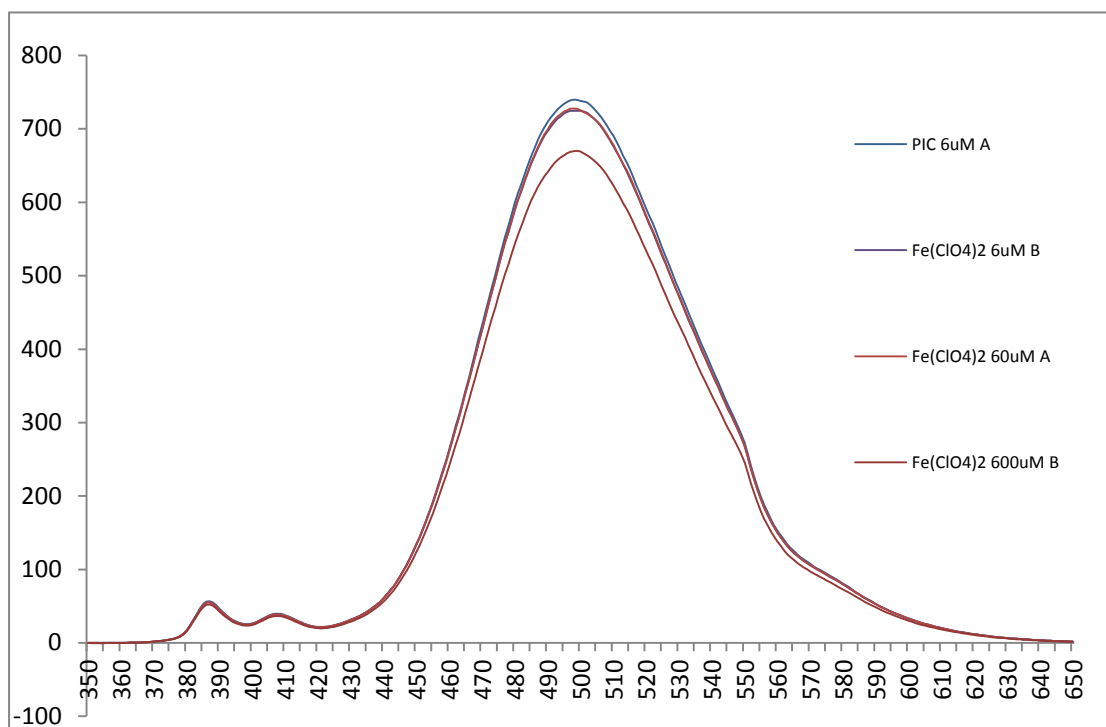
Figures 2.21g. Emission spectra of **PIC** (6 μM) in CH$_3$CN upon addition of 1 eq., 10 eq. and 100 eq. of Fe(ClO$_4$)$_2$.
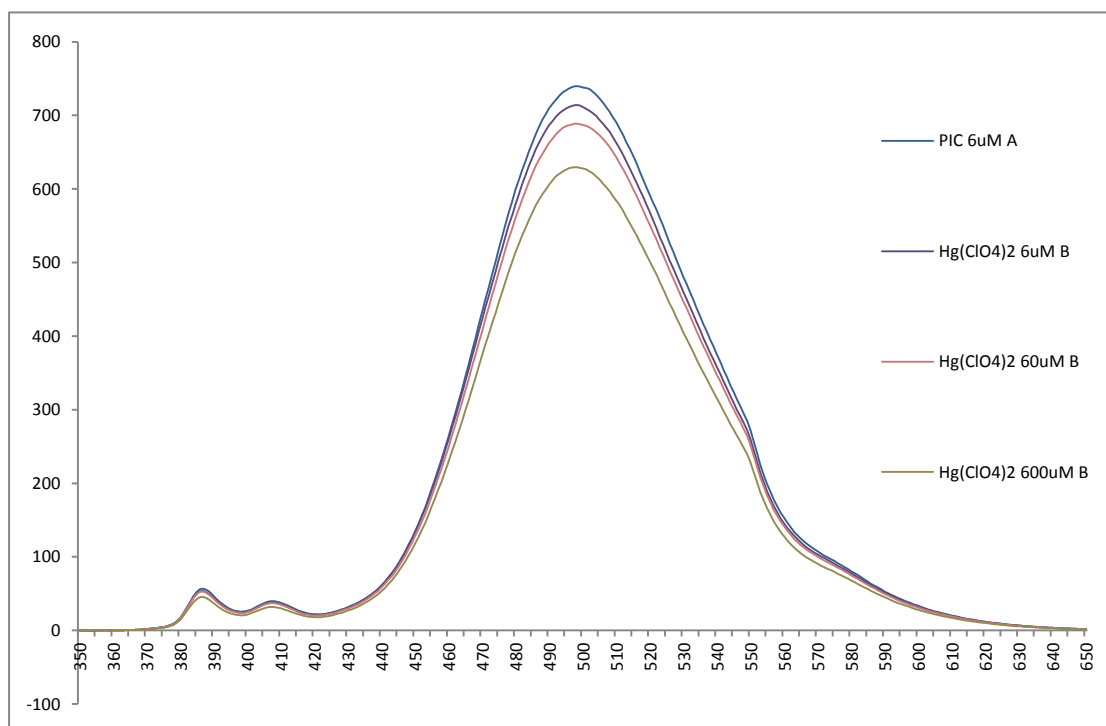
Figures 2.21h. Emission spectra of **PIC** (6 μM) in CH$_3$CN upon addition of 1 eq., 10 eq. and 100 eq. of Hg(ClO$_4$)$_2$ with **PIC**.

Upon the addition of $Co(ClO_4)_2$, $Fe(ClO_4)_2$ and $Hg(ClO_4)_2$ (Figures 2.21f-h.), a slight quenching of excimer emission of the host was observed; however no discernable change could be observed upon addition of even 100 eq. of perchlorate salts of Cd, Pb, Ni, Ag or Zn (Figures 2.21a-e.). In sharp contrast, the addition of $Cu(ClO_4)_2$ caused a dramatic quenching of excimer emission. With as little as 10 eq. of $Cu(ClO_4)_2$ fluorescence intensity was decreased by a factor of ~7-8 and almost complete quenching occurred following exposure of the host to 100 eq. of copper perchlorate (Figures 2.21i.).
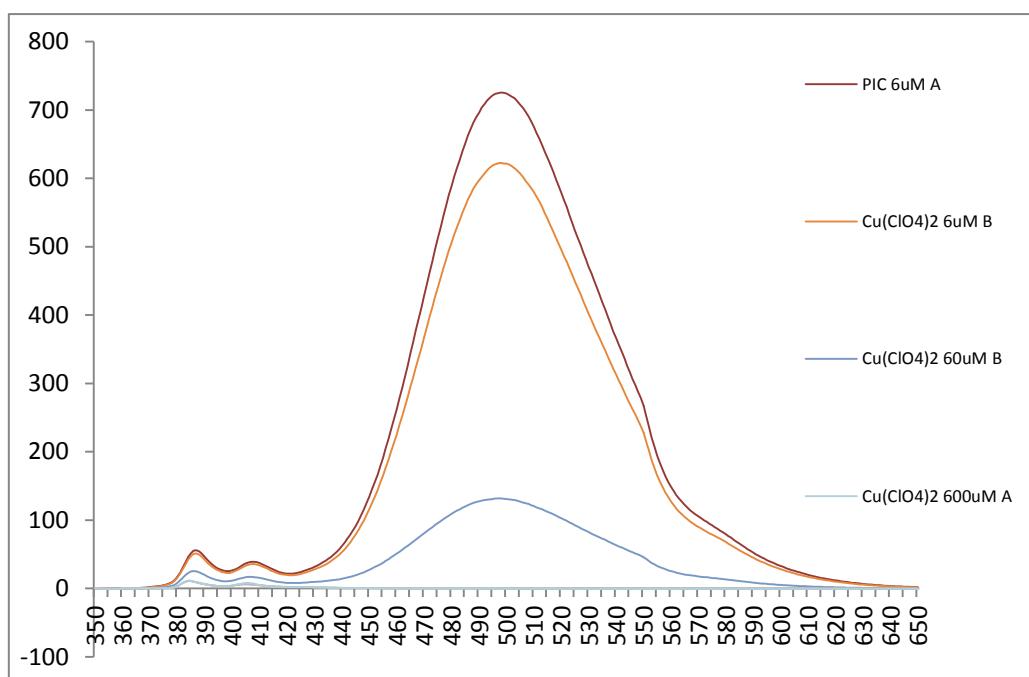
Figures 2.21i. Emission spectra of **PIC** (6 μM) in CH_3CN upon addition of 1 eq., 10 eq. and 100 eq. of $Cu(ClO_4)_2$.

2.6.2.5. Fluorescence spectra of **monoPiM** in the presence of various perchlorate salts.

As expected, **monoPiM** bearing only one pyrene subunit, and no calixarene scaffold, shows no significant spectral changes upon addition of 20 equivalents of most heavy metals (120 μM, 20 eq. to host **monoPiM**), whereas Cu^{2+}, Co^{2+} and Hg^{2+} ions resulted in very slight quenching of the host (Figure 2.22).
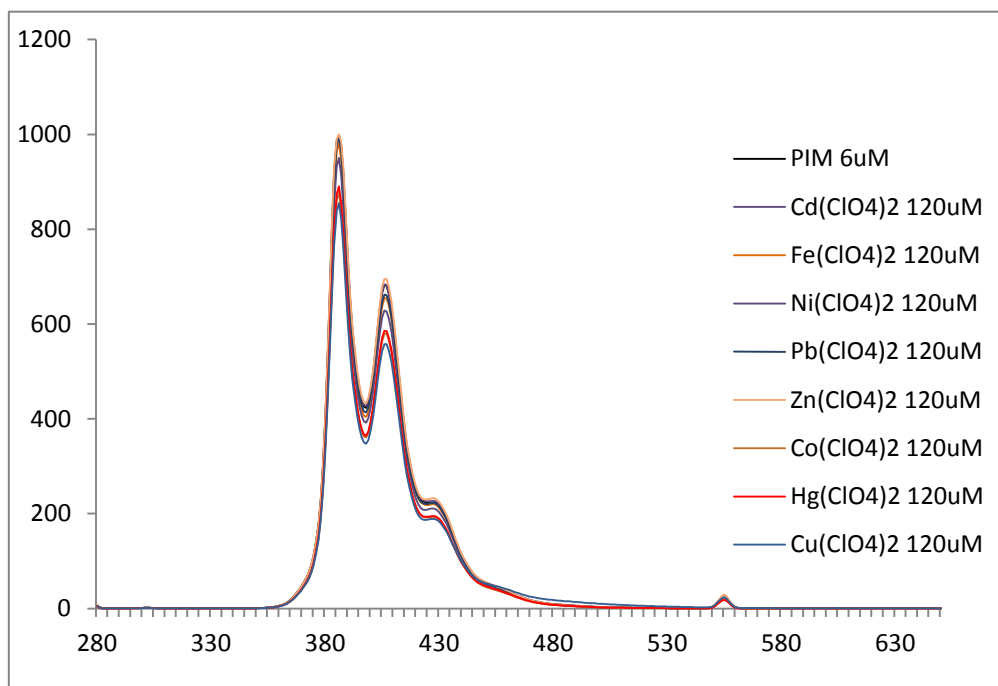
Figure 2.22. The fluorescence emission spectra of **monoPiM** (6 μM) upon the addition of 20 eq. of Cd(II), Fe(II), Ni(II), Pb(II), Zn(II), Co(II), Hg(II) or Cu(II) ions.

2.6.2.6. Ion-selectivity study for **PIC**.

To study the potential of PIC as an ion-selective chemosensor for Cu^{2+}, the effect of competing metal-ions on quenching by Cu^{2+} was explored. To individual solutions of **PIC** (6 μM) in the presence of 20 eq. of $Cu(ClO_4)_2$ were added, in turn, 20 eq. of each of the following metal perchlorates, Co^{2+}, Fe^{2+}, Hg^{2+}, Ni^{2+}, Pb^{2+}, Zn^{2+}, Cd^2. The results of these experiments are summarized in the Figure 2.23 below. The blue bar shows the relative intensity of the fluorescence signal at 498 nm for **PIC** (6 μM) to that of **PIC** in the presence of 20 eq. of the named metal salt. The red bar show the relative intensity of the fluorescence signal at 498nm for **PIC** (6 μM) to that of **PIC** in the presence of both 20 eq. of the named metal salt and 20 eq. of Cu^{2+} (all spectra recorded in CH_3CN). The data clearly show effective host quenching is retained upon the addition of Cu^{2+} ion in the presence of all other cations studied. **PIC** is thus a highly selective chemosensor for Cu^{2+} ion.
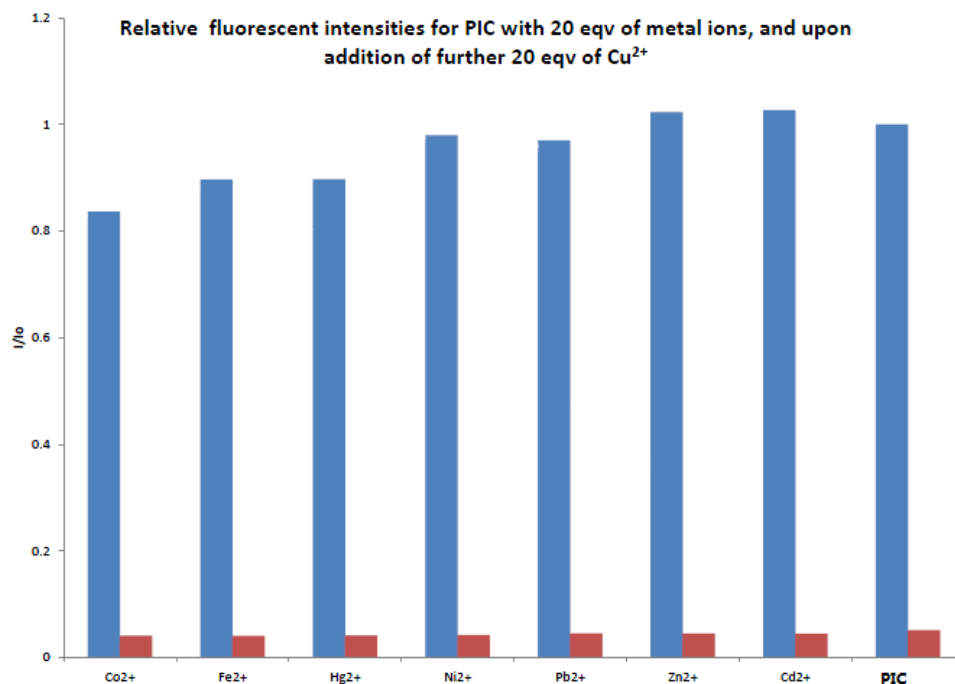
Figure 2.23. Selective fluorescence quenching of **PIC** by Cu^{2+} in the presence of a range of metal-ions. All samples were measured in CH$_3$CN and excitation was at 343 nm. The relative intensity of the fluorescence signal at 498 nm for **PIC** (6 μM) to that of **PIC** in the presence of 20 eq. of the named metal salt is shown by the blue bar. The red bar show the relative intensity of the fluorescence signal at 498nm for **PIC** (6 μM) to that of **PIC** in the presence of both 20 eq. of the named metal salt and 20 eq. of Cu^{2+}.

2.6.2.7. Anion study.

The ability of **PIC** to detect Cu^{2+} ions from perchlorate salts is highly evident from the data presented above. We were anxious to study the influence, if any, of the counter ion and thus began to study the fluorescence profile of **PIC** in the presence of a range of copper salts. Thus, copper nitrate, chloride and acetate salts were studied. Fluorescence spectra were recorded for samples where the host, **PIC**, was present at 6 μM and guests at 6 μM, 300 μM and 600 μM, *i.e.* 1, 50 and 100 eq., and the results are summarized in Figures 2.24a-c.
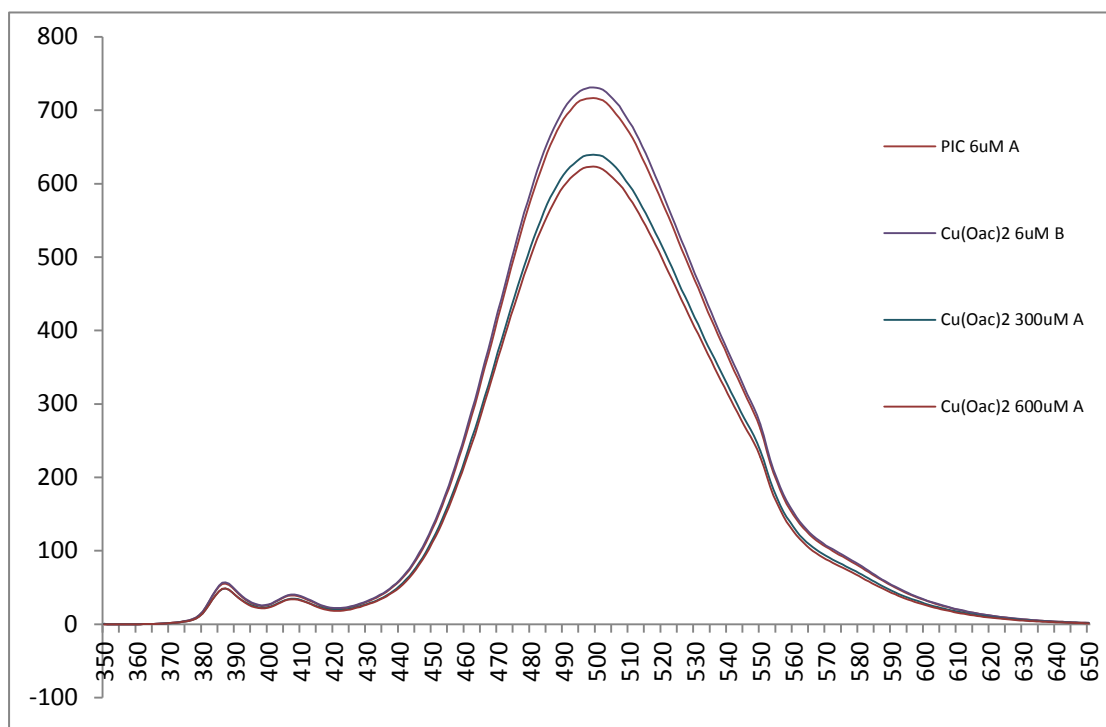
Figure 2.24a. The fluorescence emission changes of **PIC** (6 μM) upon the addition of Cu(OAc)$_2$ (1 eq., 10 eq. and 100 eq.).
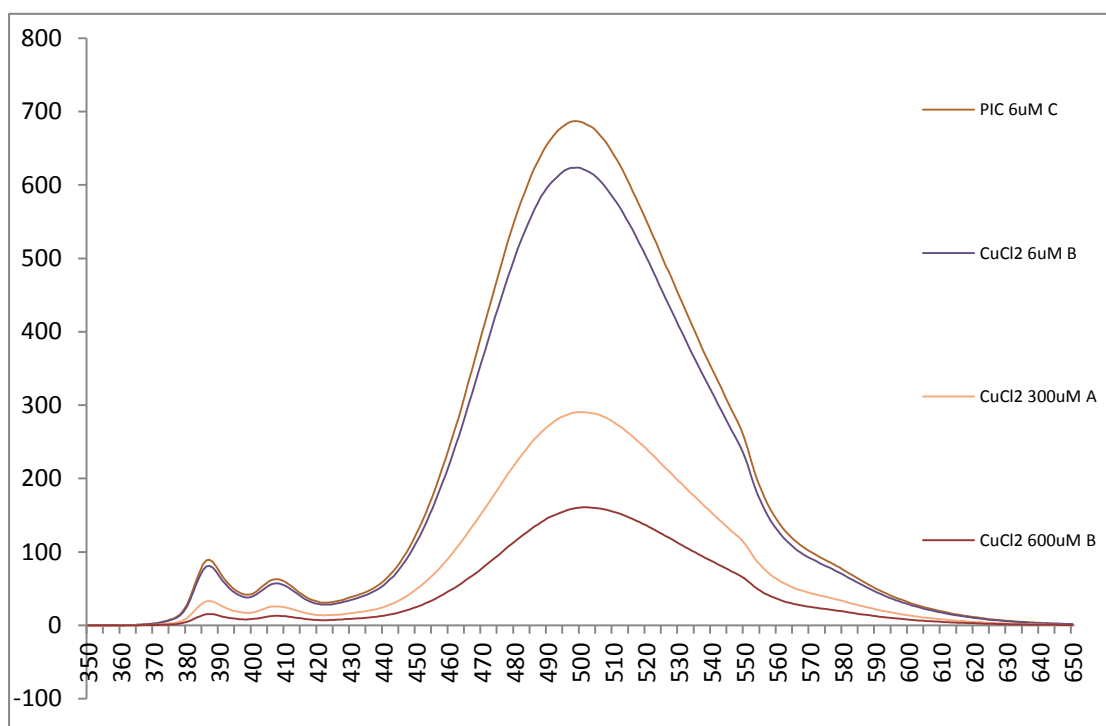
Figure 2.25b. The fluorescence emission changes of **PIC** (6 μM) upon the addition of CuCl$_2$ (1 eq., 10 eq. and 100 eq.).
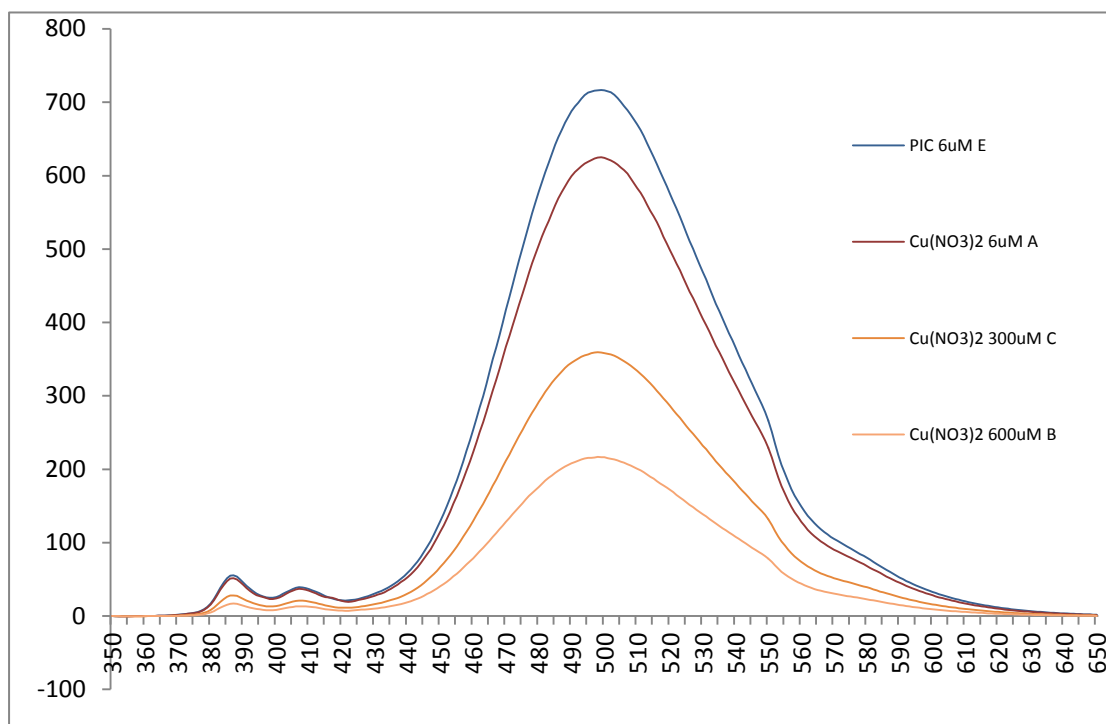
Figure 2.25c. The fluorescence emission changes of **PIC** (6 μM) upon the addition of Cu(NO$_3$)$_2$ (1 eq., 10 eq. and 100 eq.).

The data clearly show that, compared to the perchlorate analogue, Cu(OAc)$_2$ has very limited ability to quench the fluorescence signal of **PIC**. Thus the addition of 100 eq. of Cu(OAc)$_2$ results in less host quenching than 1 eq. of Cu(ClO$_4$)$_2$. CuCl$_2$ and Cu(NO$_3$)$_2$, are about one order of magnitude less effective quenchers than Cu(ClO$_4$)$_2$. From this data it is obvious that the extent of fluorescence quenching by copper ions is directly related to the nature of the counter ion and the extent of dissociation of the various copper salts in acetonitrile[62].

2.6.3. Binding stoichiometry of **PIC** with Cu^{2+}.

2.6.3.1. Job's method study[63].

To determine the stoichiometry of reaction between **PIC** and Cu^{2+}, a Job's plot was constructed. A Job plot is used to determine the stoichiometry of a binding event which is widely used in analytical chemistry, instrumental analysis, and advanced chemical equilibrium texts and research articles. This method is named after P. Job, who first introduced this methodology in 1928.[64]

In solutions where two species are present (i.e. species A and species B), one species (A) may bind to the other species (B). In some cases, more than one molecule of the former will bind with a single molecule of the later. A Job's plot can be used to determine the stoichiometry of A binding to B. In this method, the total molar concentration of the two binding species (like a ligand and metal) is kept as constant, however their mole fractions are varied. A signal capable of recognition of complex formation, e.g. an absorption signal, is plotted against the mole fractions of these two components. The stoichiometry of the two species is obtained from the maximum (or minimum) of the corresponding plot.[65]

2.6.3.2. Experiments to create a Job's plot

To construct the desired Job's plot illustrating the stoichiometry association between **PIC** and $Cu(ClO_4)_2$, a solution of $Cu(ClO_4)_2$ in CH_3CN was prepared at 24 µM; the host **PIC** was prepared at 12 μM in the same solvent. Thus appropriate quantities were drawn from the stock solutions to prepare the samples indicated in Table 2.3 and Figure 2.26.

Reagent, Volume / Host-guest ratio	PIC μL	Cu^{2+} μL	CH$_3$CN μL
6 : 0	1500	0	1500
5.6 : 0.4	1400	50	1550
5 : 1	1250	125	1625
4.4 : 1.6	1100	200	1700
4 : 2	1000	250	1750
3.6 : 2.4	900	300	1800
3 : 3	750	375	1875
2.4 : 3.6	625	450	1925
2 : 4	500	500	2000
1.6 : 4.4	400	550	2050
1 : 5	250	625	2125

Table 2.3. The preparation of samples required to construct a Job's plot.

The total concentration of host and guest was kept as 6 μM in all Job plot samples. e.g. concentration of host and guest 5.6 and 0.4 μM, which needs 1400 μL of host, 50 μL of Cu^{2+} and 1500 μL of CH$_3$CN, means the concentration of host in the prepared sample is 5.6 μM and the concentration of Cu^{2+} is 0.4 μM. The change of fluorescence intensity at 498 nm with increasing Cu^{2+} to **PIC** was monitored and data is shown in Figure 2.26.
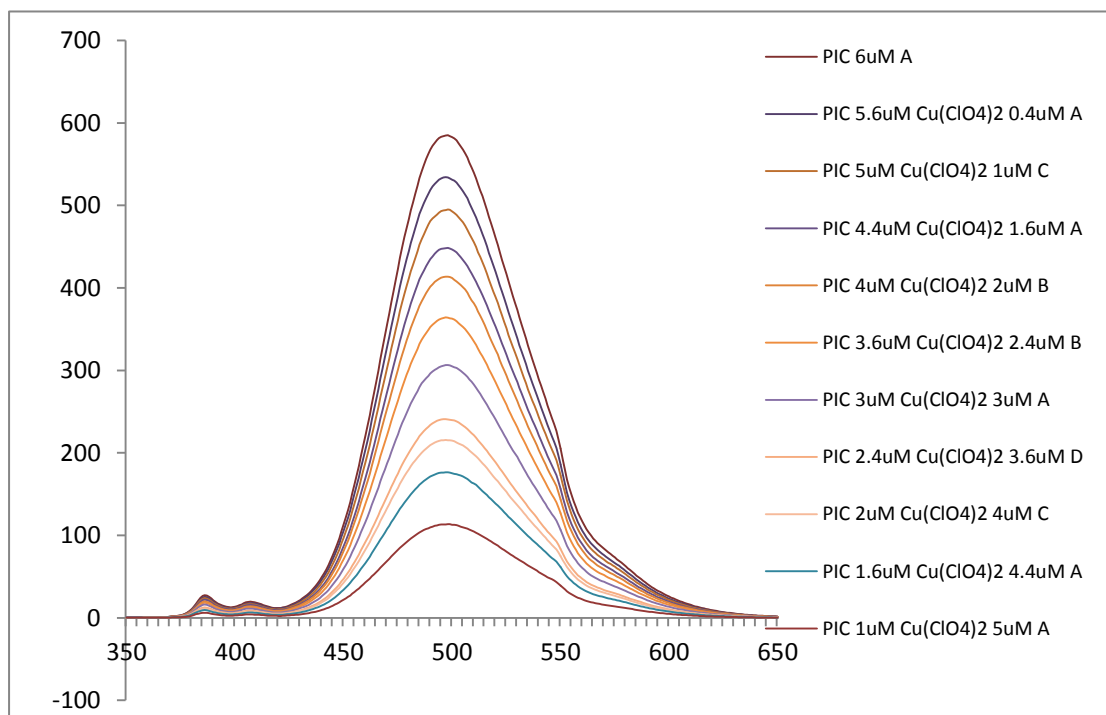
Figure 2.26. Emission spectra for **PIC** in the presence of various amounts of Cu(ClO4)$_2$-- total species concentration 6.0 μM.

The data from Figure 2.26 were used to create the Jobs plot as follows. For each sample, following excitation at 343 nm the intensity of maximum absorption (@ 498 nm) was recorded. On the X axis, the mole fraction of the ligand [X] is defined as:

$$[X] = \frac{Cl}{Cl + Cm}$$

Where *Cl* is the concentration of ligands,

Cm is the concentration of the metal-ions

Cl+Cm is the total concentrations of ligand and cation which is kept as a constant, 6.0 μM.

On the Y-axis, *ΔF*[X]=(Fl-Fm)*[X]*, where *Fl* is the absorption (498 nm) of ligand **PIC** at 6.0 M, and Fm is the absoption (498 nm) of a particular Job's plot sample.
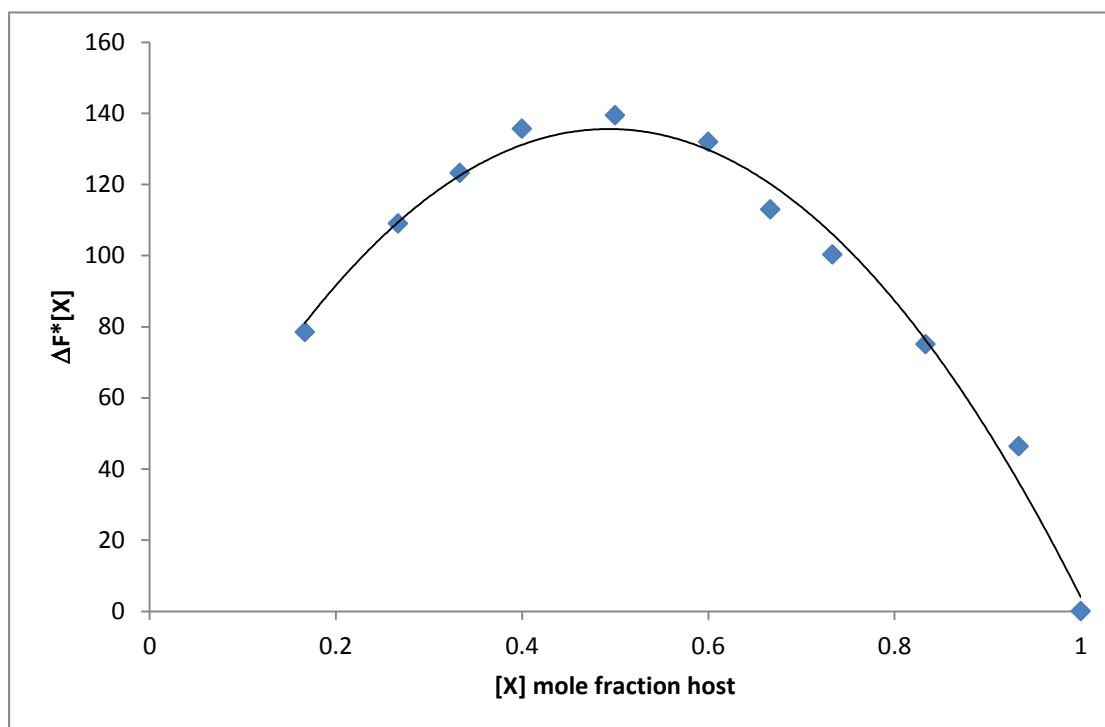
Figure 2.27. Job's plot[66] of **PIC** with Cu^{2+} in a total concentration of 6.0 μM.

Analysis of the plot so constructed, Figure 2.27, indicates the maximum absorption occurs around 0.5. This indicates formation of a 1:1 complex between **PIC** and Cu^{2+} ions.

2.6.3.3. Stern-Volmer study.[67]

The Stern–Volmer relationship allows an exploration of the kinetics of a photophysical intermolecular deactivation process, and fluorescence and phosphorescence are examples of such intramolecular deactivation (quenching) processes. A deactivation process is said to be intermolecular when the presence of another chemical species can accelerate the decay rate of a species in its excited state. Stern-Volmer plots can help understand quenching behaviour as a function of quencher concentration. The Stern Volmer equation[63] which relates the ratio of the fluorescence intensity in the presence and absence of a quenching molecule to the concentration of the species, it is given as follows:

$$I_o/I = 1 + K_{sv}[Q]$$

where I_o is the fluorescence intensity of the host, **PIC**.

I is the fluorescence intensity of the host plus guest, **PIC**-Cu^{2+} complex,

K_{sv} is the Stern-Volmer constant,

[Q] is the concentration of the guest Cu^{2+}.

The samples for Stern-Volmer analysis were prepared as follows. Stock solutions of guest $Cu(ClO_4)_2$, at 24 μM and host **PIC** at 12 μM were prepared in CH_3CN. Samples required preparing a plot of I_o/I against [Q]. Calculated volumes of the metal salt were titrated with the host so that the final concentration of the guest in the 3000 μL cuvette was 0, 1.2, 2.4, 3.6, 4.8, 6, 9, 12 μM. The calculation of the required volume of all solutions and the molar ratio of host-guest are shown in Table 2.4. e.g. **PIC**:Cu^{2+} = 6:1.2 means the concentration of host in the host-guest system is 6 μM whereas the concentration of guest copper is 1.2 μM. For this fluorescent sample, 1500 μL of host, 150 μL of $Cu(ClO_4)_2$ and 1350 μL of CH_3CN are needed (Table 2.4).

The Stern-Volmer plot constructed following collection of fluorescence emission data (excitation at 343 nm and recording intensity of emission at 498 nm) upon addition of $Cu(ClO_4)_2$ to a CH_3CN solution of **PIC** is shown below in Figure 2.28. On the X-axis is mole fraction of quencher [Q] (metal-ions) the Y-axis shows the ratio I_0/I. I_0 is defined as the emission intensity of **PIC** at 498 nm. It is defined as the emission intensity of **PIC** in the presence of quencher at 498 nm. The data, shown in the Figure 2.28a, did not fit well to a straight line; the linear trend-line has a R^2 = 0.9776. Attempts were also made to fit to a curve; the fits to a second order plot, shown in Figure 2.28b, had R^2 = 0.9941. On the basis of these data, it is likely that a combination of static or dynamic quenching applies to this system.

Reagents, Volume PIC: Cu^{2+} (μM)	PIC (μL)	Cu(ClO$_4$)$_2$ (μL)	CH$_3$CN (μL)
6: 1.2	1500	150	1350
6: 2.4	1500	300	1200
6: 3.6	1500	450	1050
6: 4.8	1500	600	900
6: 6	1500	750	750
6: 9	1500	1125	375
6: 12	1500	1500	0

Table 2.4. The preparation of samples required to construct a Stern-Volmer plot.
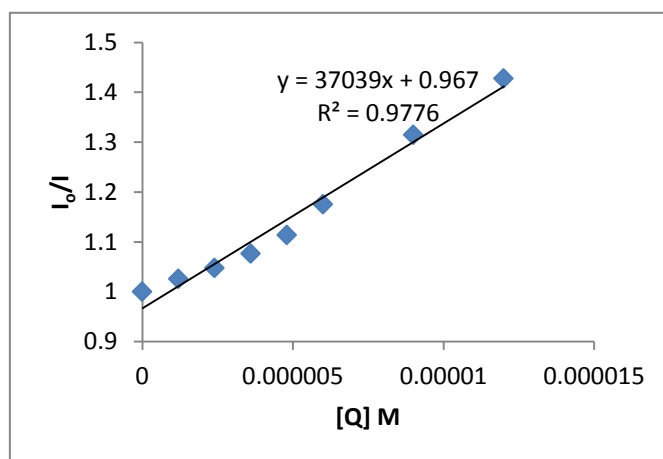
Figure 2.28a. The Stern-Volmer plot obtained from the fluorescence emission changes (at 498 nm) of **PIC** (6 μM) upon the addition of Cu(ClO$_4$)$_2$ (0, 0.2, 0.4, 0.6, 0.8, 1.0, 1.5 and 2.0 eq.).
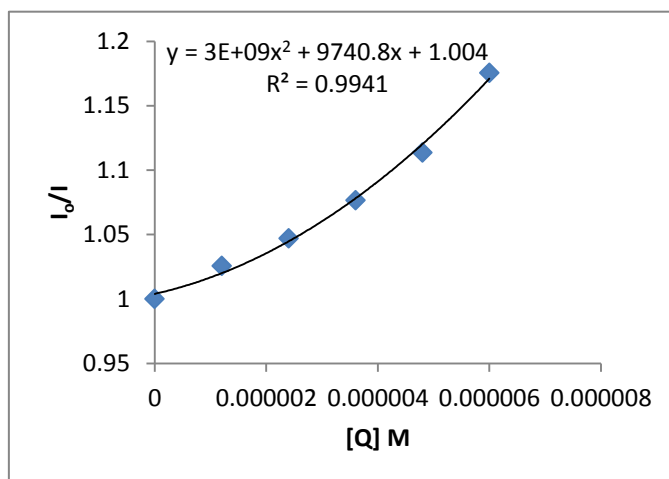
Figure 2.28b. The Stern-Volmer plot obtained from the fluorescence emission changes (at 498 nm) of **PIC** (6 μM) upon the addition of $Cu(ClO_4)_2$ (0, 0.2, 0.4, 0.6, 0.8 and 1.0 eq.).

Two types of fluorescence quenching dominate host-guest systems: Dynamic quenching and Static quenching. In Dynamic quenching, energy transfer occurs from the donor in its excited state. Static quenching occurs when the molecules form a complex in the ground state, e.g. before excitation occurs. The Stern-Volmer plots arising from systems exhibiting these different types of quenching are shown in Figure 2.29. In general static quenching results in a straight line plot as does data from dynamic quenching, on the other hand quenching as a result of both static and dynamic processes presents as a curve with an upward slope.[63] Based on such knowledge we propose that quenching due to formation of a **PIC-**Cu^{2+} complex arises due to both dynamic and static quenching effects.

DYNAMIC QUENCHING | **STATIC QUENCHING**

collisional process

$$\frac{I_0}{I}=\frac{\Phi_0}{\Phi}=\frac{\tau_0}{\tau}=1+K_{SV}[Q]$$

STERN-VOLMER $K_{SV}=k_q\tau_0$

sphere of effective quenching

$$\frac{I_0}{I}=\exp(V_q N_a[Q])$$

formation of a non-fluorescent complex

$$\frac{I_0}{I}=\frac{\Phi_0}{\Phi}=1+K_S[Q]$$

+ Transient effect due to diffusion

+ DYNAMIC QUENCHING

$$\frac{I_0}{I}=(1+K_{SV}[Q])\exp(V_q N_a[Q])$$

+ DYNAMIC QUENCHING

$$\frac{I_0}{I}=(1+K_{SV}[Q])(1+K_S[Q])$$

DYNAMIC QUENCHING (with transient effects) + STATIC QUENCHING

$$\frac{I_0}{I}=(1+K_{SV}[Q])\frac{\exp(V_q N_a[Q])}{Y}$$

Figure 2.29. The various cases of dynamic and static quenching were summarized.[63]

Possible points of interaction between **PIC** and the copper guest ions are proposed in Figure 2.30. With the knowledge of the coordination chemistry mentioned in the Introduction to this thesis, the proposed structure for the complex formed between **PIC** and the Cu^{2+} ion is shown in Figure 2.30. Unfortunately it proved impossible to grow a crystal structure of **PIC** with a Cu^{2+} guest to give unambiguous information on the coordination sites, thus in an effort to decipher the points of interaction between host and guest a ^1H NMR study was undertaken at the Institute of Technology, Tallaght. The instrument was a Bruker Avance 500 MHz spectrometer and spectra were recorded in CD_3CN:$CDCl_3$, 4:1. The host compounds were prepared at 0.65 mM. Spectra were recorded for **PIC** and **monoPiM** alone, and also in the presence of 0.5, 1.0 and 2.0 equivalents of copper perchlorate. Cu^{2+} ions are paramagnetic and we undertook this experiment with the knowledge that extensive signal broadening of signals representing protons in the vicinity of these

ions can be problematic. A parallel study was conducted with zinc perchlorate as a reference "guest" unable to quench the fluorescence of **PIC**.
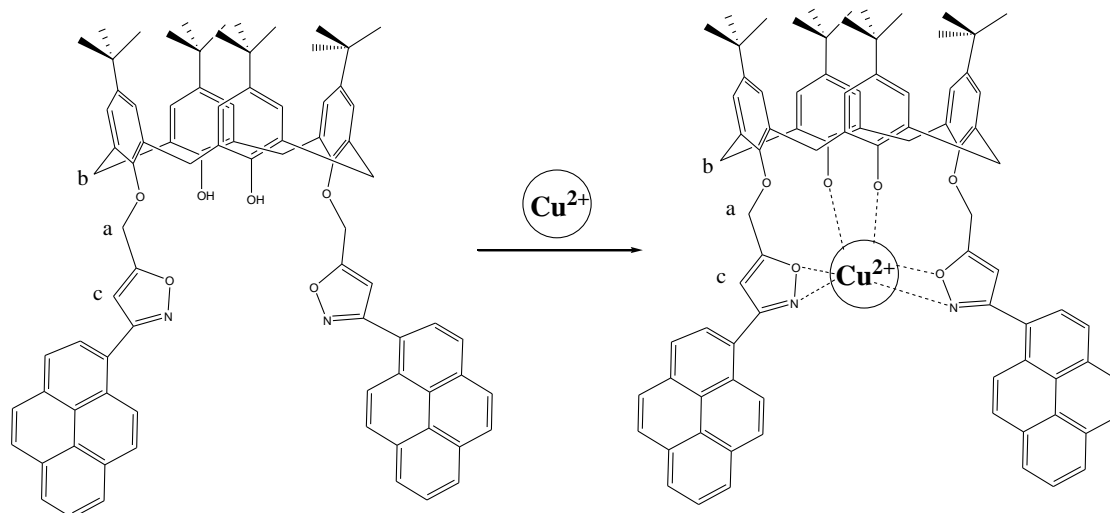
Figure 2.30. The proposed structure for **PIC** with Cu^{2+} ions. The indicated protons **a**, **b** and **c** were followed in the NMR study.

2.6.3.4. NMR study.

To determine if the isoxazole nucleus or the calixarene framework was most important for attracting the guest key signals to monitor include the resonance signal for the isoxazole proton, the phenolic proton and the pyrene aromatic protons. In the host molecule, **PIC** (Figure 2.30), the isoxazole proton (H_c) resonates at 6.43 ppm, H_a resonates at 5.28 ppm, H_b resonates at the range of 3.50 and 4.15 ppm, and the phenolic OH at 7.92 ppm. Some significant spectral changes can be observed in the ^{1}H NMR Spectra of **PIC** upon the addition of Cu^{2+} ion (Figure 2.31a) whereas there is nearly no change to the **PIC** data in the presence of Zn^{2+} ions (Figure 2.32a).

With the addition of 0.5 eq. Cu^{2+} to **PIC**, the isoxazole ring proton H_c undergoes a downfield shift and peak broadening. After adding a further 0.5 eq., a slight upfield shift was observed and the peak became sharper. Finally when 2.0 eq. of metal salt was added, the isoxazole proton peak became totally broadened and deshielded by a further 0.018 ppm. All the aromatic protons between 8-7 ppm became broader but

only a very small chemical shift difference can be seen (0.01%). The H_a methylene protons of the -OCH_2-isoxazole unit were shifted from 5.2370 to 5.2873 ppm. In contrast, whilst the methylene protons of the calixarene framework did become broader there was almost no chemical shift change. Significantly the signals representing the aromatic protons of the calixarene skeleton remained sharp over the range of spectra recorded.
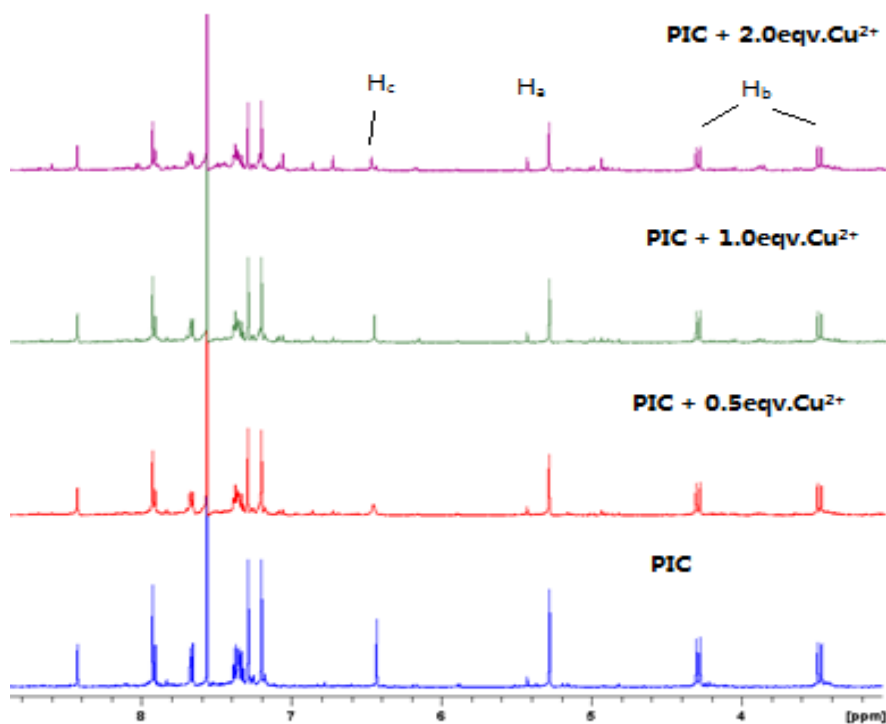
Figure 2.31a. ^{1}H NMR spectra of host **PIC** in the presence of 0.0. 0.5, 1.0 and 2.0 eq. of Cu^{2+} ion.

Interestingly, upon the addition of Cu^{2+} to **monoPiM** (Figure 2.31b), the ^{1}H NMR spectra exhibit a palpable broadening of all pyrene aromatic protons (H_a in Figure 2.30.) (in the range of 8.1-8.6 ppm). In contrast the aromatic protons and the CH_2O resonances of aryl-OCH_2-isoxazole (H_b in Figure 2.30.) framework did not change at all. The isoxazole proton (H_c) was deshielded from 6.981 to 6.993 ppm and appeared somewhat broadened.
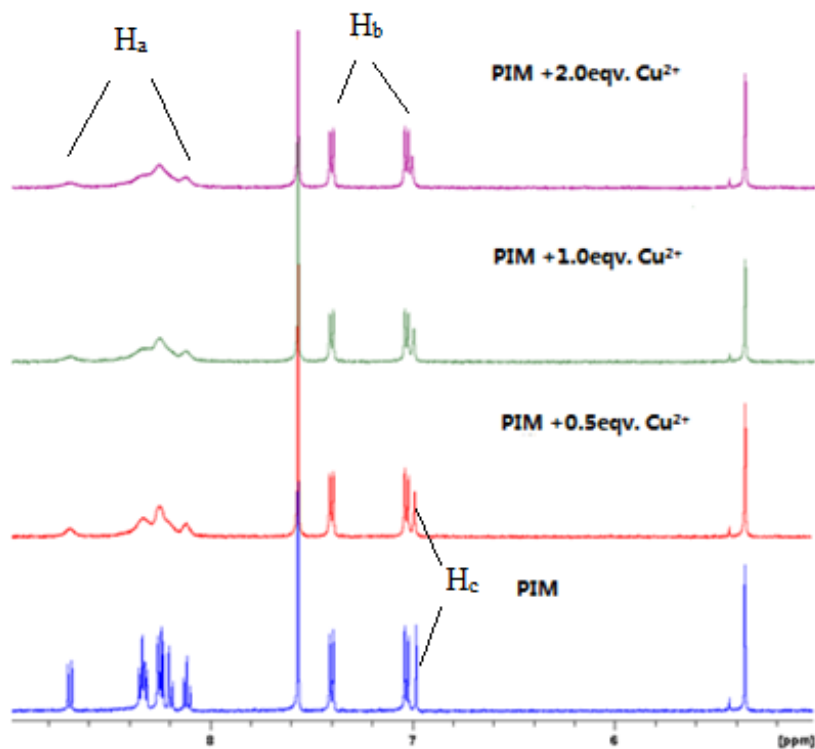
Figure 2.31b. ^{1}H NMR spectra of **monoPiM** with 0.5, 1.0 and 2.0 eq. of Cu^{2+} ion.

Comparing the data obtained for the hosts in the presence of Cu^{2+}, to that obtained following the addition of Zn^{2+} to both **PIC** and **monoPiM**, it was obvious, in both cases that no significant spectral changes resulted from the addition of even 2.0 eq. of Zn^{2+} (Figure 2.32a-b). All the aromatic peaks became very slightly broad but not nearly to the extent observed when Cu^{2+} was added. With this data, the high selectivity of **PIC** for Cu^{2+} ion is confirmed. These qualitative observations could, with further study be analyzed to give quantitative information on the binding of **PIC** and copper ions.
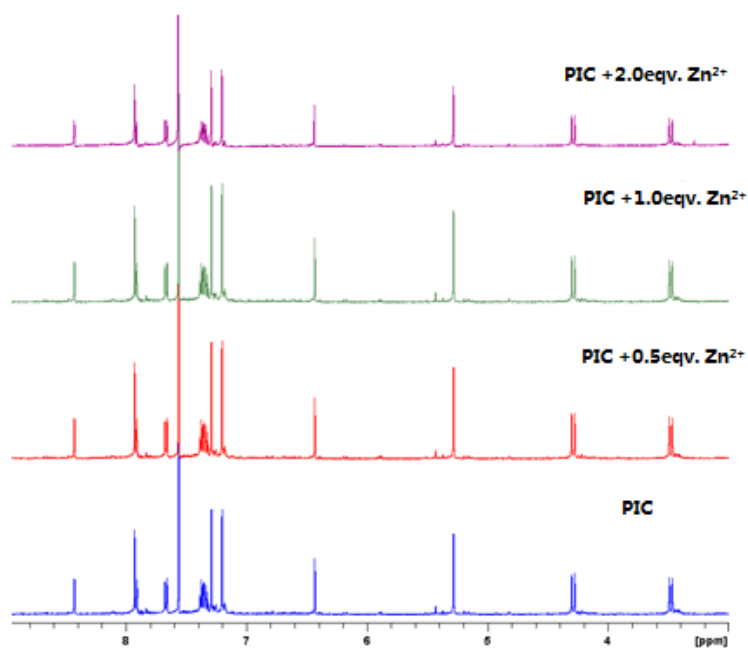
Figure 2.32a. ^{1}H NMR spectra of host **PIC** with 0.0, 0.5, 1.0 and 2.0 eq. of Zn^{2+} ion.
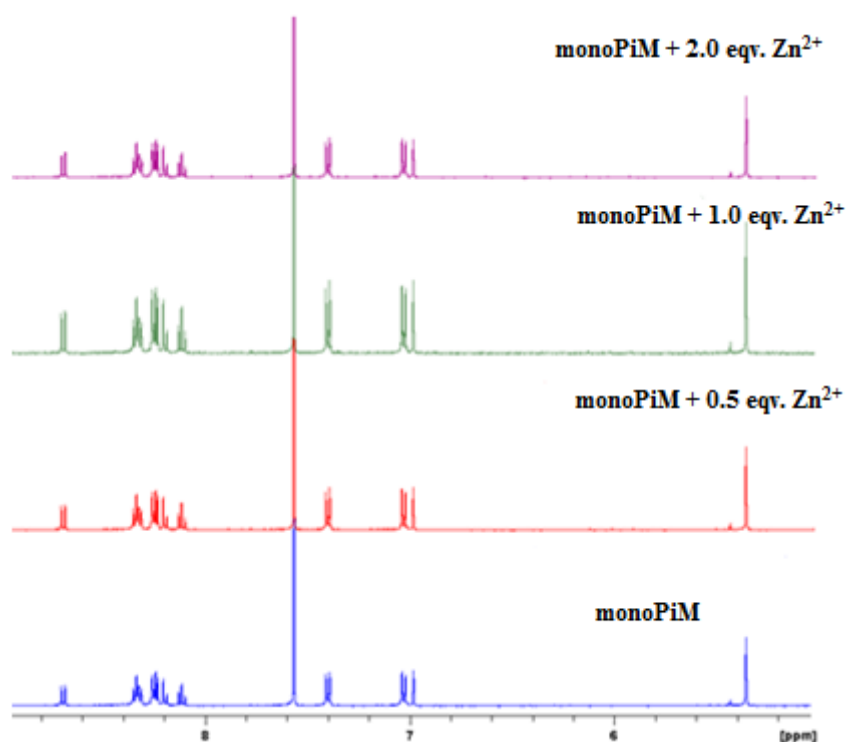
Figure 2.32b. ^{1}H NMR spectra of host **monoPiM** with 0.0, 0.5, 1.0 and 2.0 eq. of Zn^{2+} ion.

2.6.4. Conclusion.

A highly Cu^{2+} selective fluorogenic calix[4]arene chemosensor **PIC** has been designed and synthesized. Upon addition of Cu^{2+}, a dramatic fluorescence quenching

of the **PIC** host was observed. Moreover, the effects of anions (e.g. Cl$^-$, NO$_3^-$) on fluorescence intensity were studied and it was observed that the most effective quenching arose from the perchlorate salt. Analysis of the data by Job's plot indicated 1:1 complexation between the host and guest (**PIC** and Cu^{2+}). That the data from a Stern-Volmer plot fitted no better, or worse, to a second order curve than to a straight line does not allow any conclusion to be drawn on the relative importance of dynamic and static quenching processes in the host-guest system.

2.7. 1,3-Dipolar cycloaddition by "copper-free" click reaction.

2.7.1 Overview.

"Click chemistry" illustrates a variety of organic reactions which proceed rapidly, under mild reaction conditions and afford products in high yield.[45] Among the click reactions reported to date, the bioorthogonal, Copper-free azide alkyne Huisgen cycloaddition, developed by Carolyn Bertozzi, is most attractive. The reaction which uses a ring-strained cyclooctyne as an activated alkyne partner has been applied, without toxicity, in living cells. The reaction, known as a strain-promoted alkyne-azide cycloaddition (SPAAC) is widely used in chemical biology, and it is generically illustrated for a bioconjugation protocol in Figure 2.33 below. It has been applied to labeling of biomolecules[68] (proteins, lipids) and modification of oligonucleotides[45] as well as cell and tissue surface engineering applications.[69] SPAAC takes advantage of ground-state destabilization, or ring strain of the eight-membered ring, to accelerate triazole formation under mild conditions, including physiological or ambient conditions.[70] It was developed as a faster alternative to the Staudinger ligation (Figure 2.34). The Staudinger reaction is a chemical reaction in which the combination of an azide with a phosphite or phosphine affords an iminophosphorane intermediate.
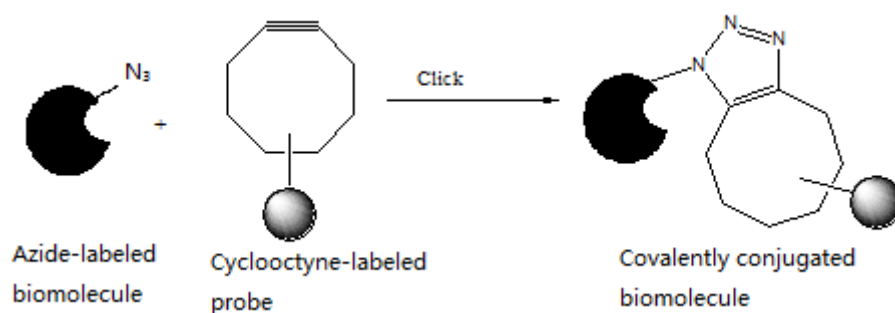
Figure 2.33. The Copper-Free azide alkyne Huisgen cycloaddition,.
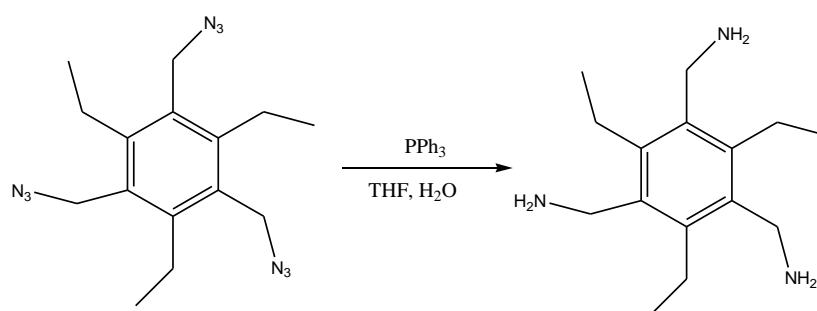
Figure 2.34. The Staudinger reaction[71]. SPAAC was developed as a faster alternative

to the Staudinger ligation

Mechanistically the SPAAC reaction proceeds as a standard 1,3-dipolar cycloaddition and the regioisomeric ring fused products are obtained as shown in Figure 2.35 below).[72]
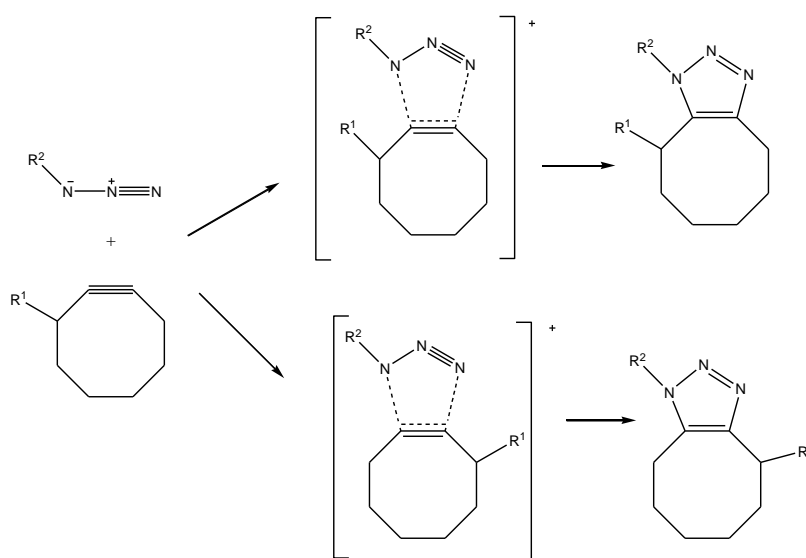
Figure 2.35. The mechanism of the copper-free SPAAC reaction.

As mentioned above, a significant advantage of the SPAAC reaction is the ability to conduct bioconjugation protocols in the absence of a potentially toxic copper catalyst. However, the avoidance of toxicity by eliminating the copper catalyst carries a penalty. The regioselectivity of the copper-promoted triazole-forming reaction is lost, and in the catalyst-free version both regioisomers are usually formed in approximately equal amounts. As part of my research toward this MSc thesis I set out to explore the hypothesis that regioselectivity in the nitrile oxide-cycloalkyne cycloaddition could be reintroduced with judicious choice of substituents on the reacting dipole and dipolarophile. I wished to explore the possibility that substituents capable of *H*-bonding, on the dipole, and on the dipolarophile, may be effective in promoting one alignment over the other in the transition state leading to ring formation. To this end, I prepared a range of (hydroxyalkoxy)benzaldehyde oximes and explored the regioselectivity of their cycloaddition to hydroxyalkoxy-substituted cyclooctynes.

2.7.2. Synthesis and characterization of **70** and **71**.

3-(Cyclooct-2-yn-1-ylmethoxy)propan-1-ol (**69**)[73], first reported within the research group by Dr. Singh, was selected as the cyclooalkyne of choice. The pendant hydroxyl group gives this molecule the possibility to *interact* during the transition state, with dipoles bearing either H-bond donor, or H-bond acceptor substituents. This potential interaction we anticipated may be sufficient to anchor the reactants towards regioselective cycloaddition.

The preparation of this substituted alkyne was technically challenging. The first step of the sequence is the dibromosubstitution of cycloheptene. The reactants, cycloheptene and bromoform, in the presence of KO^{t}Bu, were stirred at 0 ℃ in dark for 6 hours, prior to standing in dark overnight at r.t. The dibromobicycle compound **67** was obtained in 45% yield. Ring opening of **67** with 1,4-butanediol was achieved in the presence of silver perchlorate to afford the bromoalkene **68** which was used for the next step without purification. Sodium-hydride-induced elimination of HBr from **68** gave the desired product **69** in 50% yield (Scheme 2.6).

CHBr$_3$

KO^{t}Bu

Pentane

0° C, 6 hours under Ar,
then r.t. 18 hours under Ar

Br   Br

67

Ag(ClO$_4$)$_2$
toluene/pyridine/dark
reflux, 4 hours

1,4-butandiol

HO

NaH

DMF/THF
r.t. 5 hours

HO

Br

O

O

69

68
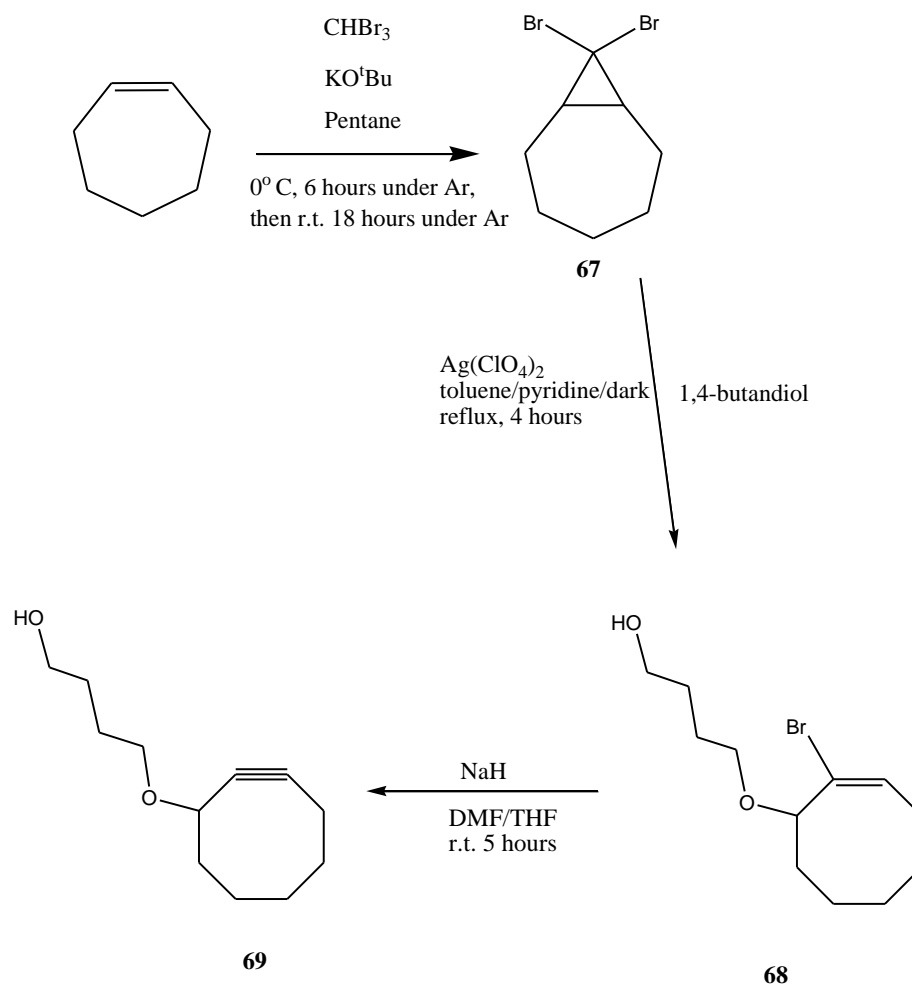
Scheme 2.6. The synthesis route to the desired cyclooctyne **69**.

Oximes selected for study were the *o-* and *p*-(2-hydroxyethoxy)benzaldehyde oximes **54** and **56** as well as the *p*-(6-hydroxyhexyloxy)benzaldehyde oxime. These substrates we believed could inform on the relationship between linker length and orientation of the potential H-bonding groups on the regioselectivity of the cycloaddition reaction. The desired oximes **54** and **56** were prepared uneventfully from their parent aldehydes and cycloaddition was initially investigated between the nitrile oxide generated from **54** and the cyclic alkyne **69**.

The cycloaddition was explored by heating the reactants in the presence of chloramine-T at reflux in aqueous ethanol for 18 hours (Scheme 2.7). After that, the crude reaction products were examined by ^{1}H NMR spectroscopy (Figure 2.36). The relative intensity of the signals representing protons CH-O (H$_c$) was used to judge the regioselectivity of the reaction. The resonances for these diagnostic protons in the

regioisomeric products appeared at ~4.7 and 4.5 ppm (CDCl$_3$). They were of approximately equal intensity (~1:1 ratio) (Figure 2.36) and the crude products, formed without regiochemical preference were purified by flash column chromatography (SiO$_2$, ethyl acetate:hexane = 3:1). The two isomers separated well and were characterized individually (31% and 38% yield Figure 2.37 and Figure 2.38). The failure of the pendant hydroxy groups on the reactants to induce regioselectivity was disappointing, but it is possible that the linker between dipole and hydroxyl terminus was not of the correct length to facilitate a H-bonding attraction to the dipolarophile so favouring one regiochemical alignment over the other.

Scheme 2.7. The synthesis route to the two regiosiomers; **A** has been assigned to the stereoisomer with the more downfield H$_c$ (at 4.7 ppm), and **B** to the one at 4.5 ppm.

Figure 2.36. ^{1}H NMR spectrum (CDCl$_3$, 300 MHz) of the crude products of

cycloaddition between oxime **56** and cycloalkyne **69**.
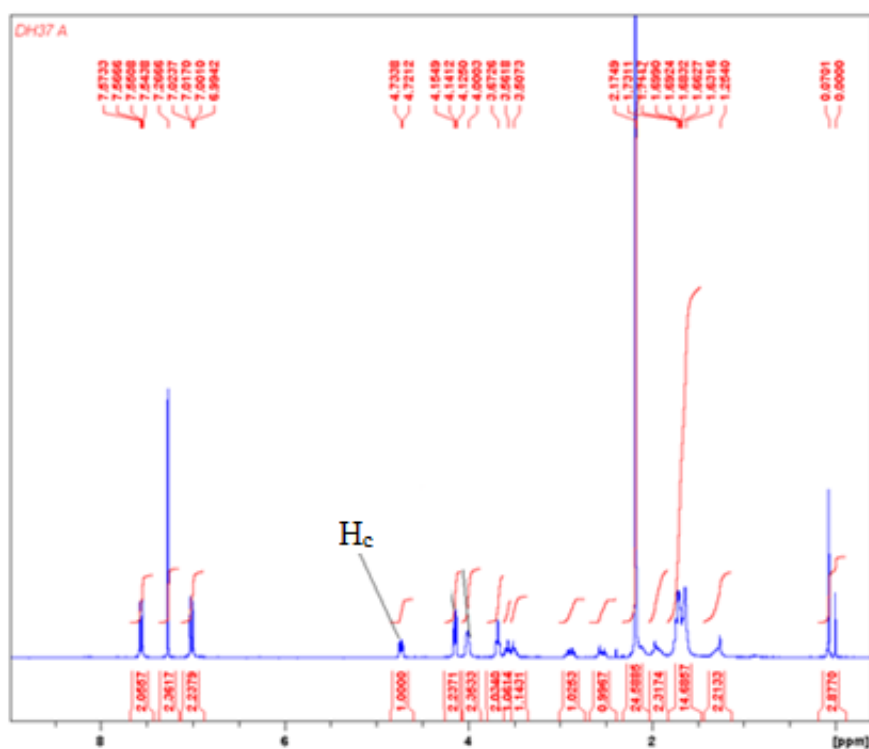
Figure 2.37. ^{1}H NMR spectrum (CDCl$_3$, 300 MHz) of the regioisomer **A** in which the

H$_c$ proton is more downfield than the one in **B**.
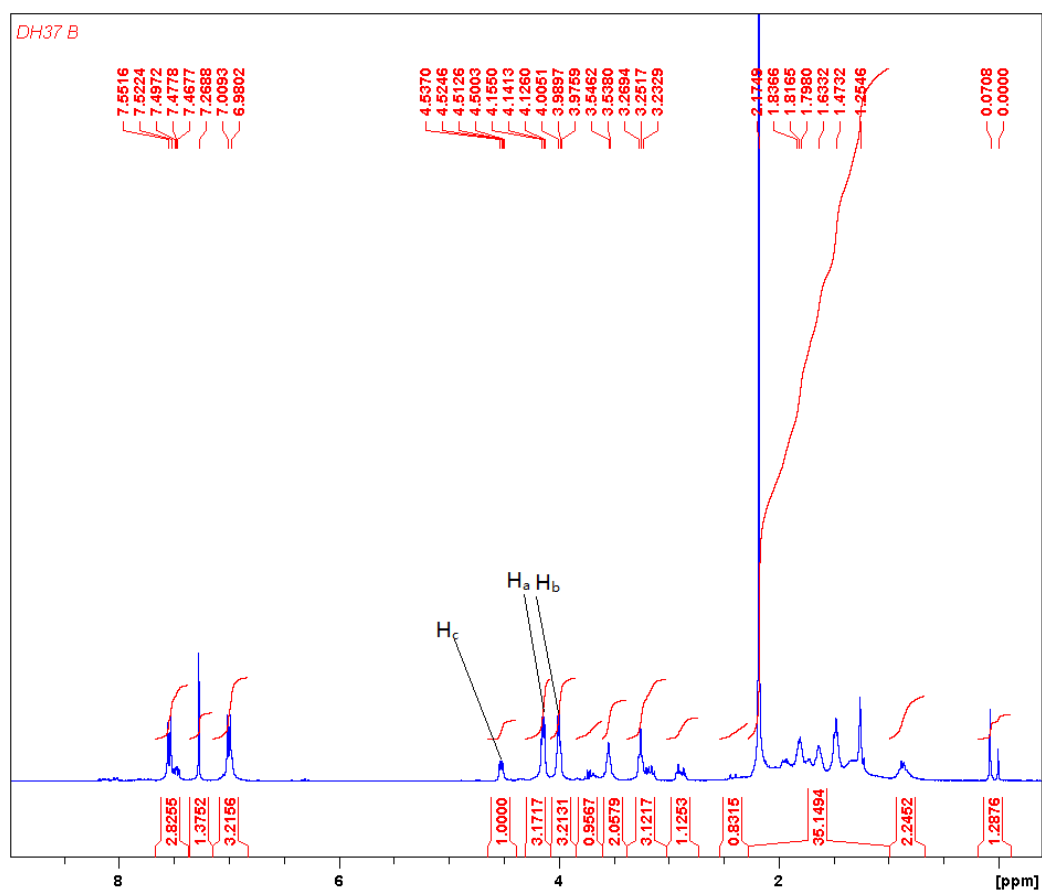
Figure 2.38. ^{1}H NMR (CDCl$_3$, 300 MHz) of regioisomer **B**.

The proton NMR data of regiosiomer **A** was assigned with the assistance of a ^{1}H^{1}H 2D-COSY spectrum (Figure 2.39). The significant cross peaks on this spectrum are those between H$_c$ (at 4.72 ppm) with H$_a$ and H$_b$ at (2.18 and 1.95 ppm). The cross peaks at 7.53 and 7.00 are those indicating coupling between the aromatic protons. Cross peaks at 4.13 and 3.99 indicate coupling of the two OCH$_2$ methylene groups of the hydroxyethoxy chain. The remaining cross peaks arise from the CH$_2$'s of longer chain and the eight-membered ring. (The protons of regioisomer **B** were assigned in the same way).
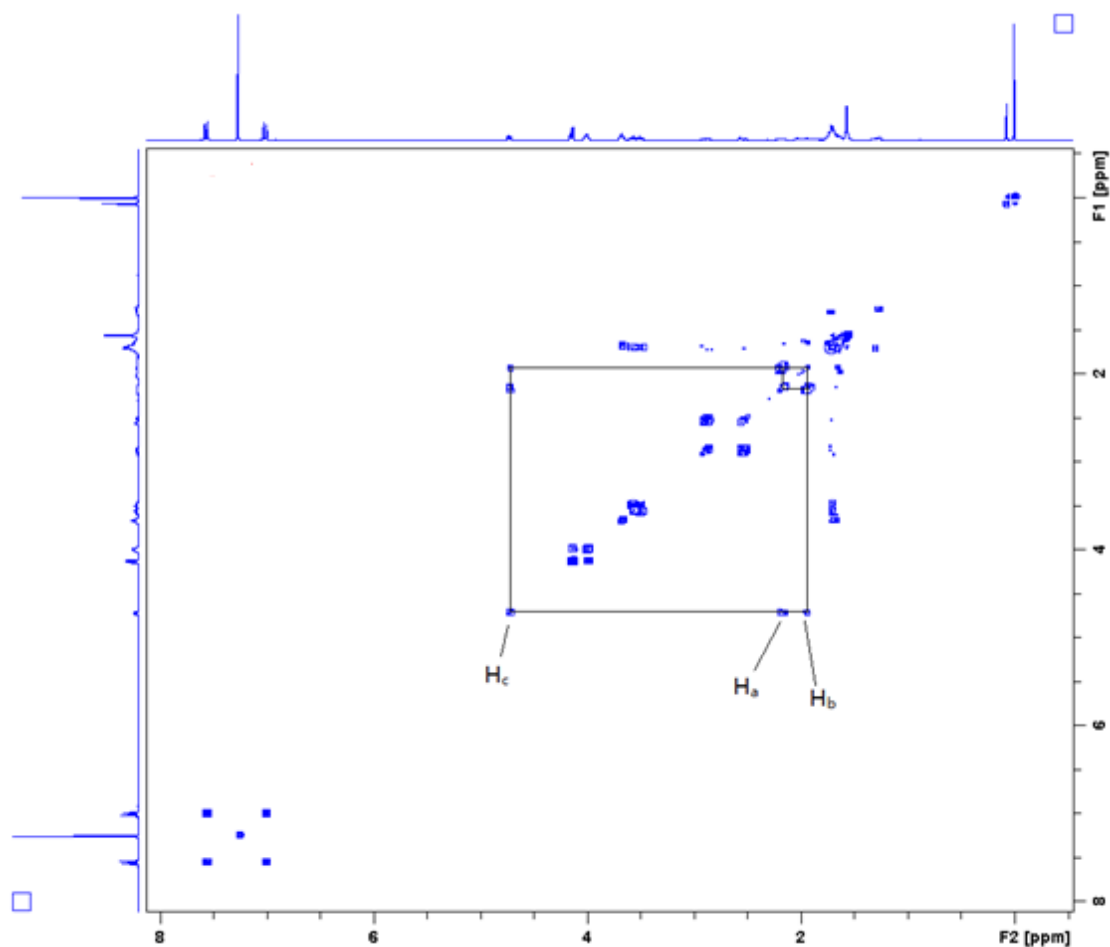
Figure 2.39. ^{1}H^{1}H 2D-COSY spectrum of regioisomer **A**.

2.7.3. Synthesis and characterization of **72** and **73.**

A study of the regioselectivity of the cycloaddition between the nitrile oxide generated from the *o*-isomer of (2-hydroxyethoxy)benzaldehyde oxime **54** and the cyclooctyne **69** provided an opportunity to comment on steric effects on regioselectivity. Cycloaddition with **54** was conducted under the same reaction conditions. ^{1}H NMR spectrum of the crude reaction products (Figure 2.40.) showed only a marginal regioselectivity. Thus the relative integral of the diagnostic OCH signals at 4.74 and 4.36 ppm indicate the isomers were present in a ratio of 1:1.26. Thus the different steric demands of the nitrile oxide appear to have had little influence over the regioselectivity of the reaction. Unfortunately, despite exploring a wide variety of solvent systems, it proved impossible to obtain separate samples of the regioisomeric cycloadducts. After attempted purification by flash column

chromatography (SiO$_2$, EtOAc:hexane, 3:1), the cycloaddition products, containing both isomers **72** and **73**, was obtained as a yellow gum, 63% yield.
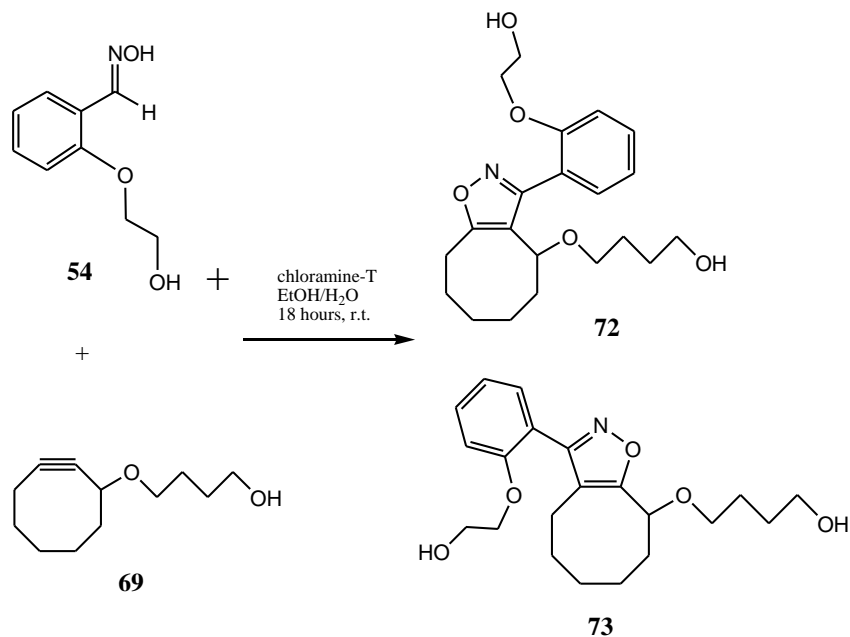
Equation 2.6. The cycloaddition between **54** and **69** to afford two isomers **72** and **73.**
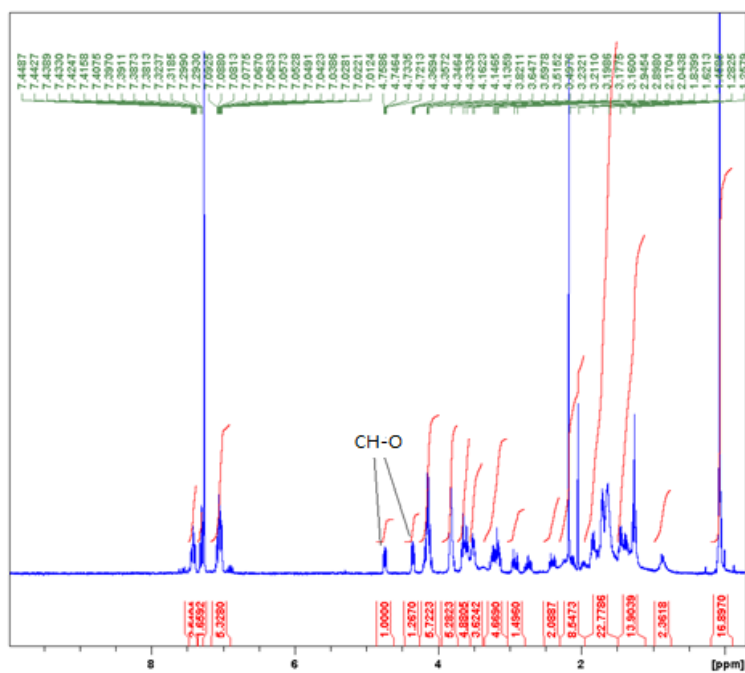
Figure 2.40. The ^{1}H NMR spectrum (CDCl$_3$, 300 MHz) of the crude products resulting from cycloaddition between oxime **54** and cycloalkyne **69**.

2.7.4. Synthesis and characterization of **74** and **75**

The nitrile oxide generated from *p*-(6-hydroxyhexyloxy)benzaldehyde oxime (obtained from previous group researchers), which contains a longer CH_2 chain, again provided an opportunity to study the potential influence of *H*-bonding interactions. The proton NMR spectrum of the crude products of reaction (Equation 2.7) between this oxime and the cyclic alkyne under the standard conditions is shown in Figure 2.41. Once again the indicator of the selectivity is taken as the relative size of the integrals for the resonances representing the OCH ring protons. The ratio of these signals was determined to be 0.9:1.0 and thus in this case we disappointingly conclude no regioselectivity could be induced by the pendant groups with potential for *H*-bonding. The pure product (both isomers) was obtained from column chromatography (SiO_2, EtOAc: hexane, 6:1) in 73% yield.
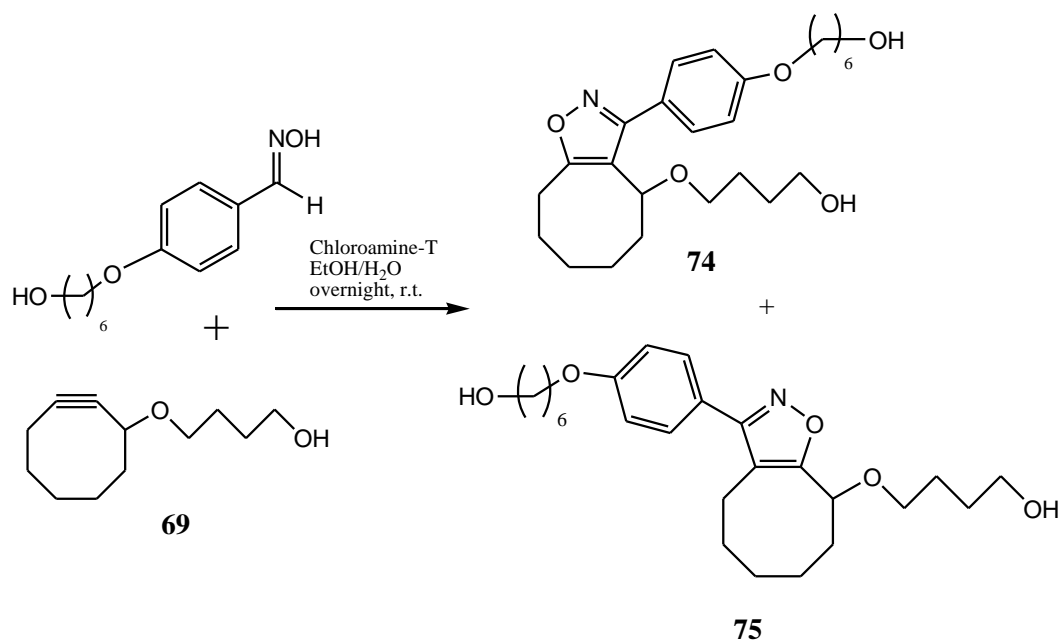
Equation 2.7. The copper-free cycloaddition of *p*-(6-hydroxyhexyloxy)benzaldehyde oxime and **69.**
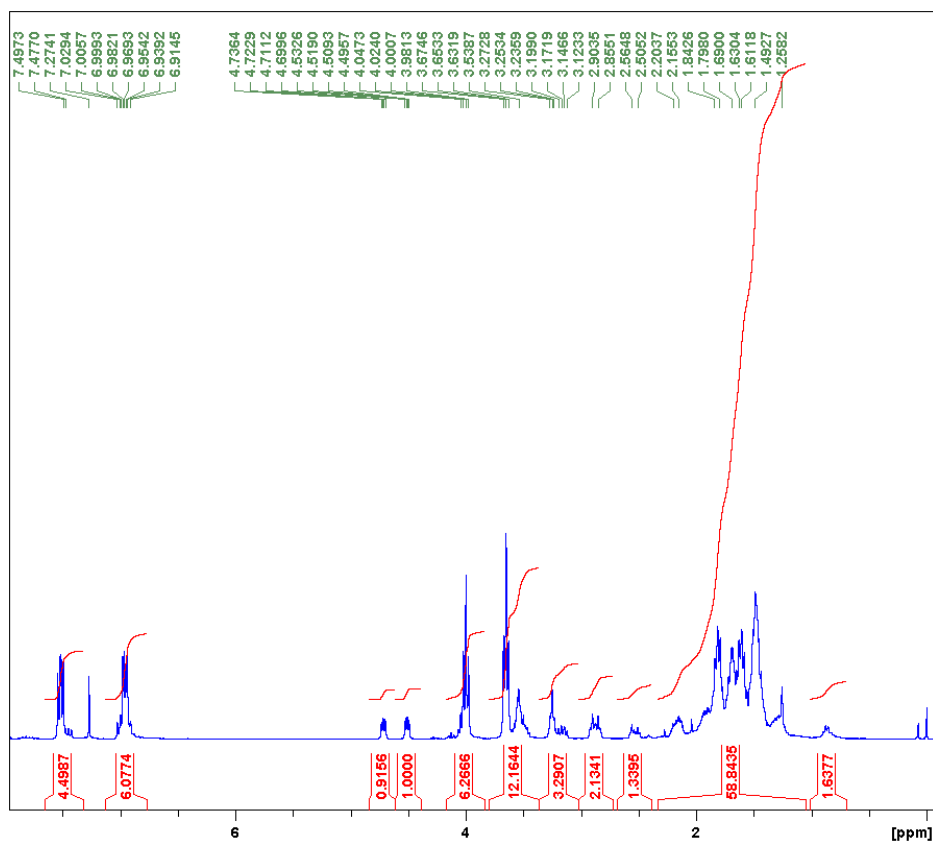
Figure 2.41. The ^{1}H NMR spectrum (CDCl$_3$, 300 MHz) of pure product (contains both **74** and **75**).

2.7.5. Conclusion.

The SPAAC explored between hydroxyalkoxybenzaldehyde-oxime-derived nitrile oxides and hydroxybutoxycyclooctynes progressed readily albeit without any attractive regioselectivity. The choice of aqueous ethanol as solvent is to facilitate dipole formation from the oxime by reaction with chloramine-T. It is of course likely that *H*-bonding of the individual reactant partners to solvent molecules far outweighed any chance for interaction between the hydroxyl groups of the dipole and dipolarophile to be able to influence alignment in the transition state leading to cycloadduct formation. In the future this reaction will be repeated using e.g. chlorooximes as precursors to nitrile oxides and a solvent incapable of H-bonding.

Chapter 3
Experimental

3.0. **Instrumentation**.

Reagents and starting materials were supplied by Sigma-Aldrich and Alfa Aesar which were used without purification. Solvents were used as purchased except DMF and toluene which were distilled before use. Products were characterized by NMR, IR and Mass spectroscopy. NMR spectra were recorded on a Bruker Avance 300 MHz spectrometer at room temperature in $CDCl_3$ solution. IR spectra were recorded as KBr discs or liquid films between NaCl plates using a Perkin Elmer system 2000-FT-IR spectrophotometer. MS was recorded in LC/TOF-MS model 6210 Time-Of-Flight LC/MS with an electrospray source positive and negative (ESI+/−), capillary 3500 V, nebuliser spray 30 psig, drying gas 5 L/min and source temperature 325 ℃. The fragmentor was used at 175 V. The LC was run on a 1200 series model and injection volumes were typically 10 μL. Column used was an Agilent Eclipse XBD-C18. A diameter of 5-micron was employed. UV/vis spectra were recorded using a Unicam UV 500 spectrometer. For fluorescence data, the excitation and emission spectra were recorded on a JASCO FP-6300 spectrafluorometer. The further NMR study for **PIC** was recorded on a Bruker Avance 500 MHz spectrometer at the Institute of Technology Tallaght, Ireland.

3.1. 1-Pyrenecarbaldehyde oxime (51)[74]

51
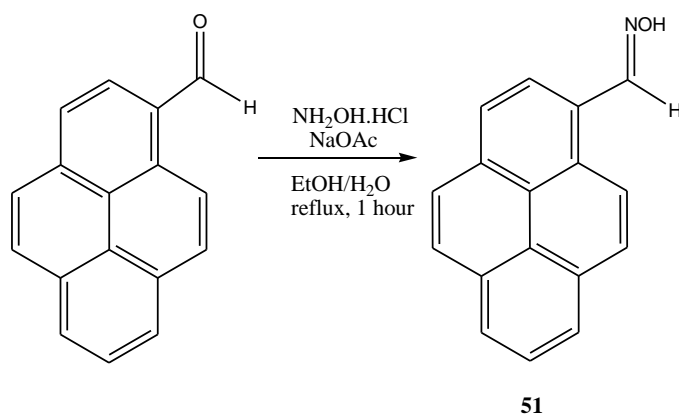
1-Pyrenecarbaldehyde (0.20 g, 0.8 mmol), $NH_2OH \cdot HCl$ (0.18 g, 2.6 mmol) and EtOH (8 mL) were added into a 50 mL round bottomed flask. NaOAc (0.24 g, 3.5 mmol) in water (4 mL) was added. The mixture was heated at reflux (80 ℃) for 1 hour. After cooling, water (10 mL) was added and the mixture was extracted with EtOAc (10 mL x 3). The organic layers were combined, washed with base and dried over anhydrous $MgSO_4$. The solvent was removed under vacuum. The product was obtained as yellow solid (0.19 g, 89 %). M.p. = 179-186 ℃.

^{1}H NMR (300 MHz, CDCl$_3$) δ: 9.15 (1H, s, CH=N), 8.60 (1H, d, J = 9.3 Hz, ArH), 8.38 (1H, d, J = 8.1 Hz, ArH), 8.25-8.01 (7H, m, ArH), 7.57 (1H, br. s, OH). Data are in good agreement with the literature.[74]

3.2. Benzaldehyde oxime (52)[51]

52
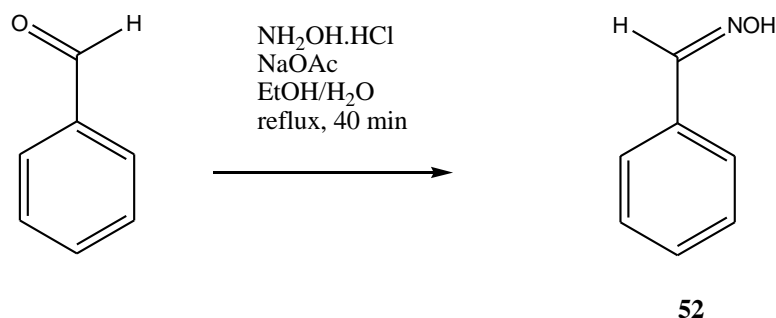
Benzaldehyde (2.00 g, 18.9 mmol), hydroxylamine hydrochloride (3.96 g, 56.6 mmol) and EtOH (80 mL) were added into a 250 mL round bottomed flask. NaOAc (5.29 g, 75.6 mmol) in water (40 mL) was added. The mixture was heated at reflux (80 ℃) for 40 minutes. After cooling, water (100 mL) was added. The mixture was extracted with EtOAc (60 mL x 3). The organic layers were combined, washed with 5% NaOH

(30 mL x 2) and dried over anhydrous MgSO$_4$. The solvent was removed under vacuum. The product was obtained as a light-yellow oil (0.34 g, 66 %), suitable for usage without further purifications. M.p. = 119-125 ℃.

^{1}H NMR (300 MHz, CDCl$_3$) δ: 8.23 (1H, s, CH=N), 7.89-7.60 (2H, m, ArH), 7.58-7.28 (3H, m, ArH). Data are in good agreement with the literature.[51]

3.3. 1-Naphthalenecarbaldehyde oxime (53)[51]

53
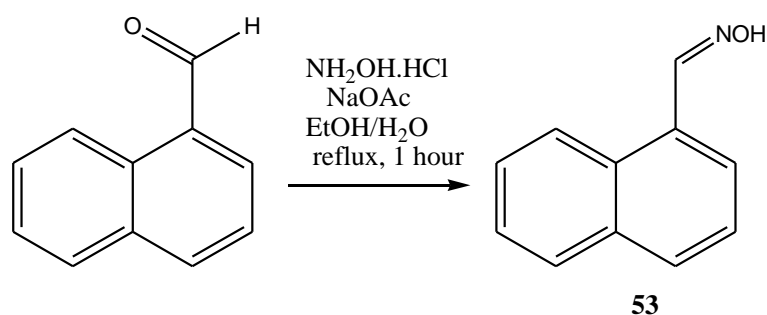
1-Naphthalenecarbaldehyde (1.00 g, 6.3 mmol), hydroxylamine hydrochloride (1.35 g, 19.3 mmol) and EtOH (40 mL) were added into a 100 mL round bottomed flask. A solution of NaOAc (1.79 g, 25.5 mmol) in water (20 mL) was added. The mixture was heated at reflux (80 ℃) for 1 hour. After cooling, water (100 mL) was added. The mixture was extracted with EtOAc (20 mL x 3). The organic layers were combined, washed with 5% NaOH (20 mL x 2) and dried over anhydrous MgSO$_4$. The solvent was removed under vacuum. The product was obtained as a light-yellow solid (1.20 g, 87 %), suitable for next experiment without further purifications. M.p. = 92-96 ℃.

^{1}H NMR (300 MHz, CDCl$_3$) δ: 8.82 (1H, s, CH=N), 8.45 (1H, d, J = 8.7 Hz, ArH), 7.92-7.87 (2H, m, ArH), 7.77 (1H, d, J = 7.2 Hz, ArH), 7.61-7.46 (3H, m, ArH). Data are in good agreement with the literature.[51]

3.4. 2-(2-Hydroxyethoxy)benzaldehyde oxime (54)[48]

54
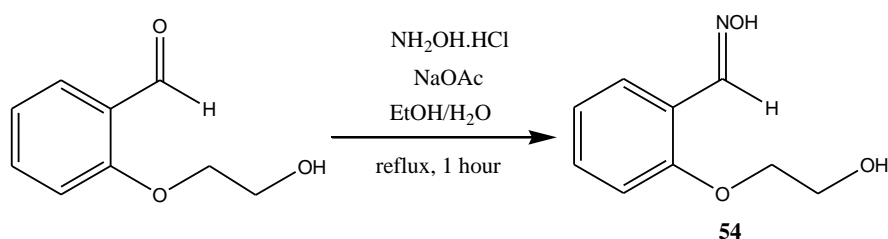
2-(2-Hydroxyethoxy)benzaldehyde (2.01 g, 12.0 mmol), $NH_2OH \cdot HCl$ (2.53 g, 36.1 mmol) and ethanol (80 mL) were added into a 250 mL round bottomed flask. NaOAc (3.37 g, 48.1 mmol) in water (40 mL) was added. The solution was stirred at reflux (85 ℃) for 1 hour. After cooling to room temperature, the ethanol was removed under vacuum. The aqueous residue was extracted with ethyl acetate (3 x 20 mL) and washed with water (20 mL). After drying over anhydrous $MgSO_4$, the EtOAc was evaporated to afford the product as a white solid (1.58 g, 73 %) which was pure enough for further reaction. M.p. = 98-100 ℃.

^{1}H NMR (300 MHz, $CDCl_3$) δ: 8.39 (1H, s, CH=N), 7.56 (1H, dd, J = 1.5 & 7.5 Hz, ArH), 7.38-7.31 (1H, m, ArH), 7.03-6.94 (2H, m, ArH), 4.16 (2H, t, J = 4.5 Hz, CH_2), 3.97 (2H, t, J = 4.5 Hz, CH_2). ^{13}C NMR (75 MHz, $CDCl_3$) δ: 157.2, 147.4, 131.2, 128.5, 121.5, 121.2, 113.5, 70.5, 61.3; IR (KBr) 3392, 3219, 1601, 1251, 764 cm^{-1}; HRMS (ESI) calcd for [M+Na]$^+$, $C_9H_{11}NO_3Na$, 204.0631, found 204.0640.

3.5. 2-(3-Hydroxyethoxy)benzaldehyde oxime (55)[48]

55
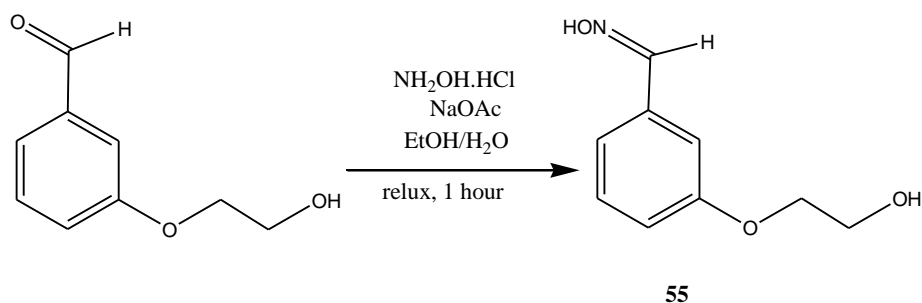
2-(3-Hydroxyethoxy)benzaldehyde (2.02 g, 12.2 mmol), $NH_2OH \cdot HCl$ (2.53 g, 36.14 mmol) and ethanol (80 mL) were added into a 250 mL round bottomed flask. NaOAc (3.37 g, 48.1 mmol) in water (40 mL) was added. The solution was stirred at reflux (85 ℃) for 1 hour. After cooling to room temperature, the ethanol was removed under vacuum. The aqueous residue was extracted with ethyl acetate (3 x 20 mL), washed with water (20 mL) and dried over anhydrous $MgSO_4$. The solvent was removed under vacuum. The desired compound was obtained as a pale yellow solid (1.53 g, 71 %) suitable for use without further purification. M.p. = 94-96 ℃.

^{1}H NMR (300 MHz, $CDCl_3$) δ: 8.10 (1H, s, CH=N), 7.87 (1H, br s, OH), 7.33-7.30

(1H, m, ArH), 7.20-7.12 (2H, m, ArH), 6.98-6.93 (1H, m, ArH), 4.11 (2H, t, J = 4.5 Hz, CH$_2$), 3.98 (2H, t, J = 4.5 Hz, CH$_2$). ^{13}C NMR (75 MHz, CDCl$_3$) δ: 157.0, 147.7, 131.5, 128.9, 121.6, 121.5, 113.4, 70.6, 61.1; IR (KBr) 3352, 3156, 1600, 1260, 907, 795 cm^{-1}; HRMS (ESI) calcd for [M+H]$^+$, C$_9$H$_{12}$NO$_3$, 182.0814, found 182.0810.

3.6. 4-(2-Hydroxyethoxy)benzaldehyde oxime (56)[48]

56
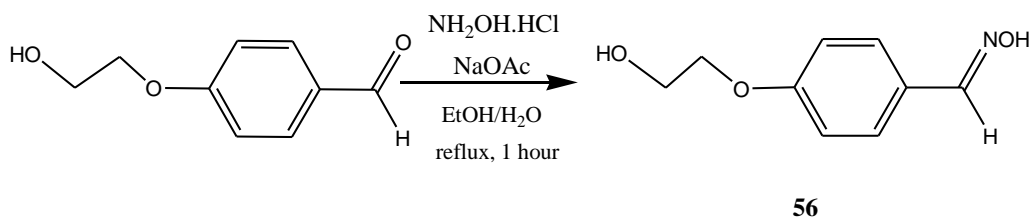
4-(2-Hydroxyethoxy)benzaldehyde (1.00 g, 6.0 mmol), NH$_2$OH.HCl (1.76 g, 25.1 mmol) and ethanol (40 mL) were added into a 100 mL round bottomed flask. NaOAc (1.69 g, 24.1 mmol) in water (20 mL) was added. The solution was stirred at reflux (85 ℃) for 1 hour. After cooling to room temperature, the solvent was removed under vacuum. The aqueous residue was extracted with ethyl acetate (3 x 40 mL), washed with water (2 x 20 mL) and dried over anhydrous MgSO$_4$. The solvent was removed under vacuum. The desired product was obtained as a white solid (0.90 g, 90 %) pure enough for the further reaction. M.p. = 109-111 ℃.

^{1}H NMR (300 MHz, CDCl$_3$) δ: 8.08 (1H, s, CH=N), 7.52 (2H, d, J = 9.0 Hz, ArH), 7.19 (1H, br s, OH), 6.93 (2H, d, J = 9.0 Hz, ArH), 4.12 (2H, t, J = 4.5 Hz, CH$_2$), 4.00 (2H, t, J = 4.5 Hz, CH$_2$). ^{13}C NMR (75 MHz, CDCl$_3$) δ: 160.1, 149.9, 128.5, 125.2, 114.8, 69.3, 61.4; IR (KBr) 3262, 1605, 1259, 836 cm^{-1}; HRMS (ESI) calcd for C$_9$H$_{11}$NO$_3$Na, [M+Na]$^+$, 204.0628, found 204.0624.

3.7. 9-Anthraldehyde oxime (57)[75]

57
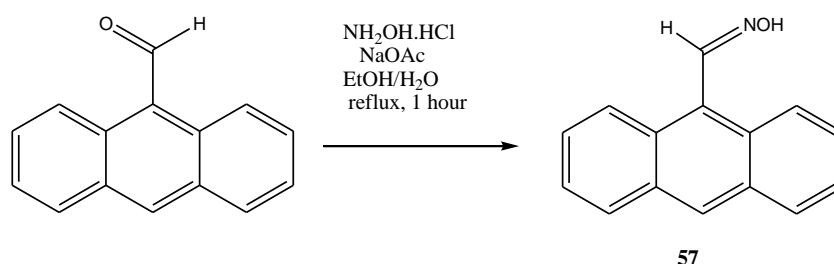
9-Anthracenecarbaldehyde (1.00 g, 4.8 mmol), NH$_2$OH.HCl (1.02 g, 1.4 mmol) and EtOH (40 mL) were added into a 100 mL round bottomed flask. NaOAc (1.36 g, 19.4 mmol) in water (20 mL) was added. The mixture was heated at reflux (80 ℃) for 1 hour. After cooling, water (10 mL) was added and the mixture was extracted with EtOAc (20 mL x 3). The organic layers were combined, washed with 5% NaOH (10 mL x 2) and dried over anhydrous MgSO$_4$. The solvent was removed under vacuum. The product was obtained as a yellow solid (0.80 g, 75 %). M.p. = 164-174 ℃.

^{1}H NMR (300 MHz, CDCl$_3$) δ: 9.22 (1H, br s, OH), 8.51 (1H, s, CH=N), 8.42 (2H, d, J = 8.7 Hz, ArH), 8.03 (2H, d, J = 8.7 Hz, ArH), 7.90 (1H, s, ArH), 7.60-7.47 (4H, m, 4 x ArH). Data are in good agreement with the literature.[75]

3.8. *1H*-Indole-3-carbaldehyde oxime (58)[51]
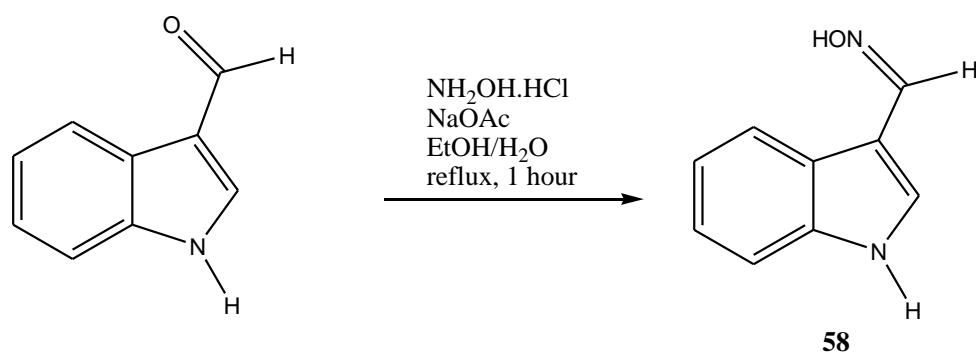
1H-Indole-3-carbaldehyde (0.11 g, 0.7 mmol), hydroxylamine hydrochloride (0.16 g, 2.3 mmol) and ethanol (4 mL) were added into a 50 mL round bottomed flask. NaOAc (0.22 g, 3.1 mmol) dissolved in water (2 mL) was added. The mixture was heated at reflux (80 ℃) for 1 hour. After cooling, water (6 mL) was added. The mixture was extracted with ethyl acetate (3 x 10 mL). The organic layers were combined, washed with base and then dried over anhydrous MgSO$_4$. Solvent was removed under vacuum. The product was obtained as a pink solid (0.11 g, 85 %). M.p. = 195-203 ℃.

^{1}H NMR (300 MHz, CDCl$_3$) δ: 11.57 (1H, br. s, OH), 11.17 (1H, s, NH), 8.22 (1H, d, J = 2.4 Hz, CH=N), 7.85 (1H, d, J = 7.5 Hz, ArH), 7.78 (1H, s, CH-N), 7.44 (1H, d, J = 7.8 Hz, ArH), 7.20-7.08 (2H, m, ArH). ^{13}C NMR (75 MHz, CDCl$_3$) δ: 139.4, 136.3, 131.6, 127.4, 123.0, 121.2, 118.7, 112.5, 107.8; *m/z* [M+H]$^+$ calculated for C$_9$H$_9$N$_2$O

161.0821.

3.9. 1-*tert*-Butyl-4-(prop-2-ynyloxy)benzene (59)[52]
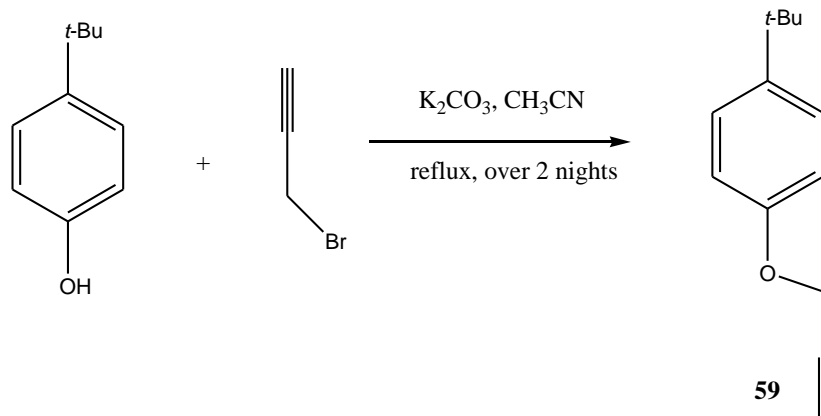
K$_2$CO$_3$ (1.38 g, 10.0 mmol) and 4-*tert*-butylphenol (1.00 g, 6.7 mmol) were added to a solution of CH$_3$CN (15 mL) and propargyl bromide (0.95 g, 8.0 mmol). The mixture was heated at reflux for 2 days and left standing overnight at room temperature. Water (30 mL) was added and the mixture was extracted with DCM (15 mL x 2). The combined organic layers were dried and the solvent was removed under vacuum. The crude product was purified by flash column chromatography (SiO$_2$, DCM:hexane, 1:4). The desired product was obtained as a pale yellow oil (1.07 g, 86 %).

^{1}H NMR (300 MHz, CDCl$_3$) δ: 7.32 (2H, d, J = 8.4 Hz, ArH), 6.92 (2H, d, ArH, J = 8.4 Hz), 4.66 (2H, d, J = 2.1 Hz, CH$_2$), 2.50 (1H, t, J = 2.1 Hz, C≡C-H), 1.30 [9H, s, (CH$_3$)$_3$]. Data are in good agreement with the literature.[52]

3.10. 5-[(4-*tert*-Butylphenoxy)methyl]-3-(pyren-6-yl) isoxazole (60)
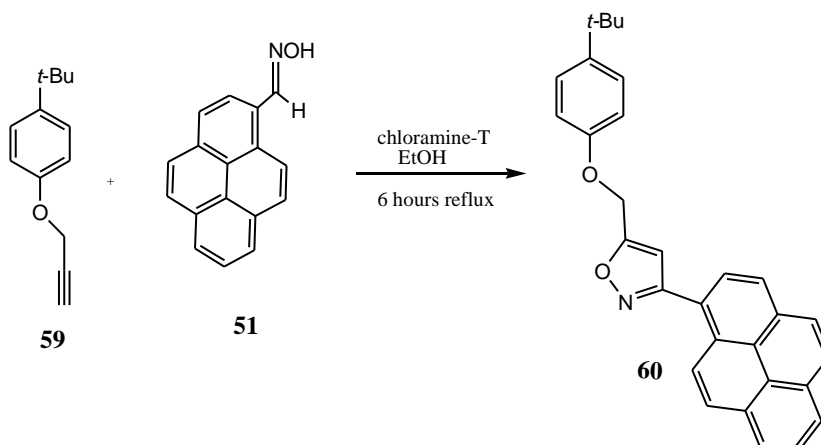
A mixture of **59** (0.20 g, 1.1 mmol) and EtOH (30 mL) was added into a 100 mL round bottomed flask. **51** (0.13 g, 0.5 mmol) and chloramine-T[76] (0.12 g, 0.5 mmol) were added. The mixture was heated at reflux for 2 hours. Reaction progress was followed by TLC (SiO$_2$, DCM:MeOH, 100:1). After an interval of 2 hours, a second portion of oxime and of chloramine-T (0.5 mmol each) was added. The mixture was heated at reflux for another 2 hours. After this interval, a third portion of oxime and chloramine-T (0.5 mmol each) was added. The reaction was stopped after a total of 6 hours heating. Water (50 mL) was added. The mixture was extracted with chloroform (15 mL x 3). The organic layers were combined, washed with 5% NaOH (10 mL x 3) and dried over anhydrous MgSO$_4$. The solvent was removed by evaporation under reduced pressure. The crude product was purified by flash column chromatography (SiO$_2$, DCM:MeOH, 100:1). The desired product was obtained as a yellow solid (0.29 g, 62%). M.p. = 142-152 ℃.

^{1}H NMR (300Hz, CDCl$_3$) δ:8.67 (1H, d, J = 9.6 Hz, ArH), 8.26-8.05 (8H, m, ArH), 7.37 (2H, d, J = 9.3 Hz, ArH), 7.00 (2H, d, J = 9.1 Hz, ArH), 6.82 (1H, s, isoxazole CH), 5.31 (2H, s, OCH$_2$), 1.32 [9H, s, C(CH$_3$)$_3$]; ^{13}C NMR (75 Hz, CDCl$_3$) δ: 168.3, 163.1, 155.6, 144.7, 132.3, 131.2, 130.7, 124.5, 123.4 (ArC, isoxazole C); 128.7, 128.5, 127.2, 126.5, 126.3, 125.8, 125.6, 124.7, 124.8, 114.3, 105.1 (ArCH, isoxazole CH); 61.7 (OCH$_2$); 34.2 [(CH$_3$)$_3$-C]; 31.5 [(CH$_3$)$_3$-C]; m/z [M+H]$^+$ calculated for C$_{30}$H$_{26}$NO$_2$ 432.1958; found 432.1976.; IR: 2863, 1603, 1509, 1184, 848, 826 cm^{-1}.

3.11. **3-(Anthracen-10-yl)-5-[(4-*tert*-butylphenoxy)methyl] isoxazole (61)**
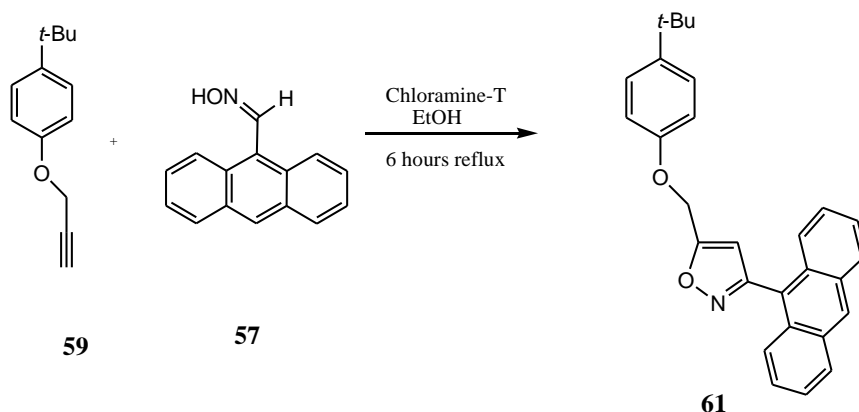
59 (0.25 g, 1.4 mmol) and EtOH (40 mL) were added into a 100 mL round bottomed flask. **57** (0.15 g, 0.7 mmol) and chloramine-T[76] (0.15 g, 0.7 mmol) were added. The mixture was heated at reflux for 2 hours. Reaction progress was followed by TLC (SiO$_2$, DCM:petroleum ether, 1:2). After 2 hours, a second portion of alkyne and chloramine-T (0.7 mmol each) was added. The mixture was heated at reflux for another 2 hours. After this interval, a third portion of alkyne and chloramine-T (0.7 mmol each) was added. The reaction was stopped after a total of 6 hours heating. Water (100 mL) was added. The mixture was extracted with chloroform (30 mL x 3). The organic layers were combined and washed with 5% NaOH (15 mL x 3) and dried over anhydrous MgSO$_4$. The solvent was removed by evaporation under reduced pressure. The crude product was purified by flash column chromatography (SiO$_2$, DCM:petroleum ether, 1:2, R$_f$ = 0.4). The desired product (**61**) was obtained as a yellow liquid (0.27 g, 98 % yield).

^{1}H NMR (300 MHz, CDCl$_3$) δ: 8.58 (1H, s, ArH), 8.06 (2H, dd, J= 1.8 & 7.2 Hz, ArH), 7.87-7.83 (2H, m, ArH), 7.52-7.42 (4H, m, ArH), 7.39-7.34 (2H, m, ArH), 7.01-6.97 (2H, m, ArH), 6.61 (1H, s, isoxazole CH), 5.38 (2H, s, OCH$_2$), 1.32 (9H, s, C(CH$_3$)$_3$); ^{13}C NMR (75 MHz, CDCl$_3$) δ: 167.7, 161.0, 155.7, 144.8, 131.2, 130.6, 129.1, 128.55, 126.6, 126.5, 125.6, 125.4 122.9, 114.5 106.9 (isoxazole CH, isoxazole C, ArC, ArCH), 61.8 (O-CH$_2$), 34.2 [$\underline{C}$(CH$_3$)$_3$], 31.5 [C($\underline{C}$H$_3$)$_3$]. HRMS [2M+Na]$^+$ calculated for C$_{56}$H$_{50}$N$_2$NaO$_4$ 837.3663, found 837.3681. IR: 2962, 1605, 1512, 1363, 1363, 1232, 998, 893, 732 cm^{-1}.

3.12. 2-{5-*tert*-Butyl-3-ethyl-2-[(3-phenylisoxazol-5-yl)methoxy]benzyl}-4-*tert*-butyl-6-methylphenol (62)
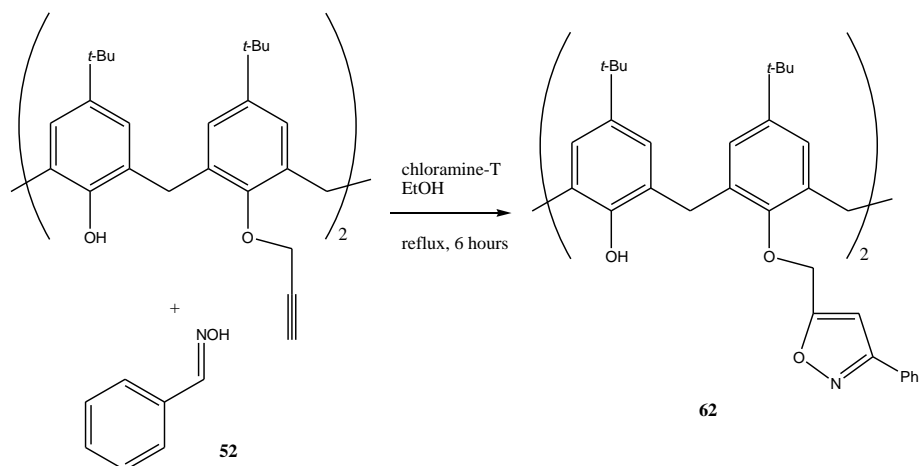
52[48] (25.1 mg, 0.2 mmol) and chloramine-T (47.3mg, 0.2 mmol) were placed in a 50 mL round bottomed flask and dissolved in EtOH (10 mL). The 2-[5-*tert*-butyl-3-ethyl-2-(prop-2-ynyloxy)benzyl]-4-*tert*-butyl-6-methylphenol[18] (100 mg, 0.1 mmol) was added. The mixture was heated at reflux for 2 hours. Reaction progress was followed by TLC (SiO$_2$, DCM:MeOH, 100:1). After that, a portion of alkyne and chloramine-T (0.2 mmol each) was added. The mixture was heated at reflux for another 2 hours. After this interval, another portion of alkyne and chloramine-T (0.2 mmol each) was added. The reaction was stopped after a total of 6 hours heating. After cooling to r.t., water (20 mL) was added. The mixture was extracted with chloroform (3 x 15 mL). The organic layers were combined, washed with 5% NaOH (2 x 15 mL) and dried over anhydrous MgSO$_4$. The solvent was removed under vacuum. The product was purified by flash column chromatography (SiO$_2$, DCM:MeOH, 100:1), and was obtained as a white solid (136 mg, 44 % yield). M.p.= 140-148 ℃.

^{1}H NMR (300 MHz, CDCl$_3$) δ: 7.71-7.75 (4H, m, ArH), 7.30-7.41 (6H, m, ArH), 7.06 (4H, s, ArCH), 6.92 (2H, s, isozoxale CH), 6.77 (4H, s, ArH), 6.68 (2H, s, OH), 5.20 (4H, s, CH$_2$-O), 4.23 (4H, d, J = 13.2 Hz, CH$_2$-Ar), 3.20 (4H, d, J = 13.2 Hz, CH$_2$-Ar), 1.20 & 0.92 [36H, 2 x s, C(CH$_3$)$_3$]; ^{13}C NMR (75 MHz, CDCl$_3$) δ: 168.3 (2 x isozaxole C=N), 162.5 (2 x isozaxole O-$\underline{C}$=C), 150.3, 149.5, 147.7, 141.9, 132.3, 130.0, 128.9, 128.7, 128.7, 127.8, 127.7, 127.0, 126.8, 125.8, 125.2 (22 x ArC, 22 x ArCH), 102.0 (2 x C-$\underline{C}$=N), 68.5 (2 x CH$_2$-O), 34.0, 33.9 [4 x $\underline{C}$(CH$_3$)$_3$], 31.7, 30.9 (36 x C-$\underline{C}$H$_3$); IR: 3410, 2960, 1649, 1442, 1393, 1173 cm^{-1}; HRMS: *m/z* [M+Na]$^+$

calculated for $C_{64}H_{70}O_6NaN_2$ 985.5126, found at 985.5114.

3.13. 2-(5-*tert*-Butyl-3-ethyl-2-{[3-(4-(2-hydroxyethoxy)phenyl)isoxazole-5-yl]methoxy}benzyl)-4-*tert*-butyl-6-methylphenol (63)
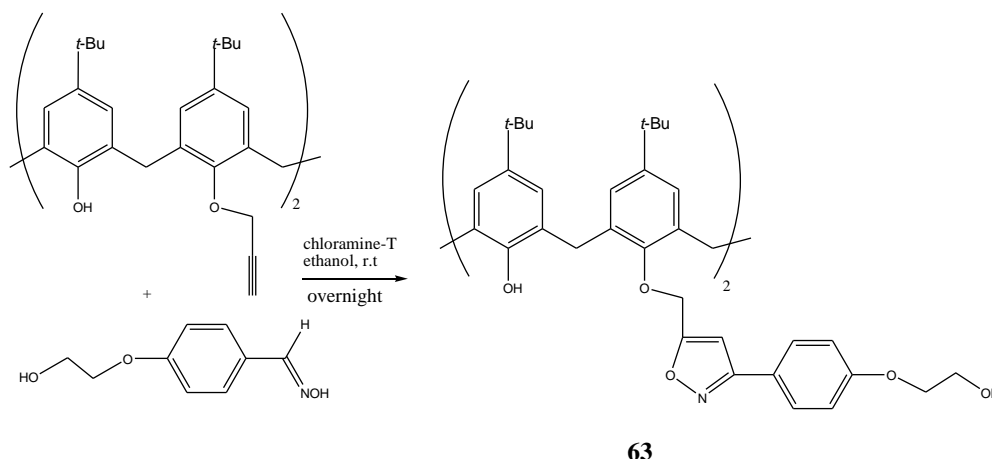

63

58 (52.0 mg, 0.3 mmol) and chloramine-T[76] (84.3 mg, 0.4 mmol) were placed in a 50 mL round bottomed flask and dissolved in ethanol (10 mL). The 2-[5-*tert*-butyl-3-ethyl-2-(prop-2-ynyloxy)benzyl]-4-*tert*-butyl-6-methylphenol[18] (50.0 mg, 0.1 mmol) was added. The mixture was stirred at room temperature overnight. Water (15 mL) was added. Chloroform (15 mL x 3) was added to extract the mixture. The organic layer was then washed with 5% NaOH (20 mL x 2) after drying with MgSO$_4$. The solvent was removed under vacuum. The crude product was purified by flash column chromatography (SiO$_2$, EtOAc:hexane:methanol = 7:12:1, R$_f$ = 0.33). The pure product was obtained as a white solid (35.3 mg, 46%). M.p. = 146-154 ℃.

^{1}H NMR (300 MHz, CDCl$_3$) δ: 7.64 (4H, dd, J=2.1 & 6.9 Hz, ArH) 7.07 (4H, s, ArH), 6.94-6.86 (5H, m, ArH), 6.78 (4H, s, ArH), 6.73 (1H, s, isoxazole CH), 5.18 (4H, s, O-CH$_2$-isozoxale ring), 4.25 (4H, d, J = 13.5 Hz, CH$_2$-Ar), 4.15-4.08 (8H, m, OCH$_2$), 3.97 (H,)3.35 (4H, d, J = 13.5 Hz, CH$_2$), 2.04 (4H, s, OH), 1.29, 0.93 [36H, s, (CH$_3$)$_3$];
^{13}C NMR (75 MHz, CDCl$_3$) δ: 168.2, 160.0, 150.4, 149.6, 147.7, 132.3, 128.3, 127.7, 125.8, 125.2, 121.6, 114.87 (ArC, ArCH, isoxazole C), 101.4 (isoxazole CH), 69.3, 68.7, 61.4 (OCH$_2$), 34.0, 33.9 [C̲(CH$_3$)$_3$, CH$_2$], 31.68, 30.93 [C(C̲H$_3$)$_3$]; MS: *m/z*

[M+Na]$^+$ calculated for $C_{68}H_{78}N_2NaO_{10}$ 1105.5549, found at 1105.5563; IR: 3422, 2961, 1610, 1484, 1363, 1255, 1177, 911, 734 cm^{-1}.

3.14. 2-{5-*tert*-Butyl-3-ethyl-2-[(3-(naphthalen-1-yl)isoxazol-5-yl)methoxy]benzyl}-4-*tert*-butyl-6-methylphenol (64)
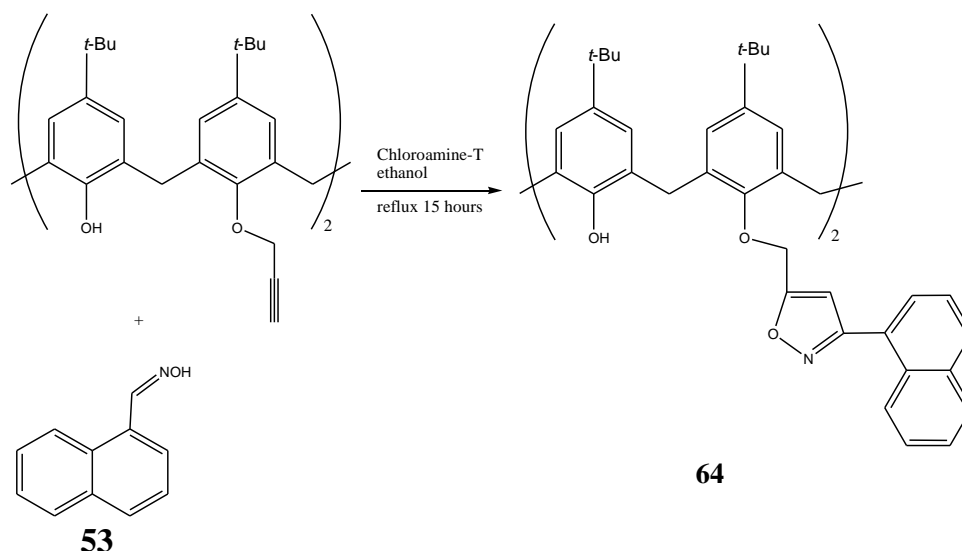
53[51] (0.20 g, 1.2 mmol) and chloramine-T (0.55 g, 2.4 mmol) were placed in a 100 mL round bottomed flask and dissolved in 40 mL EtOH. The calixarene-alkyne (0.21 g, 0.30 mmol) was added. The mixture was heated at reflux (80 ℃) for 7 hours and reaction progress followed by (TLC SiO$_2$, DCM:hexane, 85:15), then water (50 mL) was added. The mixture was extracted with DCM (20 mL x 3). The organic lagers were combined, washed with 5% NaOH (10 mL x 2) and dried over anhydrous MgSO$_4$. The solvent was removed under vacuum. The crude product was purified by flash column chromatography (SiO$_2$, DCM hexane, 85:15). The desired product was obtained as white solid (0.14 g, 43 % yield).

^{1}H NMR (300 MHz, CDCl$_3$) δ: 8.40-8.35 (2H, m, ArH), 7.45 (4H, d, J = 9.0 Hz, ArH), 7.62-7.59 (2H, dd, J = 1.2 Hz & 7.2 Hz, ArH), 7.52-7.48 (4H, dd, J = 3.6 & 6.0 Hz, ArH), 7.50-7.39 (2H, t, J = 7.5 Hz, ArH), 7.07 (4H, s, ArH), 6.79 (4H, s, ArH), 6.75 (2H, s, isoxazole H/ OH), 6.68 (2H, s, OH/ isoxazole H), 5.21 (4H, s, CH$_2$-O), 4.26 (4H, d, J = 13.2 Hz, CH$_2$), 3.35 (4H, d, J = 13.2 Hz, CH$_2$), 1.29 & 0.93 (36H, s, C(CH$_3$)$_3$); ^{13}C NMR (75 MHz, CDCl$_3$) δ: 167.4, 162.6, 150.4, 149.5, 147.6, 141.9

(ArC, isoxazole C), 133.8, 132.4, 130.9, 130.2, 128.5, 127.9, 127.8, 127.0, 126.4, 126.2, 125.8, 125.7, 125.2, 125.2 (ArC & ArCH), 105.6 (isoxazole CH), 68.1 (2 x OC$\underline{H}_2$), 34.0 (CH$_2$), 33.9 [$\underline{C}$(CH$_3$)$_3$] 31.7, 30.96 [C(C$\underline{H}_3$)$_3$]; IR: 3421, 2962, 1607, 1483, 1362, 909 cm^{-1}; HRMS: *m/z* [M+H]$^+$ calculated for C$_{72}$H$_{75}$O$_6$N$_2$, calculated 1063.5620, found 1063.5628.

3.15.   2-{5-*tert*-Butyl-3-ethyl-2-[(3-(pyren-1-yl)isoxazol-5-yl)methoxy]benzyl}-4-*tert*-butyl-6-methylphenol (65)
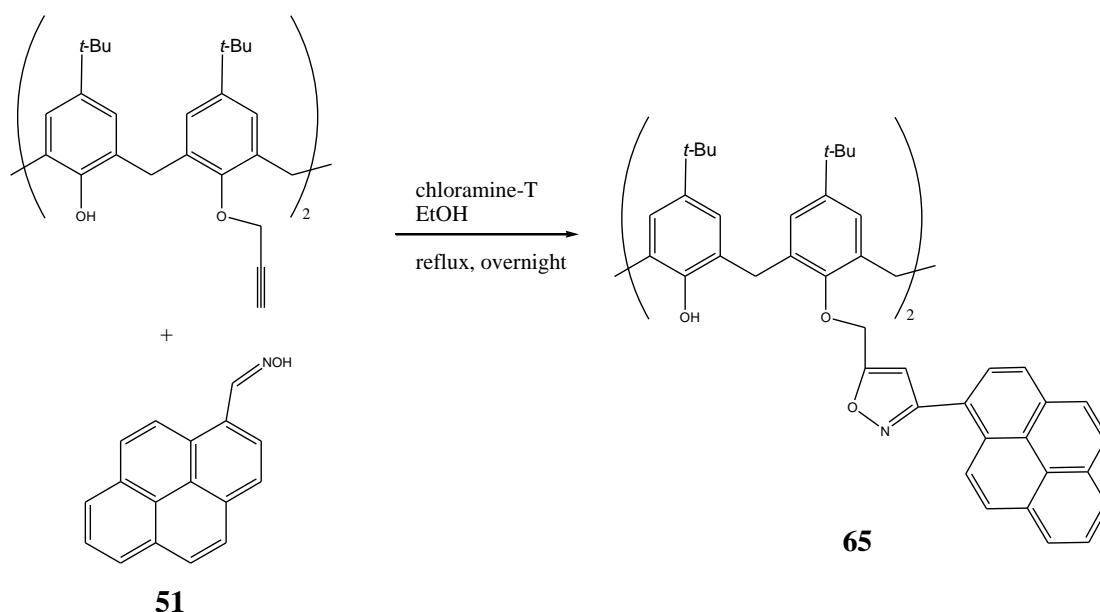
A mixture of **51** (0.37 g, 1.5 mmol) and chloramine-T (0.42 g, 1.8 mmol) was placed in a 50 mL round bottomed flask and dissolved in EtOH (30 mL). The 2-(5-*tert*-butyl-3-ethyl-2-(prop-2-ynyloxy)benzyl)-4-*tert*-butyl-6-methylphenol[18] (0.26 g, 0.3 mmol) was added. The mixture was heated at reflux (80 ℃) overnight and reaction progress followed by TLC (SiO$_2$, DCM:petroleum ether:methanol= 1:1:0.01). On completion of the reaction, water (30 mL) was added and the mixture was extracted with chloroform (3 x 10 mL). The organic layers were combined, washed with 5% NaOH (2 x 10 mL) and dried over anhydrous MgSO$_4$. The solvent was removed under vacuum. The crude product was purified by flash column chromatography (SiO$_2$, DCM:MeOH, 100:1). The crude product was crystalized from DCM/petroleum ether (1:2) and obtained as a white solid (0.24 g, 54 %). Melting

point: 208-222 ℃. R_f = 0.35, DCM:petroleum ether = 2:1.

^{1}H NMR (300 MHz, CDCl₃) δ: 8.54 (2H, d, J = 9.3 Hz, ArH), 8.07 (4H, m, ArH), 7.97-7.88 (10H, m, J = 9.3 H, ArH), 7.76 (2H, d, J = 9.0 Hz, ArH), 7.11 (4H, s, ArH), 6.97 (2H, s, isoxazole CH), 6.88 (2H, s, OH), 6.84 (4H, s, ArH), 5.29 (4H, s, CH₂-O), 4.37 (4H, d, J = 13.2 Hz, CH₂), 3.40 (4H, d, J = 13.2 Hz, CH₂), 1.31 [18H, s, C(CH₃)₃], 0.97 [18H, s, C(CH₃)₃]; ^{13}C NMR (75 MHz, CDCl₃) δ: 167.6, 163.1, 150.5, 149.6, 147.8, 142.0, 132.44, 132.0, 131.0, 128.7, 128.1, 127.8, 127.0, 126.0, 125.9, 125.5, 125.3, 125.2, 124.8, 124.6, 124.2, 122.9 (ArC, ArCH, isoxazole C), 105.42 (isoxazole CH), 68.54 (CH₂-O), 34.03, 33.91 [C̲(CH₃)₃, CH₂], 31.72, 31.00 [C-(C̲H₃)₃]; HRMS: *m/z* [M+H]⁺, Calculated for C₈₄H₇₉N₂O₆ 1211.5933, found at 1211.5959; IR: 3429, 2960, 1603, 1484, 1362, 1189, 846 cm⁻¹.

3.16. 3-(Anthracen-10-yl)-(4-*tert*-butylcalix[4]arene)isoxazole (66)
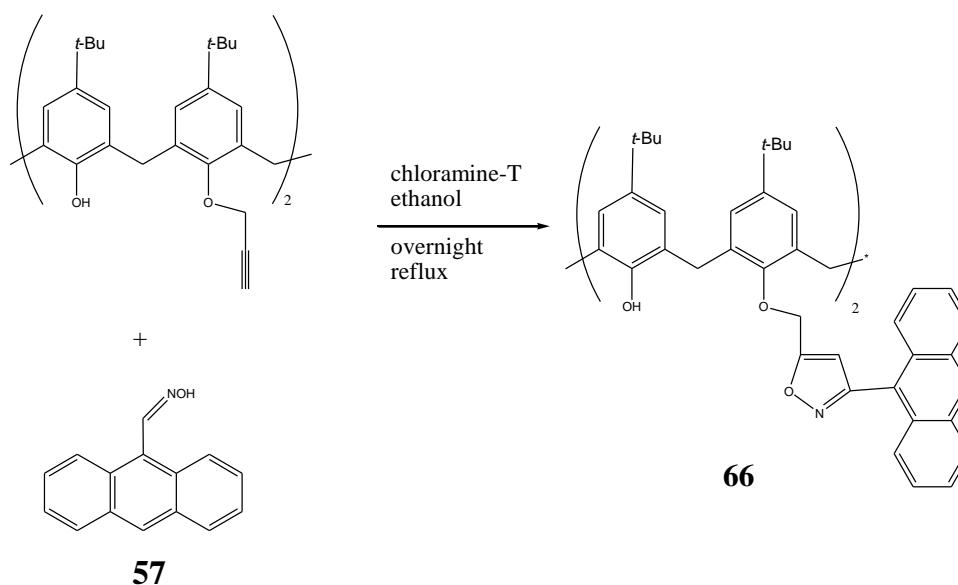

57 (0.19 g, 0.7 mmol) and chloramine-T (0.20 g, 0.9 mmol) were placed in a 100 mL round bottomed flask and dissolved in EtOH (60 mL). The 2-[5-*tert*-butyl-3-ethyl-2-(prop-2-ynyloxy)benzyl]-4-*tert*-butyl-6-methylphenol[18] (0.30 g, 0.4 mmol) was added. The mixture was heated at reflux (80 ℃) for 3 hours and another portion of oxime (0.90 g) and chloramine-T (0.20 g) were added. The mixture was heated at reflux (80 ℃) overnight. On completion of the reaction, water (30 mL) was added and the mixture was extracted with chloroform (10 mL x 3). The organic layers were

combined, washed with 5% NaOH (10 mL x 2) and dried over anhydrous MgSO$_4$. The solvent was removed under vacuum. The crude product was purified by flash column chromatography (SiO$_2$, petroleum ether:ethyl acetate, 3:1). The crude product was crystalized from petroleum ether/ethyl acetate (3:1) and the product was obtained as a white solid (0.25 g, 51 %). Melting point: 174-190 ℃.

^{1}H NMR (300 MHz, CDCl$_3$) δ: 8.43 (2H, s, ArH), 7.93 (4H, d, J = 7.8 Hz, ArH), 7.79 (4H, d, J = 7.8 Hz, ArH), 7.43-7.33 (8H, m, ArH), 7.09 (4H, s, ArH), 6.80 (4H, s, ArH), 6.70 (2H, s, OH), 6.48 (2H, s, isoxazole CH), 5.27 (4H, s, ArOCH$_2$), 4.29 (4H, d, J = 13.2 Hz, CH$_2$), 3.37(4H, d, J = 13.2 Hz, CH$_2$), 1.31 (18H, s, C(CH$_3$)$_3$), 0.94 (18H, s, C(CH$_3$)$_3$); ^{13}C NMR (75 MHz, CDCl$_3$) δ: 167.9, 161.0, 150.4, 149.6, 147.7, 141.9, 132.5, 131.1, 130.6, 129.0, 128.4, 127.8, 126.5, 125.8, 125.6, 125.3, 125.2 (ArC, ArCH, isoxazole C) , 108.1 (isoxazole CH), 67.7(O-CH$_2$), 34.0, 33.9 [$\underline{C}$(CH$_3$)$_3$], 31.7, 31.0 [C($\underline{C}$H$_3$)$_3$, CH$_2$]; HRMS: *m/z* [M+Na]$^+$ calculated for C$_{80}$H$_{78}$N$_2$NaO$_6$ 1185.5752, found 1185.5670; IR: 3447, 2960, 1625, 1483, 1362, 1207, 888, 735 cm^{-1}.

3.17. **8,8-Dibromobicyclo[5.1.0]octane (67)**[73]

67
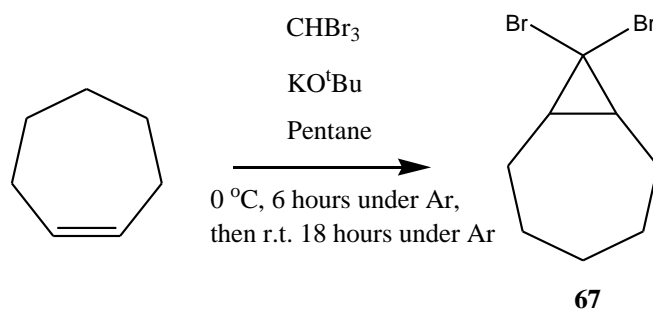
A stirred suspension of cycloheptene (1.92 g, 20.0 mmol) and potassium *tert*-butoxide (2.58 g, 23.0 mmol) in anhydrous pentane (50 mL) was cooled to 0 ℃ and maintained at this temperature over a period of 6 hours using an ice-salt bath. A solution of bromoform (5.05 g, 20.0 mmol) in anhydrous pentane (50 mL) was added dropwise under argon over 6 hours. The reaction was allowed to warm to room temperature overnight. Water (200 mL) was added. The aqueous layer was extracted with pentane (30 mL x 3) and dried over anhydrous sodium sulphate. The solution was filtered and the solvent was removed under vacuum. Unreacted cycloheptene was

removed under a high vacuum. The crude product, a yellow oil (2.42 g, 45 %), was stored in the freezer.

^{1}H NMR (300 MHz, CDCl$_3$) δ: 2.32-2.10 (2H, m, 2 x BrCCH), 1.90-1.71 (8H, m, 4 x CH$_2$), 1.2 (2H, m, CH$_2$). Data are in good agreement with the literature.[73]

3.18. **4-[(2-Bromocyclooct-en-1-yl)oxy]butan-1-ol (68)**[73]
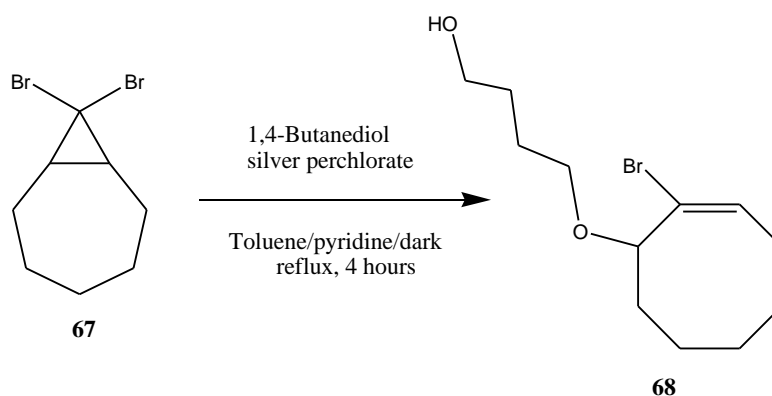
A solution of **67** (0.75 g, 2.8 mmol) in a mixture of toluene (1.5 mL) and pyridine (2.0 mL) was added to a suspension of 1,4-butandiol (7.61 g, 84.4 mmol) and silver perchlorate (1.75 g, 8.5 mmol) in toluene (2.0 mL). The mixture was heated at reflux for 4 hours in the dark, after which the silver salts were filtered. Water (5 mL) was added. The mixture was extracted with diethyl ether (3 x 10 mL) and the combined organic layers were dried over anhydrous MgSO$_4$. The solvent was removed under vacuum to give the crude product as a yellow oil (0.30 g, 68 %).

^{1}H NMR (300 MHz, CDCl$_3$) δ: 6.17 (1H, dd, J = 4.2 & 11.7 Hz, CH=CBr), 3.86 (1H, dd, J = 5.4 & 9.9 Hz, OCH-CBr), 3.72-3.57 (3H, m, CH$_2$O and one H from OCH$_2$), 3.61-3.46 (1H, m, one H in from OCH$_2$), 1.24-1.98 (14H, m, 7 x CH$_2$). Data are in good agreement with the literature.[73]

3.19. 3-(Cyclooct-2-yn-1-ylmethoxy)propan-1-ol (69)[73]

68

69
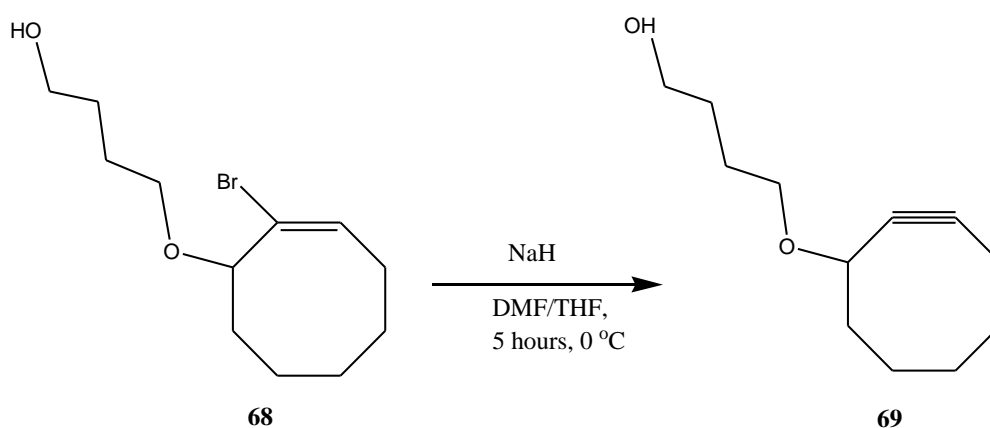
68 (0.30 g, 3.1 mmol) was dissolved in DMF (10 mL) and NaH (0.30 g, 60% in paraffin, 12.5 mmol) was added. Anhydrous THF (10 mL) was added. The mixture was stirred at room temperature and reaction progress monitored by TLC (DCM: hexane = 2:3). After 5 hours, the reaction mixture was cooled in a salt-ice bath and carefully neutralized by drop-wise addition of 1M HCl. The mixture was extracted with diethyl ether (20 mL x 3) and dried over anhydrous Na_2SO_4. The solvent was removed under vacuum to give a pale, yellow oil[73] (0.14 g, 66 %), which was further dried to remove any residual solvent (DMF).

^{1}H NMR (300 MHz, CDCl$_3$) δ: 4.21-4.15 (1H, m, CH-O), 3.67-3.60 (3H, m, CH_2-O and one H from CH_2-O), 3.36 (1H, t, J = 7.5 Hz, one H from O-CH_2), 2.20-1.61 (14H, m, CH_2). Data are in good agreement with the literature.[73]

3.20.   4-{3-[4-(2-Hydroxyethoxy)phenyl]-4,5,6,7,8,9-hexahydrocycloocta[*d*] isoxazol-4-yloxy}butan-1-ol & its regioisomer 4-{3-[4-(2-hydroxyethoxy)phenyl]-4,5,6,7,8,9-hexahydrocycloocta[*d*] isoxazol-9-yloxy}butan-1-ol (70 & 71)
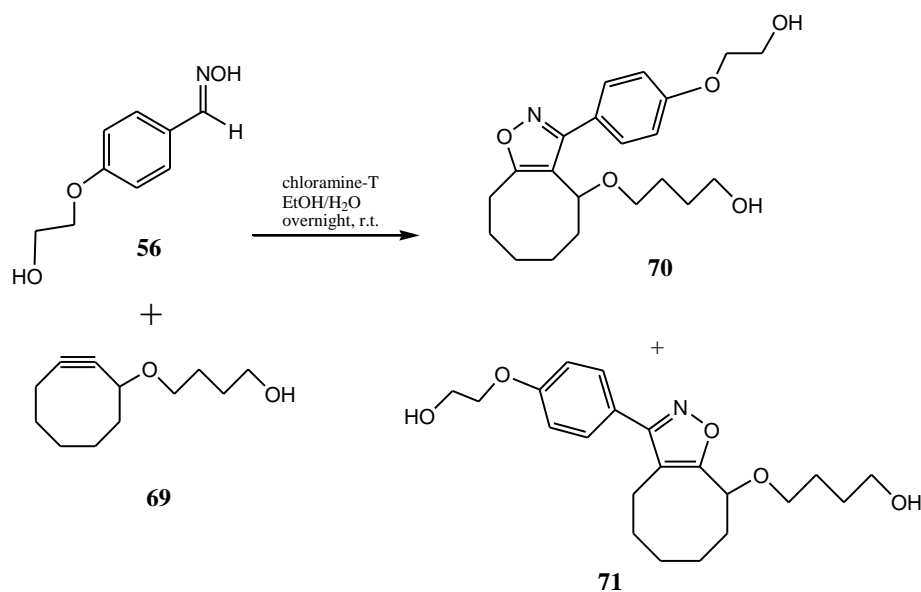
4-(2-Hydroxyethoxy)benzaldehyde oxime[48] (38.0 mg, 0.3 mmol) and chloramine–T[76] (59.8 mg, 0.3 mmol) were placed in a round bottomed flask and dissolved in 50% aqueous (EtOH, 8 mL). The mixture was stirred until all reactants dissolved and was then added directly to 3-(cyclooct-2-yn-1-ylmethoxy)propan-1-ol (20.6 mg, 0.1 mmol)[73]. The combined reactants were stirred at room temperature overnight. Water (20 mL) was added and the mixture was extracted with ethyl acetate (3 x 30 mL). The organic layer was collected and washed twice with 5% NaOH (15 mL). After drying over $MgSO_4$, the solvent was removed under vacuum. ^{1}H NMR analysis of the crude mixture showed complete consumption of the starting alkyne and that the crude products comprised regioisomeric isoxazoles in ~1:0.93 ratio. The crude products (yellow gum) were separated by flash column chromatography (SiO_2, EtOAc:hexane, 3:1).

The minor regioisomer, A, [(12.3 mg, 31%); R_f = 0.33, SiO_2, ethyl acetate:hexane = 3:1] eluted before the major regioisomer B [(15 mg, 38%), R_f = 0.2, SiO_2, ethyl acetate:hexane = 3:1].

Isomer A: ^{1}H NMR (300 MHz, $CDCl_3$) δ: 7.53 (2H, dd, J = 2.1 Hz & 6.6 Hz, 2 x ArH), 7.00 (2H, dd, J = 2.1 Hz & 6.6 Hz, 2 x ArH), 4.72 (1H, dd, J = 3.6 Hz & 7.2 Hz, HC-C=C), 4.13 (2H, t, J = 4.5 Hz, O-CH$_2$), 3.99 (2H, t, J = 4.5 Hz, HO-CH$_2$), 3.67 (2H, t, J = 5.7 Hz, HO-CH$_2$), 3.57-3.50 (2H, m, -O-CH$_2$), 2.90-2.83 (1H, m, CH$_2$-C=C), 2.58-2.51 (1H, m, CH$_2$-C=C), 2.22-1.96 (1H, m, -O-CH), 1.73-1.64 (10H,

m, CH$_2$); ^{13}C NMR (75 MHz, CDCl$_3$) δ: 167.85 (ArC), 161.18 (ArC), 158.53 (C=N), 128.63 (2 x ArCH), 121.34 (C=$\underline{C}$-O), 113.77 (2 x ArCH), 112.08 (C=$\underline{C}$-C), 72.89(alkene CH), 68.66(CH$_2$O), 68.23(CH$_2$O), 61.70(CH$_2$OH), 60.39(CH$_2$OH), 33.13-18.42 (CH$_2$); IR: 3408, 2933, 1612, 1440, 1252, 1086 cm^{-1}; Mass: m/z [M+Na]$^+$ calculated for C$_{21}$H$_{29}$NNaO$_5$, calclated 398.1938, found at 398.1920.

Isomer B: ^{1}H NMR (300 MHz, CDCl$_3$) δ:7.56 (2H, d, J=6.0 Hz, ArH), 7.00 (2H, dd, J = 6.0 Hz, ArH), 4.50 (1H, dd, J = 3.6 Hz, 7.5 Hz, HC-C=C), 4.13 (2H, t, HO-C$\underline{H}_2$, J = 4.5 Hz)), 4.00 (2H, t, HO-C$\underline{H}_2$, J = 4.5 Hz), 3.57-3.52 (4H, m, 2 x O-CH$_2$-), 2.88 (1H, m, CH$_2$), 2.54-2.51 (1H, m, CH$_2$), 2.17-1.25 (12H, m, -O-CH, CH$_2$); ^{13}C NMR (75 MHz, CDCl$_3$) δ: 170.86 (ArC), 162.16 (ArC), 159.57 (C=N), 130.13 (2 x ArCH), 122.37 (C=C-O), 114.59 (2 x ArH), 72.07 (CH), 69.36 (CH$_2$O), 69.30(CH$_2$O), 68.22 (CH$_2$OH), 62.69 (CH$_2$OH), 34.80-21.97 (CH$_2$); IR: 3411, 2931, 1612, 1446, 1252, 1082, 961 cm^{-1}; mass: m/z [M+H]$^+$ calculated for C$_{21}$H$_{30}$NO$_5$ 376.2118, found at 376.2107.

## 3.21. 4-{3-[2-(2-Hydroxyethoxy)phenyl]-4,5,6,7,8,9-hexahydrocycloocta[*d*]isoxazol-9-yloxy}butan-1-ol & its reigoisomer4-{3-[2-(2-hydroxyethoxy) phenyl]-4,5,6,7,8,9–hexahydrocycloocta[*d*]isoxazol-4-yloxy}butan-1-ol (72 & 73)
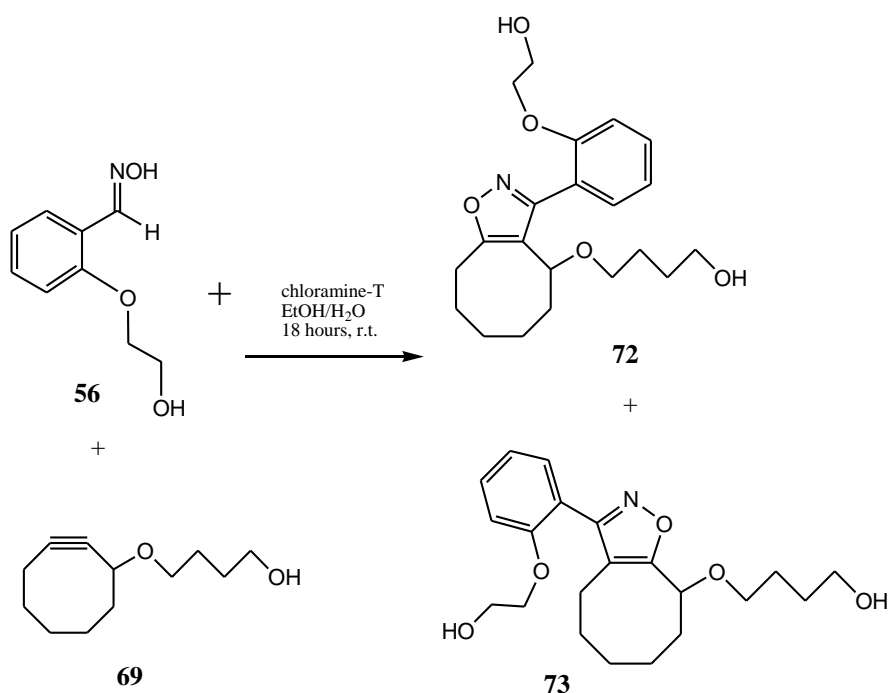
2-(2-Hydroxyethoxy)benzaldehyde oxime[48] (38.0 mg, 0.26 mmol) and chloramine–T (59.8 mg, 0.26 mmol) were placed in a round bottomed flask and dissolved in 50% aq. Ethanol (4 mL). The mixture was stirred until all reactants dissolved and was then added directly to the 3-(clyclooct-2-yn-1-ylmethoxy) propan-1-ol)[73] (20.6 mg, 0.11 mmol). The combined reactants were stirred at room temperature for 18 hours. Water (20 mL) was added and the reaction mixture extracted with ethyl acetate (3 x 30 mL). The organic layer was collected and washed with 5% NaOH (15 mL x 2). After drying over anhydrous $MgSO_4$ the solvent was removed under vacuum. ^1H NMR spectroscopic analysis of the crude mixture showed complete consumption of the starting alkyne and that the crude products comprised regioisomeric isoxazoles in ~1:2 ratio. The crude products were purified by flash column chromatography (SiO_2 EtOAc:hexane=3:1, R_f = 0.3); however, the regioisomeric products could not be separated and were obtained as a yellow gum (24.6 mg, 63% yield).

^1H NMR (300 MHz, $CDCl_3$) δ (both isomers): 7.45-7.38 (1H, m, ArH), 7.29 (1H, d, J = 6.5 Hz, ArH), 7.09-7.01 (2H, m, ArH), 4.74 (1H, dd, J = 3.7 & 7.5 Hz, CH-O),4.36 (1H, dd, J = 3.7 & 7.5 Hz, CH-O), 4.14 (2H, t, J = 4.7 Hz, CH_2), 3.82 (2H, m, CH_2), 3.54 (2H, m, CH_2-OH), 2.92-1.25 (16H, m, CH_2); ^{13}C NMR (75 MHz, $CDCl_3$) δ: 168.96 (C=C, isoxazole), 167.18 (C=C), 160.11 (C=N), 159.41 (C=N), 155.83, 155.80, 130.04, 129.94, 120.28, 120.22, 118.73, 118.03, 114.36, 113.91, 112.94, 112.83 (ArC-O, ArCH, ArC, C=C), 75.59-59.76 (CH_2, OCH_2), 32.90-20.59 (CH_2); IR: 3400, 2930, 1619, 1455, 1259, 1084 cm^{-1}; Mass: *m/z* [M+Na]$^+$ calculated for $C_{21}H_{29}NNaO_5$ 398.1938, found 398.1955.

3.21. 6-{4-[9-(4-Hydroxybutoxy)-4,5,6,7,8,9-hexahydrocycloocta[d]isoxazol-3-yl]phenoxy}hexan-1-ol & its regioiosmer 6-{4-[4-(4-hydroxybutoxy)-4,5,6,7,8,9-hexahydrocycloocta[d] isoxazol-3-yl]phenoxy}hexan-1-ol (74 & 75)
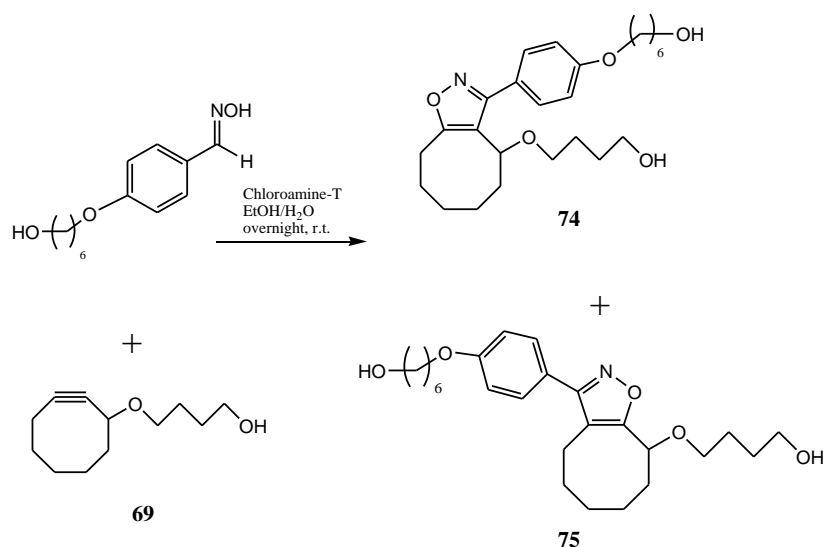
4-(6-Hydroxyhexyloxy)benzaldehyde oxime[48] (89.5 mg, 0.4 mmol) and chloramine-T (107.4 mg, 0.4 mmol) were placed in a round bottomed flask and dissolved in 50% aq. ethanol (4 mL). The mixture was added directly to the 3-(cyclooct-2-yn-1-ylmethoxy) propan-1-ol[73] (37.0 mg, 0.3 mmol) and the combined reactants were stirred at room temperature overnight. Water (10 mL) was added and the mixture was extracted with ethyl acetate (3 x 5 mL). The organic layers were collected and washed with 5% NaOH (2 x 10 mL). After drying over anhydrous $MgSO_4$, the solvent was removed under vacuum. ^1H NMR spectroscopic analysis of the crude mixture showed complete consumption of the starting alkyne and the presence of regioisomeric isoxazoles in ~1:1 ratio. The crude products were purified by flash column chromatography (50.7 mg, 63% yield) (SiO$_2$, EtOAc:hexane, 6:1, R_f = 0.5). However, it was not possible to obtain separate samples of individual regioisomers.

^1H NMR (300 MHz, CDCl$_3$) δ (both isomers): 8.10 (1H, dd, J = 9.0 &15.0 Hz), 7.50 (1H, dd, J = 5.7 & 9.0 Hz, ArH), 6.95 (2H, ArH, dd, J = 4.2 & 5.7 Hz), 4.72 (1H, dd, J = 3.7 & 7.4 Hz, CH-O), 4.50 (1H, dd, J = 3.7 & 7.4 Hz, CH-O), 4.02 (2H, t, J= 6.4 Hz, O-CH$_2$), 3.65 (2H, t, J = 6.4 Hz, O-CH$_2$), 3.54 (2H, t, J = 2.1 Hz, O-CH$_2$), 2.92-2.84 (2H, m, CH$_2$-O), 2.20-1.25 (14H, m, CH$_2$); ^{13}C NMR (75 MHz, CDCl$_3$) δ (both isomers): 169.85 (isoxazole C=C), 167.76 (isoxazole C=C), 161.28, 159.02, 128.99, 128.52, 120.6, 113.88, 113.70, 112.44, 112.09 (ArC, C=N, ArCH, ArC, C=$\underline{C}$-O, $\underline{C}$=C-O), 72.90 (CH-O), 70.97 (CH-O), 68.65 (CH$_2$), 67.15 (CH$_2$-O), 66.90

(CH$_2$-O), 61.82 (CH$_2$-OH), 61.65 (CH$_2$-OH), 33.89-18.45 (CH$_2$). IR: 3375, 2930, 1611, 1526, 1443, 1250, 1175, 1059 cm^{-1}; Both/mixed isomers: Accurate mass *m/z* [M+H]$^{+}$ calculated for C$_{21}$H$_{38}$NO$_5$ 432.2744, found 432.2754.

Reference

(1) Thomas, J. J. M.; Willy, B.; Rominger, F. *Synthesis* **2008**, *2*, 293.

(2) Sperry, J.; Wright, D. C. O. *Drug Discovery Dev.* **2005**, *8*, 723.

(3) Axel, B.; Gisela, G.; B., H.-G.; Volker, H.; Bernhard, B. *Psychopharmacology* **1999**, *144*, 333.

(4) Rowley, M.; Broughton, H. B.; Collins, I.; Baker, R.; Emms, F.; Marwood, R.; Patel, S.; Ragan, C. I. *J. Med. Chem.* **1996**, *39*, 1943.

(5) Frolund, B.; Jorgensen, A. T.; Tagmose, L.; Stensbol, T. B.; Vestergaard, H. T.; Engblom, C.; Kristiansen, U.; Sanchez, C.; Krogsaard-Larsen, P.; Liljefors, T. *J. Med. Chem.* **2002**, *45*, 2454.

(6) Talley, J. J. *Prog. Med. Chem.* **1999**, *13*, 201.

(7) Diadone, G.; Raffa, D.; Maggio, B.; Plescia, F.; Cutuli, V. M. C.; Mangano, N. G.; Caruso, A. *Arch. Pharm. Pharm. Med. Chem.* **1999**, *332*, 50.

(8) Takemaka, K.; Nakatsuka, S.; Tsujihara, T.; Koranne, P. S.; Sasai, H. *Tetrahedron: Asymmetry* **2008**, *19*, 2492.

(9) Hansen, T. V.; Wu, P.; Fokin, V. V. *J.Org. Chem.* **2005**, *70*, 7761.

(10) Perumal, P.; Praveen, C.; Kalyanasundaram, A. *Synlett* **2010**, *05*, 777.

(11) Crossley, J. A.; Browne, D. L. *J. Org. Chem.* **2010**, *75*, 5414.

(12) Sustmann, R. *Pure and Applied Chemistry* **1974**, *40*, 569.

(13) Liu, K.; Shi, W.; Cheng, P. *Dalton Trans.* **2011**, *40*, 8475.

(14) Lang, S. A. J.; Lin, Y.-U. *Comprehensive Heterocyclic Chemistry*; Pergamon Press: New York, 1984; Vol. 6.

(15) Musney, S. M.; Natale, N. R. *ChemInform Abstract: The Coordination Chemistry of Isoxazoles*, 2010.

(16) Ouellette, W.; Jones, S.; Zubieta, J. *Cryst.Eng.Comm.* **2011**, *13*, 4457.

(17) Gutsche, C. D. *Calixarene:Monographs in supramolecular chemistry*; The Royal Society of Chemistry: London, 1989.

(18) Gutsche, C. D. *Calixarenes: An Introduction*; The Royal Society of Chemistry: London, 2008.

(19) Cornforth, J. W.; Hart, P. D.; Nicholls, G. A.; Rees, R. J. W.; Stock, J. A. *Br. J. Pharmacol.* **1955**, *10*, 73.

(20) Atsushi, I.; Seiji, S. *Chem. Rev.* **1997**, *97*, 1713.

(21) Gutsche, C. D.; Iqbal, M.; Stewart, D. *J. Org. Chem.* **1986**, 742.

(22) Cornforth, I. W.; Morgan, E. D.; Pons, K. T.; Rees, R. J. W. *Tetrahdron Lett* **1973**, *29*, 1659.

(23) Hayes, B. T.; Hunter, R. F. *Chem . Ind.* **1956**, 193.

(24) Jose, P.; Menon, S. *Bioinorg. Chem. Appl.* **2007**, 65815.

(25) Gutsche, C. D.; Johnston, D. E.; Stewart, D. R. *J.Org. Chem.* **1999**, *64*, 3747.

(26) Gutsche, C. D.; Balram, D.; Kwang, H. N.; Ramamurthi, M. *Chem. Soc.* **1981**, *103*.

(27) Agrawal, Y. K.; Pancholi, J. P.; Vyas, J. M. *J. SCI. IND. RES.* **2009**, *68*, 745.

(28) Kumar, S.; Chawla, H. M.; Varadarajan, R. *Tetrahedron Lett.* **2002**, *43*, 2495.

(29) Sliwa, W.; Deska, M. *ARKIVOC* **2011**, *1*, 496.

(30) Solovyov, A. V.; Cherenok, S. O.; Kalchenko, O. I.; Atamas, L. I.; Kazantseva, Z. I.; Koshets, I. A.; Tsymbal, I. F.; Kalchenko, V. I. *AV. solovyov et al. / Journal of Molecular Liquids.* **2011**, *159*, 117.

(31) Curinova, P.; Pojarova, M.; Budka, J.; Lang, K.; Stibor, I.; Lhotak, P. *Tetrahedron* **2010**, *66*, 8047.

(32) Joseph, R.; Ramanujam, B.; Acharya, A.; Rao, C. P. *J. Org. Chem.* **2009**, *74*, 8181.

(33) Vsevolod, V. R.; Luke, G. G.; Valery, V. F.; Sharpless, K. B. *Angew. Chem. Int. Ed* **2002**, *41*, 2596.

(34) Huisgen, R. *1,3-Dipolar Cycloaddition Chemistry*; Wiley: New York, 1984; Vol. 1.

(35) Francis, A. C.; Richard, J. S. *Advanced Organic Chemistry* Springer: Virginia, 2007.

(36) Halling, K.; Torssell, K. B. G.; Hazell, R. G. A. *Acta Chemica Scandinavica.* **1991**, *45*, 736.

(37) Magdziak, D.; Lalic, G.; Lee, H. M.; Fortner, K. C.; Aloise, A. D.; Shair, M. D. *J. Am. Chem. Soc.* **2005**, *127*, 7284.

(38) Cossio, F. P.; Morao, I.; Jiao, H.; Schleyer, P. v. R. *J. Am. Chem. Soc.* **1999**,

121, 6737.

(39) Himo, F.; Lovell, T.; Hilgraf, R.; Rostovtsev, V. V.; Noodleman, L.; Sharpless, K. B.; Fokin, V. V. *J. Am. Chem. Soc.* **2005**, *127*, 210.

(40) O'Reilly, J. E. *J.Chem.Ed* **1975**, *52*, 610.

(41) Berberan-Santos, M. N. *Fluorescence of Supermolecules, Polymers, and Nanosystems.*; Springer: Lisboa, 2007.

(42) Condon, E. *Physical Review* **1926**, *28*, 1182.

(43) Franck, J.; Dymond, E. G. *J. Chem. Soc., Faraday Trans* **1926**, *21*, 536.

(44) Hercules, D. M. *Fluorescence and phosphorescence analysts*; Wiley-Interscience: New York, London, Sydney 1965.

(45) Kolb, H. C.; Finn, M. G.; Sharpless, K. B. *Angew. Chem. Int. Ed.* **2001**, *40*, 2004.

(46) Lin, N. Z.; Shao, L. G.; Shu, L. G.; Chu, L. Y.; Jin, G. Q. *Chinese Journal of Chemistry* **2008**, *26*, 1424.

(47) Rostovtsev, V. V.; Luke, G. G.; Fokin, V. V.; Sharpless, K. B. *Angew. Chem. Int. Ed.* **2002**, *14*, 41.

(48) Freeman, C.; Cheallaigh, A. N.; Heaney, F. *Tetrahedron* **2011**, *67*, 7860.

(49) Grecian, S.; Fokin, V. V. *Angew Chem Int Ed Engl* **2008**, *47*, 8285.

(50) Rolf, H. *Angewandte Chemie* **2006**, *75*, 604.

(51) Ramon, R. S.; Bosson, J.; Diez-Gonzalez, S.; Marion, N.; Nolan, S. P. *J. Org. Chem.* **2010**, *75*, 1197.

(52) Howell, S. J.; Spencer, N.; Philip, D. *Tetrahedron* **2001**, *57*, 4945.

(53) Ho, I. T.; Haung, K. C.; Chung, W. S. *Chemistry, an Asian journal* **2011**, *6*, 2738.

(54) Holm, R. H.; Kennepohl, P.; Solomon, E. I. *Chem. Rev.* **1996**, *96*, 2239.

(55) Li, G. K.; Xu, Z. X.; Chen, C. F.; Huang, Z. T. *Chem Commun (Camb)* **2008**, 1774.

(56) Schazmann, B.; Alhashimy, N.; Diamond, D. *J. Am. Chem. Soc* **2006**, *128*, 8607.

(57) Beer, P. D. *Acc. Chem. Res* **1998**, *31*, 71.

(58) Chen, W.; Christopher, J. D.; Nicholas, J. T. *Macromolecules* **1999**, *32*, 4151.

(59) Sun, Y. P.; Jung, H. Y.; Chang, S. H.; Rachid, S.; Jong, S. K.; Susan, E. M.; Jacques, V. *J. Org. Chem.* **2008**, *73*, 8212

(60) Harvey, L.; Arnold, B.; Chris, A. K.; Monty, K.; Matthew, P. S.; Anthony, B.; Hidde, P.; Paul, M. *Molecular Cell Biology* Harvey Lodish, 2007.

(61) Nam, J. J.; Byung, J. R.; Kye, C. N. *Bull. Korean Chem. Soc.* **2010**, *33*, 3129.

(62) Ho, I. T.; Chu, J.-H.; Chung, W.-S. *European Journal of Organic Chemistry* **2011**, *2011*, 1472.

(63) Valeur, B. *Molecular Fluorescence: Principles and Applications*; WILEY-VCH: New York, 2001.

(64) Shi, Y.; Fan, D. J.; Li, S. X.; Zhang, H. J.; Perrett, S.; Zhou, J. M. *Protein science : a publication of the Protein Society* **2007**, *16*, 1165.

(65) Zachary, D. H.; Patrick, M. C. *J. Chem. Educ.* **1986**, *63*, 162.

(66) Senthilvelan, A.; Ho, I. T.; Chang, K. C.; Lee, G. H.; Liu, Y. H.; Chung, W. S. *Chemistry* **2009**, *15*, 6152.

(67) Joseph, R. L. *Principles of Fluorescence Spectroscopy*; Springer: USA, 2006.

(68) Muia, R. P.; Yu, H.; Prescher, J. A.; Hellman, U.; Chen, X.; Bertozzi, C. R.; Campetella, O. *Glycobiology* **2010**, *20*, 833.

(69) van Dongen, S. F. M.; Janvore, J.; van Berkel, S. S.; Marie, E.; Piel, M.; Tribet, C. *Chemical Science* **2012**, *3*, 3000.

(70) Tummatorn, J.; Batsomboon, P.; Clark, R. J.; Alabugin, I. V.; Dudley, G. B. *J. Org. Chem.* **2012**, *77*, 2093.

(71) Gololobov, Y. G. *Tetrahedron* **1981**, *37*, 437.

(72) Gold, B.; Shevchenko, N. E.; Bonus, N.; Dudley, G. B.; Alabugin, I. V. *J. Org. Chem.* **2012**, *77*, 75.

(73) Singh, I.; Heaney, F. *Chem Commun (Camb)* **2011**, *47*, 2706.

(74) Gutsmiedl, K.; Fazio, D.; Carell, T. *Chemistry* **2010**, *16*, 6877.

(75) Xiaochun, H.; Nicholas, R. N. *J. Heterocyclic Chem.* **2001**, *38*, 415.

(76) Shetty, M.; Gowda, B. T. *A Study of Substituent Effect on the Oxidative Strengths of N-Chloroarenesulphonamides: Kinetics of Oxidation of Leucine and*

Isoleucine in Aqueous Acid Medium; Z. Naturforsch.: India, 2004; Vol. 59b.

Appendix

Detailed analysis of spectral data supporting 3-(Anthracen-10-yl)-5-[(4-*tert*-butyl-phenoxy)methyl]isoxazole (**AIC**), **64**.

To demonstrate the interpretative skills used in the characterization of the new compounds in this thesis the analytical data obtained for AIC is documented in full below. A variety of NMR spectral techniques were exploited: ^{1}H, ^{13}C, HSQC, DEPT 45, 2D-COSY. All new compounds were examined by ^{1}H and ^{13}C NMR. The peaks were assigned with regard to the resonance position and multiplicity.
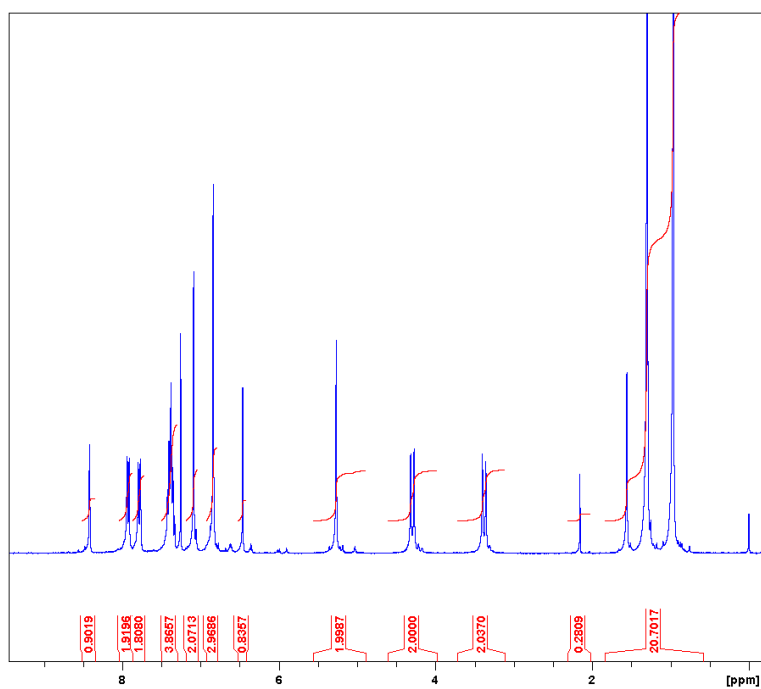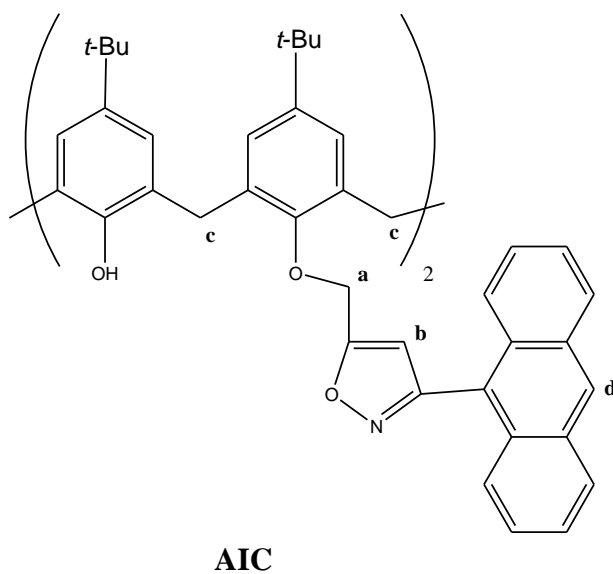

AIC

Figure A1. ^{1}H NMR Spectrum(300 MHz, CDCl$_3$) of **AIC**.

The peaks around 4.30 and 3.39 ppm in Figure A1 represent the protons of the calixarene CH_2 groups (H_C) which are confirmed in the 2D-COSY spectrum (300 MHz, $CDCl_3$) (Figure A2.) which shows coupling between these signals. The signal of H_d is assigned as the downfield aromatic singlet, appearing at 8.43 ppm; it is more deshielded than the other protons in anthracene ring.

Couplings between the other anthracene protons were observed through the 2D-COSY from one multiple and two doublet peaks from 7.33 to 7.93 ppm while no proton in the calix aromatic rings can couple to these protons. The protons of CH_2O exhibit a singlet peak at 5.27 ppm. The two singlet peaks at 1.31 and 0.94 ppm are assigned as *tert*-butyl groups.

The last three singlet peaks at 7.09, 6.83 and 6.48 ppm are assigned as the protons of ArH, isoxazole CH and OH. As there is no coupling between the protons of calixarene aromatic rings, two singlet peaks can be observed at 7.09 and 6.83 ppm were determined as ArH in calixarene ring. However, the peak at 6.83 ppm integrates for three protons which mean it may contain one proton from isoxazole CH or the OH. The isoxazole peak was then confirmed by ^1H-^{13}C HSQC spectrum ($CDCl_3$, Figure A3.) which shows the coupling between the hydrogens and carbons: a carbon-hydrogen coupling is found in the HSQC spectrum. That shows the peak 6.48 ppm represents an H-atom connected to a C-atom with resonance 108.07 ppm, thus the signal at 6.48 ppm is the isoxazole proton H_b while the ArH peak at 6.83 ppm is overlapped with the OH group.

^1H NMR (300 MHz, $CDCl_3$): 8.43 (2H, s, ArH), 7.93 (4H, d, J = 7.8 Hz, ArH), 7.79 (4H, d, J = 7.8 Hz, ArH), 7.43-7.33 (8H, m, ArH), 7.09 (4H, s, ArH), 6.83 (6H, s, ArH, OH), 6.48 (2H, s, isoxazole CH), 5.27 (4H, s, $ArOCH_2$), 4.29 (4H, d, J = 13.2 Hz, CH_2), 3.37(4H, d, J = 13.2 Hz, CH_2), 1.31 [18H, s, $C(CH_3)_3$], 0.94 [18H, s, $C(CH_3)_3$];
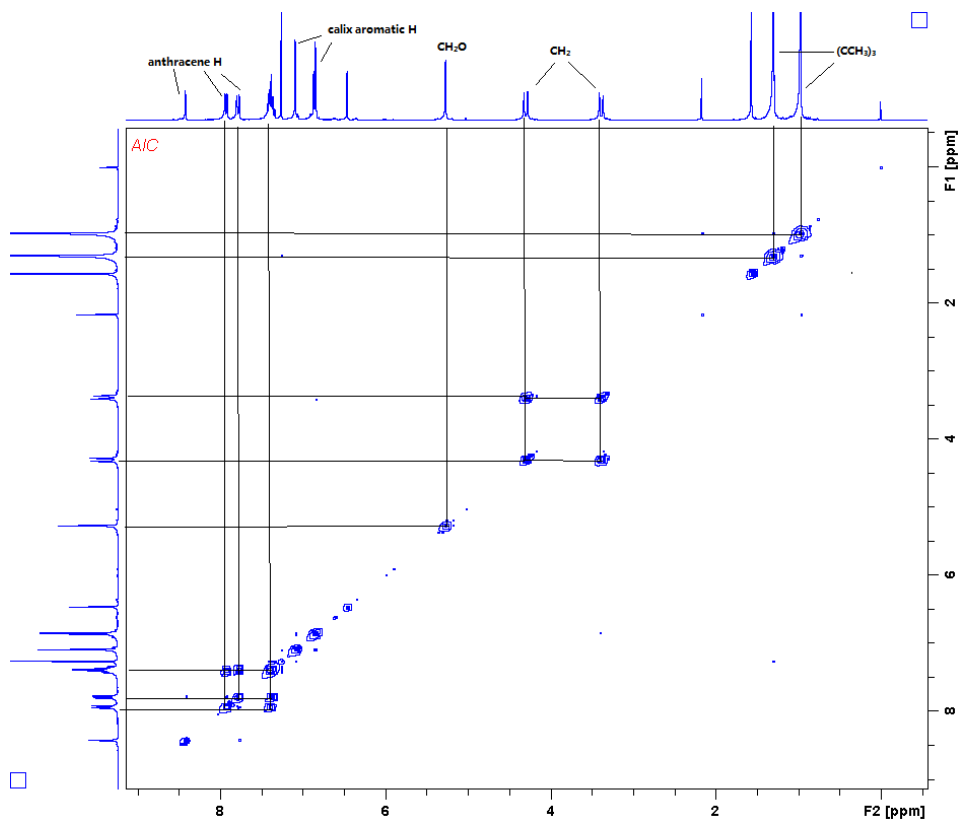
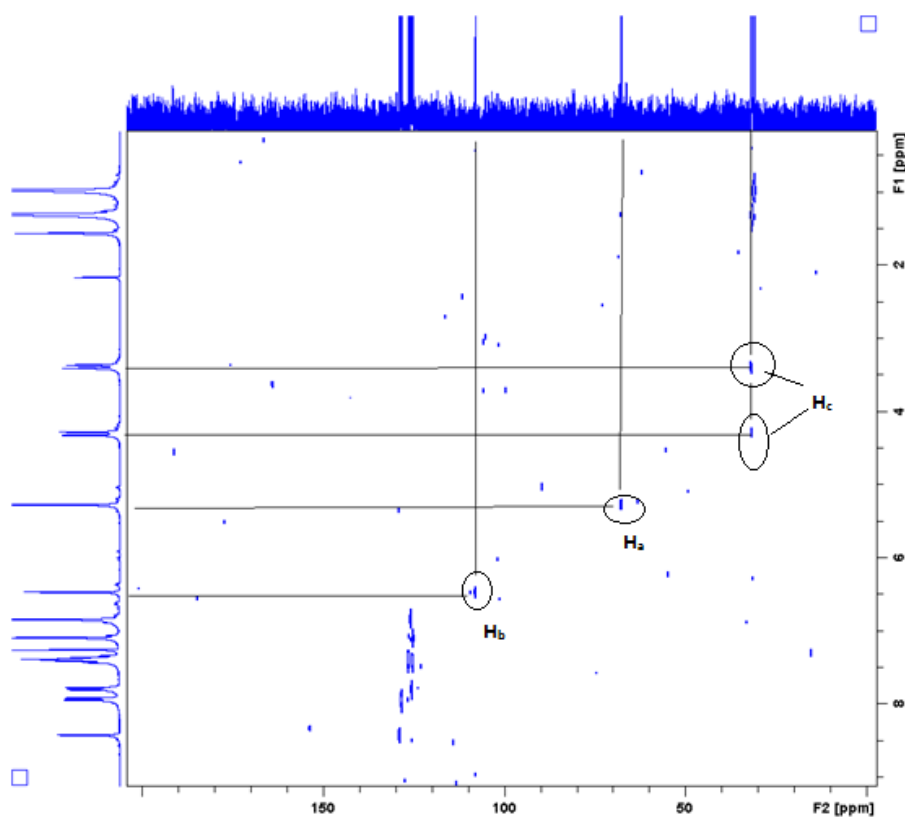Figure A2. 2D-COSY Spectrum (300 MHz, CDCl$_3$) of **AIC**.

Figure A3. HSQC spectrum (CDCl$_3$) of **AIC**.

With the help of proton-decoupled Dept 90 and Dept Q spectra (75 MHz, CDCl$_3$, in our NMR machine, Dept Q gives positive signals to C and CH$_2$ in a phase opposite to CH and CH$_3$). The signals of carbons were determined: 150.4, 149.6, 147.7, 141.9, 132.5, 131.1, 130.6, 127.9 ppm were determined as ArC. 129.0 128.4, 127.8, 126.5, 125.8, 125.6, 125.3, 125.2 ppm were determined as ArCH. Isoxazole CH peak appears at 108.1 ppm. Signals appear at 34.0, 33.9 ppm were determined as the tert-carbon [$\underline{C}$(CH$_3$)$_3$]. In the Dept Q spectrum, 67.7 and 31.9 ppm are positive signals which represent CH$_2$ and OCH$_2$. As the carbon of OCH$_2$ is more downfield that the one of CH$_2$. Thus, the peak at 67.7 ppm was assigned as OCH$_2$ signal whereas the peak 31.9 ppm was assigned as OCH$_2$ signals. The rest two signals appear at 31.7, 31.0 are the carbons of *tert*-butyl groups [C($\underline{C}$H$_3$)$_3$,].

^{13}C NMR signals are assigned as below:

^{13}C NMR (75 MHz, CDCl$_3$) δ: 167.9, 161.0, 150.4, 149.6, 147.7, 141.9, 132.5, 131.1, 130.6, 127.9, 129.0 128.4, 127.8, 126.5, 125.8, 125.6, 125.3, 125.2, 108.1, 67.7, 34.0, 33.9, 31.9, 31.7, 31.0; [M+Na]$^+$ calculated for C$_{80}$H$_{78}$N$_2$NaO$_6$ 1185.5752, found 1185.5670; IR: 3447.81, 2960.41, 1625.69, 1483.97, 1362.69, 1207.46, 888.35, 735.12 cm^{-1}.
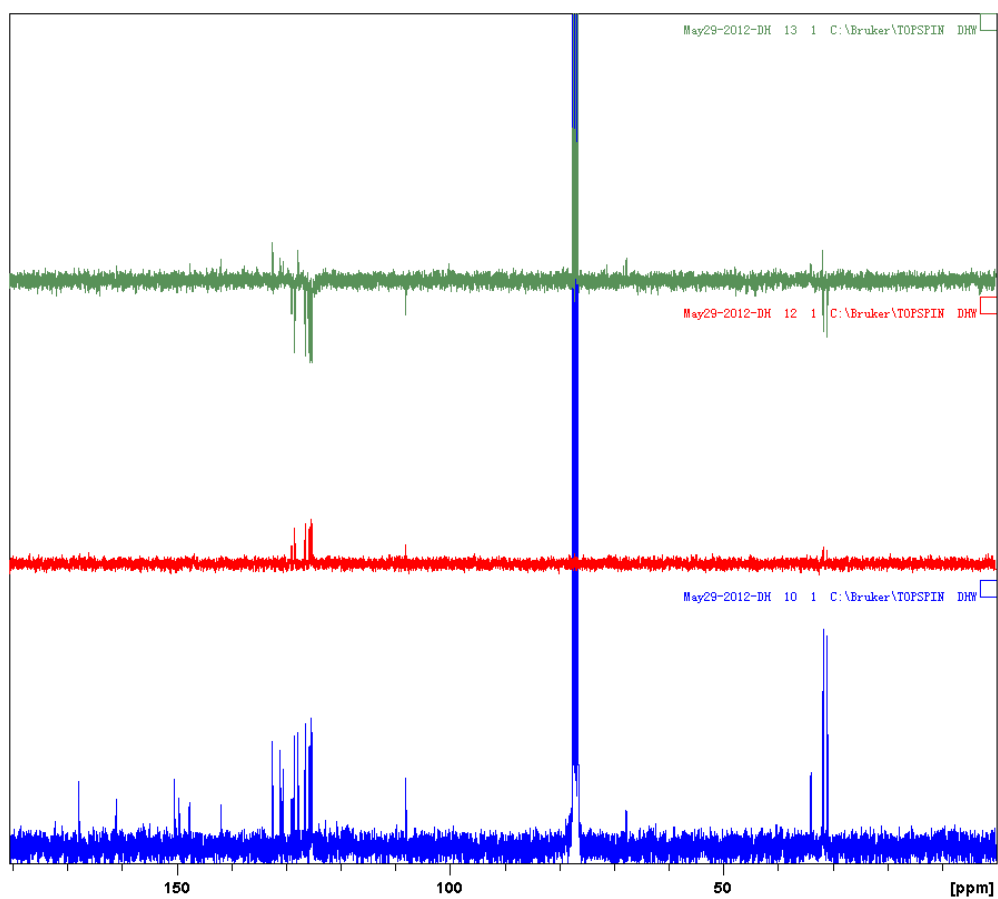
Figure A4. ^{13}C, Dept 90, Dept Q spectrum (from bottom to top) of **AIC** (75 MHz, CDCl$_3$).

Poster

I attended the 64th Irish Universities Chemistry Research Colloquium, June 14th-15th, 2012, in UNIVERSITY of LIMERICK and together with my laboratory colleague made a poster presentation centred on the progress up to that time of the work discussed in this thesis. A PDF of the poster is presented below.

Click modified calix[4]arene fluorescent sensor for Cu²⁺ ions

Haowen Daio[1], **Niall Maher[1]**, *Frances Heaney[1], John McGinley[1] and John Gallagher[2]*
1. Department of Chemistry, NUI Maynooth, 2. School of Chemical Sciences, Dublin City University
dhwert@sina.com, niall.j.maher@alumni.nuim.ie

Introduction

The potential to modify the lower rim of the calix[4]arene scaffold has made these molecules valuable templates from which a huge range of supramolecular structures have been constructed.[1] Chemosensors based on the calix-scaffold have been the subject of previous studies,[2] particularly the synthesis of metal ion selective sensors. More recently a copper promoted, triazole functionalization "click" chemistry approach to these chemosensors has been developed.[2] In this poster we describe a new sensor based upon a calix[4]arene scaffold functionalised with an isoxazole ionophore and a pryene reporter unit. Fluorescence spectra of the pyrene modified isoxazole calixarene (PIC) host alone, and in the presence of a variety of metal salts, at various host:guest ratios, were recorded. For the host sample, dual emission, monomer and excimer, was observed upon excitation at 343nm. In the presence of Cu²⁺ ions quenching of both the monomer and excimer emission was observed, while all other metals including Co²⁺, Pb²⁺, Ni²⁺ ions had little effect on the emission spectra.
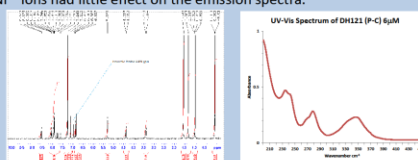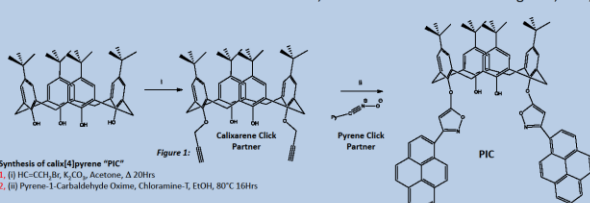
Synthesis of calix[4]pyrene "PIC"
1. (i) HC=CCH₂Br, K₂CO₃, Acetone, Δ 20Hrs
2. (ii) Pyrene-1-Carbaldehyde Oxime, Chloramine-T, EtOH, 80°C 16Hrs

Figure 1:

Shown above **Figure 1** scheme for synthesis of click modified pyrene isoxazole calixarene (PIC)
(i) The calixarene click partner was formed from the first reaction, the product was collected as crystals in 85% yield, from a solution of methanol and chloroform.
(ii) The isoxazole ring was formed by cycloaddition of 1-Pyrene oxime and the calixarene click partner. The pure product **PIC** was obtained from crystallization of column fractions using a solution of DCM and petroleum ether to give a yield of 60%.

Figure 2:
Figure 3:
The structure assigned to PIC *(Figure 1)* was confirmed by the ¹H NMR data, the ¹H NMR spectrum *(Figure 2)* showing the characteristic isoxazole proton at approx. 6.9ppm

UV data *(Figure 3)* shows three peaks at 235 nm, 277 nm, 343 nm. Excitation was preformed at these wavelengths using the fluorescence spectrometer, excitation at 343 nm was observed to give the best emission spectra

Figure 4: (a) *(b)* *(c)*
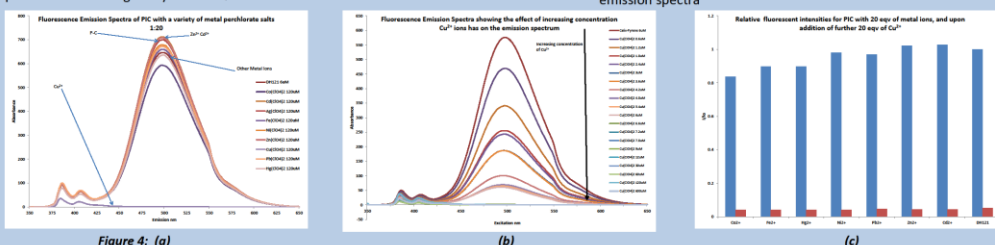
All fluorescence measurements performed at 343nm. Solutions made in 3000µL cuvette. Concentration of (PIC) kept constant (6µM) with varying concentration of guest (metal ions) 0.6µM - 600µM

(a)
- As can be seen from fluorescence emission spectrum *(a)* most metal ions have a negligible effect upon the emission spectra
- In contrast the quenching effect Cu²⁺ ions have on the fluorescence is startling
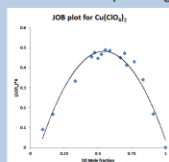
(b)
- As concentration of the Cu²⁺ ions (guest) increases so does the quenching effect
- Significant quenching can be seen with 0.6µM of Cu²⁺ ions present, a host to guest ratio of 1:0.1

(c)
- Relative intensity (Intensity/Original Intensity I/I_o) for PIC with metal salts present (blue bar)
- Relative intensity in the presence of competing Cu²⁺ ion (red bar)
- Clear that even in the presence of other metal ions, Cu²⁺ ions still result in significant fluorescent emission quenching
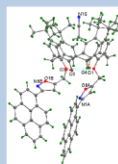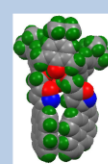- Indicates preference to binding of copper

Figure 5: *Figure 6:* *Figure 7:*

These studies revealed a 1:1 stoichiometry as can be seen in the Job Plot *(Figure 5)*, one guest molecule for each host molecule
A **K_d** of **1.52x10⁻⁶Mol⁻¹** was obtained from the Stern Volmer plot *(Figure 6)* further experiments are currently being performed.
Figure 7 above shows that PIC is an intramolecular molecule. The fluorescence emission spectrum for PIC was measured for reducing concentrations from 1x10⁻⁴M to 1x10⁻⁷M, the same relative decrease in both the monomer and excimer emission can be seen. This is indicative of intramolecular interactions between the pyrene rings.

Conclusions

A fluorescent sensor for Cu²⁺ ions was synthesised by copper free click chemistry using a calix[4]arene scaffold. Upon the addition of Cu²⁺ ion the fluorescence sensor PIC shows significant fluorescence quenching whereas the other metal ions, like Pb²⁺, Fe²⁺, have little effect on the fluorescence spectrum. The quenching effect Cu²⁺ ions have on the emission spectrum was observed even at low concentrations (0.6µM) of Cu²⁺ ions giving a host to guest ratio of 1:0.1. Further studies also points to selectivity for Cu²⁺ ions over other metal ions. A "sister" sensor using an anthracene reporter unit has been synthesised and tested in a similar fashion.
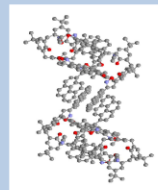
Figure 8: *Figure 9:* *Figure 10:*
Single X-ray crystal structures of calixpyrene PIC *(Figure 8 and 9)* supports the structural designation based on the ¹H NMR *(Figure 1 and 2)*
As shown in **Figure 10** the packing of PIC molecules is intermolecular as can been seen from the parallel pyrene rings from neighbouring PIC

References
1. B. Creaven, T. Gernon, J. McGinley, A. Moore and H. Tofland, *Tetrahedron.*, 2006, **62**, 9066-9071.
2. S. Y. Park, J. H. Yoon, C. S. Hong, R. S., J. S. Kim, S. E. Matthews, and J. Vicens, *J. Org. Chem.*, 2008, **73**, 8212-8218.

NUI MAYNOOTH

126